# Galvanic Vestibular Stimulation in Primates: Recording Vestibular Afferents during Transmastoid Stimulation


**Annie Kwan**

Department of Biomedical Engineering

McGill University

Montreal, Quebec, Canada

August 2016

A thesis submitted to McGill University in partial fulfillment

of the requirements of the degree of Master of Engineering

# Table of Contents

# Abstract

An increasingly popular tool to artificially activate the human vestibular system is galvanic vestibular stimulation (GVS), in which electrical stimulation is applied between surface electrodes on the mastoid processes behind the ears. To date, however, while the effects of GVS, including the perception of self-motion, eye movements, and postural sway have been well described, the neuronal correlates remain unknown. Specifically, how the vestibular system actually responds to GVS to drive perception and behaviour has not been established. Therefore, the focus of this thesis is to understand the effects of GVS on vestibular afferent activity and. in turn, correlate these neural responses to behavioural responses. To this end, I recorded the responses of individual vestibular afferent and eye movements evoked by different GVS protocols applied between surface electrodes on the mastoid processes of alert macaques. In response to sinusoidal stimulation, we show for the first time that otolith afferents, much like canal afferents, displayed an increase in both gain and phase lead as a function of frequency. In contrast, when recording eye velocity during sinusoidal GVS with the monkeys fixating on a target, the gain of torsional eye velocity relative to the peak GVS current amplitude remained relatively constant as a function of frequency.

Thus far, the prevailing view is that the GVS activation of the peripheral vestibular system is linear. However, I provide evidence that suggests that afferent responses can show significant nonlinearities in response to GVS. Notably, vestibular afferents, primarily irregular afferents, displayed asymmetric responses to currents of opposite polarity. Furthermore, we found discrepancies in the traditional linear analyses between sinusoidal and stochastic stimulation. These results reveal nonlinearities in the vestibular afferent activity in response to GVS. Taken together, the findings presented in this thesis provide the neural correlates underlying GVS-evoked

perceptual, ocular and postural responses – a fundamental step into understanding the effect of this technique required to advance its clinical and biomedical applications.

# Résumé

Un outil de plus en plus populaire pour activer artificiellement le système vestibulaire humain est la stimulation vestibulaire galvanique (SVG). La SVG consiste à appliquer une stimulation électrique entre deux électrodes de surface apposées sur les processus mastoïdes derrière les oreilles. À ce jour, alors que les effets de la SVG sur la perception des mouvements auto-générés, sur les mouvements oculaires et sur le contrôle postural ont été largement décrits, l'activité neuronale en réponse à la SVG reste inconnue. Plus précisément, le lien entre la dynamique des afférents vestibulaires et les réponses évoquées par la SVG n'a pas été établie. Par conséquent, cette thèse porte principalement sur la caractérisation des effets de la SVG sur l'activité des afférents vestibulaires et sur la corrélation entre l'activité neuronale et les réponses comportementales. À cette effet, j'ai enregistré l'activité des afférents vestibulaires ainsi que les mouvements oculaires chez deux singes et ce, pour différents protocoles de SVG de surface. Premièrement, en réponse à une stimulation sinusoïdale, nous montrons pour la première fois que les afférents otolithiques et les afférents des canaux semicirculaires ont une augmentation de gain et d'avance de phase en fonction de la fréquence. En revanche, l'enregistrement des mouvements des yeux lors d'une fixation oculaire démontre que le gain de la vitesse de torsion en fonction de l'amplitude du courant reste relativement constant et ce, indépendamment de la fréquence.

Précédemment, il était proposé que l'activation du système vestibulaire périphérique par la SGV était linéaire. Toutefois, je fournis des évidences qui suggèrent que la réponse afférente peut démontrer de la nonlinéarité en réponse à la SGV. Notamment, et de façon plus importante pour les afférents irréguliers, les afférents vestibulaires démontrent une activité asymétrique en réponse à des stimulations de polarité opposée. De plus, utilisant des analyses linéaires traditionnelles, nous avons trouvé des discordances entre la réponse aux stimulations sinusoïdales et stochastiques,

lesquelles dénotent de la nonlinéarité dans l'activité des afférents vestibulaires lors de la SGV. Dans leur ensemble, les résultats présentés dans cette thèse établissent les corrélats neuronaux soutenant les réponses perceptuelles et comportementales évoquées par la SGV tel que les mouvements oculaires et le contrôle de la posture. Cette avancée fondamentale dans notre compréhension de cette technique et de ces effets est requise pour faire avancer ses applications cliniques et biomédicales.

# Acknowledgement

I would first like to thank my supervisor, Dr. Kathleen E. Cullen for all the guidance and support over the past couple of years. I have learned an incredible amount from her. She helped me develop better critical thinking and writing skills. I will always remember all her advice as I continue in my future endeavours.

I am most grateful to all the past and present members in the lab, who made my graduate studies unforgettable. In particular, Diana Mitchell, for teaching me how conduct experiments and for always being there to answer all my questions; Alexis Dale, Mohsen Jamali, and Jerome Carriot, for helping me countless of times even when they are not in the lab; Isabelle Mackrous, for helping me translate my abstract; Adrien Xiao Shen Hu for proofreading; Kenneth Dyson, Jessica Brooks, Vanessa Chang, Omid Zobeiri, Jie Shao, Lydia Wang, and Da Woon Park for their positive feedback and encouragement.

I would also like to thank the collaborators, Drs. Patrick A. Forbes and Jean-Sébastien Blouin, for giving me the opportunity to work on such an amazing research. I am grateful for all your enthusiasm and your patience. In addition, I would thank the Biomedical Engineering graduate program director, Dr. Louis Collins, for all his advice.

My research would not be possible two extraordinary people: Walter Kucharski, a master in the workshop who makes and fixes the lab equipment while making jokes along the way; Stephen Nuara, who was always there to make sure the animals are fine and healthy.

Finally, I thank my friends and family for all their support and understandings through all the ups and downs during my studies. In particular, my big brother, for keeping me entertained.

## Contribution of Authors

Chapter 2 and 3 contain studies in collaboration with the following authors: Kwan A, Mitchell DE, Forbes PA, Blouin J-S, Cullen KE. For these two studies, I designed the stimuli, collected the behavioural and single unit data, performed the analysis, and prepared the manuscript (text and figures). Diana Mitchell contributed to the data collection and gave advice in data analysis. Dr. Patrick Forbes contributed in designing the stimuli and along with Dr. Jean-Sébastien Blouin, provided feedback based on their knowledge in human work. My thesis supervisor, Dr. Kathleen Cullen, provided guidance through each stage of the study including experimental design, surgeries, collection, analysis, and interpretation of the data, as well as the preparation of the thesis.

# Chapter 1: Literature Review

## I. General introduction

As we make movements during daily activities, our vestibular system detects the head motion in space to generate compensatory reflexes stabilizing our gaze, controlling balance and posture, as well as to provide a sense of spatial orientation and movements in our environment in order to navigate the world. There are two types of motion sensors of the vestibular system (also referred as *vestibular endorgans*) located within each inner ear: Semicircular canals, which detect angular acceleration; and otolith organs, which sense linear acceleration. Primary vestibular afferents encode and transmit motion information from these vestibular sensors to the vestibular nuclei in the brainstem and the cerebellum, which subsequently project to eye motoneurons, the spinal cord, and higher-order brain areas (Angelaki & Cullen, 2008; Cullen, 2012).

While the vestibular system is physiologically activated by motion of the head, there are several artificial means – using either heat, electricity, or magnetic field – that evoke vestibular-related responses in order to study and assess the vestibular system. One such technique is galvanic vestibular stimulation (GVS), which is electrical current applied between surface electrodes behind the mastoid processes of the ears. Ever since Purkyně first discovered GVS nearly two centuries ago by (Purkyně, 1823), the technique has been shown to induce a wide range of behavioural responses attributed to the activation of the vestibular system. This non-invasive technique has become increasingly popular not only in probing the vestibular system but as a potential tool for rehabilitation and navigation. To this day, however, how exactly GVS activates the peripheral human vestibular system to evoke the wide range of observed responses remains to be elucidated. Current views on how GVS stimulates the human vestibular afferents are based on neural

recordings in animals, with the caveat that electrical current was delivered inside the ear, a setup much different from human GVS studies. The goal of my thesis is thus to bridge the gap between the neural origins and the behavioural consequences evoked by GVS. I begin with a short overview of the peripheral vestibular system and how vestibular afferents respond to physiological stimuli. I will then follow with a review of vestibular afferent responses to the electrical stimulation delivered in the ears of different animal models and the current model in human GVS-induced responses associated with the vestibular system. Finally, I will conclude with the potential applications of GVS in different fields.

## II. Peripheral vestibular system: Encoding motion with neural activity

### A. Vestibular endorgans: Semicircular canals and otolith organs

Within the inner ear, the vestibular endorgans form the vestibular labyrinth, which is situated in the petrous part of the temporal bone in close proximity of the cochlea, the sensory organ of the auditory system. The vestibular labyrinth is composed of two types of hair-cell containing vestibular endorgans: Three semicircular canals which detect rotation, and two otolith organs which sense translation and the force of gravity.

The three semicircular canals are roughly orthogonally oriented semicircular tubes, each sensitive to rotations in their own plane (Fig. 1.1). When the head is facing forward, the horizontal semicircular canals lie nearly in the horizontal plane and are most sensitive to yaw rotations (i.e. leftward/rightward rotations about the rostral-caudal axis). The two vertical semicircular canals – the anterior (or superior) and posterior canals – are oriented vertically at about 45 degrees relative to the sagittal plane and are both sensitive to pitch and roll rotations (i.e. downward/upward rotations about the interaural axis and side to side rotation about the naso-occipital axis,

respectively). The approximate orthogonality of the three semicircular canals allows us to be able to detect and decompose three-dimensional head angular movements based on the planes of the three canals (Rabbitt, 1999). Each semicircular canal is a filled circular tube filled with a viscous fluid, where at one end is the ampulla – a bulge-like structure containing a water tight, gelatinous diaphragm called the cupula – and a neuroepithilium comprising of hair cells, the sensory receptors of the vestibular system. Stereocilia of hair cells within one ampulla are all aligned in the same direction and are embedded in the cupula. As a result, during head rotation when the viscous fluid, lagging behind due to its inertia, deflects the cupula, stereocilia of the hair cells are bent in one direction, evoking similar responses across the hair cell bundle (reviewed in Rabbitt *et al*., 2004). Depending on the direction that the stereocilia are bent, mechanoreceptors found near its tips open or close. The opening of the mechanoreceptors causes an influx of potassium and depolarizes the hair cells. Subsequently, voltage-gated calcium channels open and the calcium influx triggers the release of excitatory neurotransmitter (glutamate) onto innervating vestibular afferents, increasing the afferents' firing rate. Conversely, closing of the mechanoreceptors reduces the cation influx, which hyperpolarizes the hair cells and consequently reduces the firing rate of the innervating vestibular afferents (reviewed in Colclasure & Holt, 2003). Thus, depending on the unidirectionality of the hair cells within a semicircular canal, each semicircular canal has its own preferred direction of rotation in its plane (i.e. the direction which activates the vestibular afferents). Furthermore, for each semicircular canal on one side, there is a semicircular canal on the other side with the opposite preferred direction in the same plane of rotation. Therefore, yaw rotation toward the right would increase the firing rate of vestibular afferents innervating the right horizontal canal but simultaneously decrease the firing rate of vestibular afferents innervating the

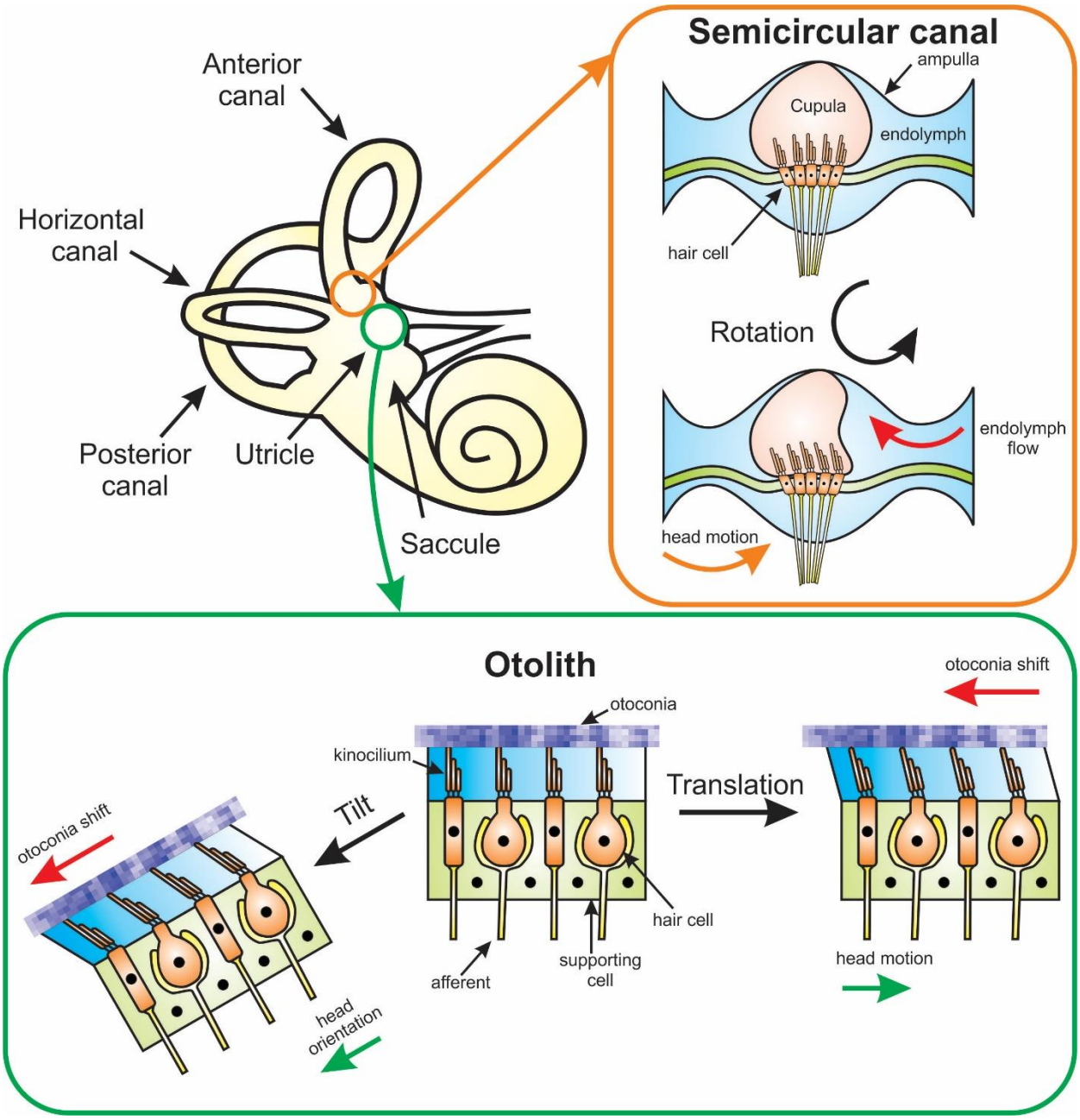


**Figure 1.1: Diagram of the vestibular sensory organs and mechanism of hair cell activation**
Semicircular canals detect rotation. Orange inset shows the organization of the hair cells within the semicircular canals. During head rotation, the endolymph lags behind and pushes on the cupula, deflecting the hair cells in the process. Otolith organs sense translation as well as head tilt relative to gravity. Green inset shows the organization of the hair cells within the otolith organs. During head translation (right), the otoconia lags behind and causes a shift between the otolithic membrane and the macula, deflecting the hair cells in the process. During head tilt (left), the force of gravity pulls the otoconia downward and causes a shift between the otolithic membrane, deflecting the hair cells in the process.

left horizontal canal. Similarly, the anterior canals form mirror symmetrical pair with their respective contralateral posterior canals (e.g. see Resine *et al*., 1998).

The two otolith organs, utricle and saccule, are aligned with the horizontal and vertical plane, respectively (Fig. 1.1). Together, they detect linear acceleration in three dimensions as well as static head tilt relative to gravity (Fernandez & Goldberg, 1976a; b; c). The hair cells of each otolith organ are arranged on a neuroepithilium sheet (macula) and the stereocilia are embedded in an overlaying gelatinous matrix (otolithic membrane) containing calcium carbonate crystals (otoconia). During linear acceleration, the otolithic membrane lags relative to the head movement along with the membranous labyrinth due to the inertial force acting upon the otoconia. This causes the deflection of the stereocilia of the hair cells and subsequent depolarization or hyperpolarization in the hair cells, depending on the direction of deflection, similar to mechanotransduction of hair cells in semicircular canals. Alternatively, during static head tilt, the force of gravity pulls down the otolith membrane relative to the membranous labyrinth, deflecting the stereocilia in the process (reviewed in Rabbitt *et al*., 2004). Unlike semicircular canals, hair cells in the otolith organs are not all arranged in the same polarization vectors (i.e. the direction of the kinocilia). A narrow curved region called the striola lies in the middle of the macula, dividing the hair cells into two zones (Fig. 1.2). No matter which side of the striola, all hair cells are oriented such that the kinocila are pointed either toward the striola, in the case of the utricular macula, or away from the striola, in the saccular macula. This causes hair cells on either side of the striola to have opposing orientation. In addition, due to the curved nature of the striola, the orientations of the hair cells are arranged in a fan-like pattern, covering all directions of a plane (reviewed in Eatock & Songer, 2011). Together, linear head acceleration in one direction can simultaneously and preferentially excite or inhibit hair cells, depending on their orientation relative to the striola.

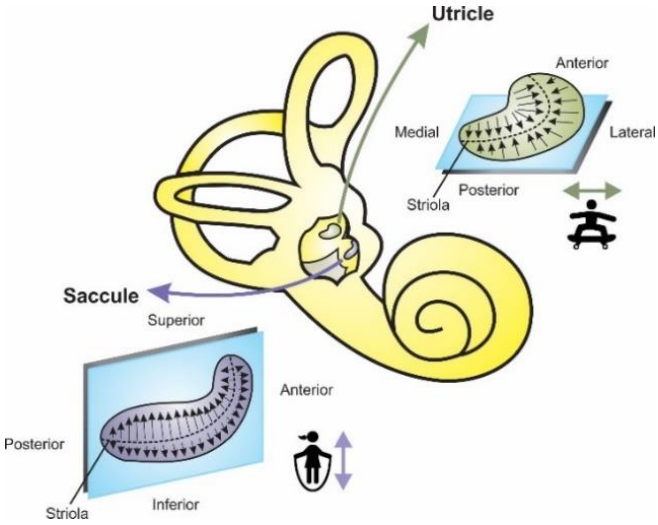


**Figure 1.2: Diagram of the utricle and saccule**
The maculae of the utricle and saccule are roughly oriented in the horizontal and vertical planes, respectively. The striola is a narrow curved linear region across the middle of the macula (dashed lines). In the utricular macula, hair cells are oriented towards the striola (arrows). In the saccular macula, hair cells are oriented away from the striola. The organization of hair cells in both the utricle and saccule forms a fan-like pattern, covering all directions of the plane.

### B. Vestibular receptor cells: Hair cells

As mentioned previously, mechanotransduction from motion to neural activity occurs at the level of hair cells in the vestibular endorgans, where the deflection of hair cells results in a change in neurotransmitter release onto the primary vestibular afferents. There exist two types of hair cells in the peripheral vestibular system (Fig. 1.3): Cylindrically-shaped type II hair cells are present in both amniotes (i.e. mammals, reptiles, and birds) and non-amniotes, while flask-shaped type I hair cells, which are phylogenetically older, are found only in amniotes (Eatock & Hurley, 2003). In addition to their morphological differences, the two types of hair cells have different cellular properties. For example, type I hair cells contain a higher density in potassium channels resulting in faster responses and therefore having greater sensitivity to high frequency stimulation compared to type II hair cells (reviewed in Eatock & Songer, 2011).

Furthermore, the two types of hair cells differ in innervation patterns by the primary vestibular afferents. Each type I hair cell is enveloped by a single cup-like afferent terminal, called the calyx. In contrast, type II hair cells receive contacts by bouton-like afferent terminals from multiple afferent fiber (Fig. 1.3). As elucidated in the following section, there are different innervation patterns of primary vestibular afferents onto the two types of hair cells. Moreover, the physiological differences between the two types of hair cells contribute to the dynamic responses of the innervating vestibular afferents.

### C. Vestibular afferents: Sensory coding of motion

Once head motion is detected by the vestibular endorgans and hair cells, the next stage of vestibular processing is to transmit this motion information to the brain in order to generate compensatory reflexes and estimate self-motion. Primary vestibular afferents, which innervate the hair cells, play the fundamental role of encoding motion into neural activity and projecting to the central vestibular areas. The following section will be a brief overview of the two different classes of vestibular afferents, as well as our current understanding of how vestibular afferents encode physiological vestibular stimulation.

In the absence of head motion, hair cells spontaneously release glutamate onto vestibular afferents such that the afferents have a resting discharge. By having a resting discharge, vestibular afferents can increase or decrease their firing rate depending on the direction of motion, and can thus transmit bidirectional motion information to the vestibular nuclei for subsequent central vestibular processing (Goldberg, 2000). Among vestibular afferents in both semicircular canals and otolith organs, there is a large distribution in the resting firing rate regularity (i.e. the distribution of the interspike intervals, ISI) which is quantified using the coefficient of variation

(standard deviation/mean) that is normalized to be independent the mean resting discharge, CV* (Goldberg *et al.*, 1984). Conventionally, vestibular afferents are functionally categorized into two groups based on their CV* (Fig. 1.3): regular afferents (CV* < 0.1) and irregular afferents (CV* > 0.1). Aside from the regularity of the resting discharge, these two types of afferents differ in morphology and response dynamics. While regular afferents provide bouton nerve ending onto type II hair cells, irregular afferents can either have calyx endings innervating type I hair cells or dimorphic endings (i.e. mixed of calyx and boutons) innervating both hair cells types. In addition, regular afferents have smaller axons, resulting in slower conduction velocity than irregular afferents. Regular afferents are also less sensitive to physiological kinetic stimulation, whether it is rotation or translation (Goldberg, 2000). Furthermore, stimulation of the efferent pathway produces smaller and slower response in regular afferents compared to irregular afferents (Goldberg & Fernandez, 1980; Sadeghi *et al.*, 2009).

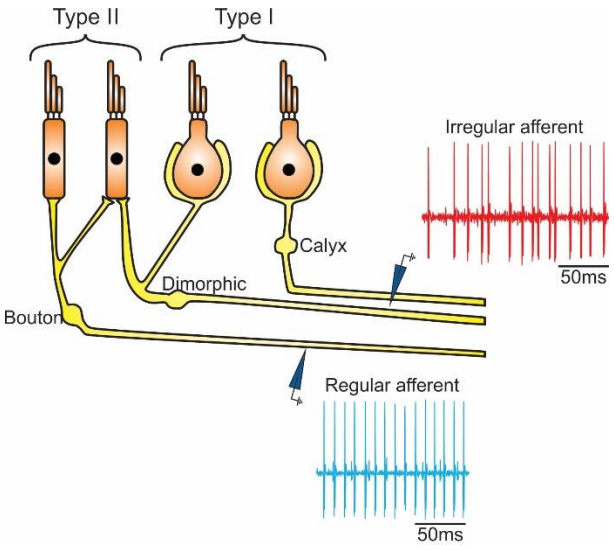


**Figure 1.3: Vestibular hair cells and primary vestibular afferents**
Regular afferents, which have regularly discharging action potentials (blue trace), form bouton nerve endings onto type II hair cells. Irregular afferents, which have more variability in their resting discharge (red trace), innervate type I hair cells with calyx nerve endings and synapse with both type I and type II hair with dimorphic (mix of bouton and calyx) nerve endings.

Following the biomechanics of the vestibular endorgans, semicircular canal afferents respond to rotational stimuli whereas otolith afferents are stimulated by translational movements. Moreover, responses from both canal and otolith afferents remained consistent, regardless of whether the motion is self-generated (i.e. active) or imposed upon (i.e. passive) (Cullen & Minor, 2002; Jamali *et al.*, 2009). The similarity in vestibular afferent responses to active and passive motion justifies the use of passive motion stimuli to investigate the response dynamics of canal and otolith afferents to rotational and translational motion, respectively, which have been utilized extensively in numerous studies (Fernandez & Goldberg, 1971; Angelaki & Dickman, 2000; Cullen & Minor, 2002; Hullar *et al.*, 2005; Ramachandran & Lisberger, 2006; Sadeghi *et al.*, 2007a; Sadeghi *et al.*, 2007b; Jamali *et al.*, 2013). Traditionally, sinusoidal or broadband noise motion stimuli of low amplitude and within the physiological relevant frequency range (0 – 25 Hz) are applied to characterize vestibular afferents. It has been shown that the firing rates of canal and otolith afferents linearly encode angular velocity and linear acceleration, respectively. More specifically, the frequency responses of canal and otolith afferents to their respective motion stimuli were found to increase in gain and phase lead as a function of frequency, with the irregular afferents having a greater frequency response (Fig. 1.4). Linear models have been established for both canal (Fernandez & Goldberg, 1971; Hullar *et al.*, 2005) and otolith (Angelaki & Dickman, 2000) afferents, which can be used to form a linear prediction the afferents' firing rate in response to motion.

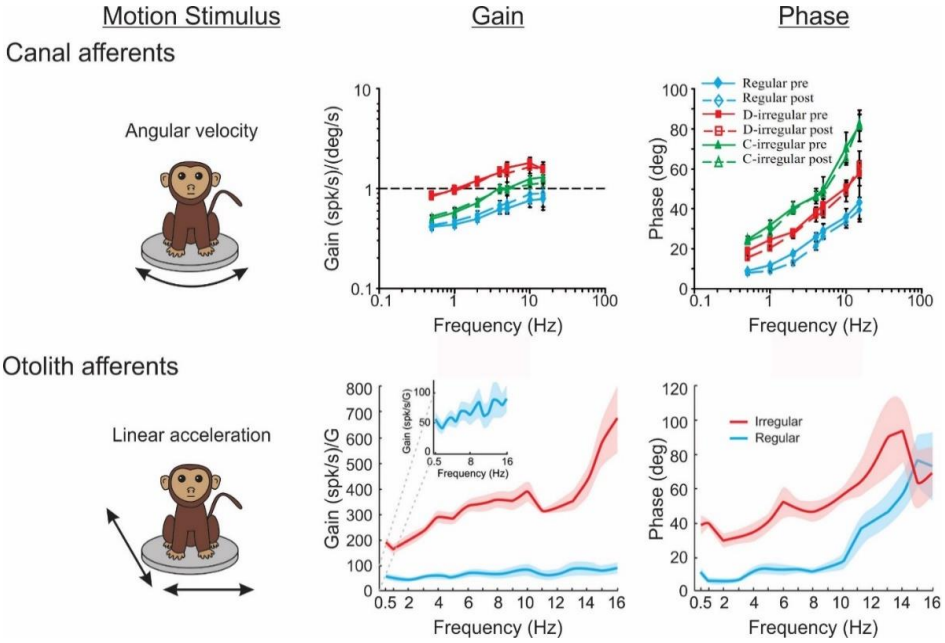


**Figure 1.4: Linear response dynamics of vestibular afferents to motion**
Semicircular canal afferents respond to head angular velocity (top) whereas otolith afferents respond to head linear acceleration (bottom). The gain and phase lead for both canal (adapted from Sadeghi *et al*., 2007b) and otolith afferents (adapted from Jamali *et al*., 20013) increase across the physiological frequency range. There is a markedly bigger difference in gain between irregular and regular afferents in otolith afferents than in canal afferents.

Although vestibular afferent responses are often considered to linearly encode motion, as described above, the motion stimuli used to characterize afferents have typically been constrained to low intensity. However, there are reports where high amplitude vestibular stimuli can drive vestibular afferents into a nonlinear regime, where afferents cannot have a negative firing rate (i.e. cutoff) and they have a maximum firing rate (i.e. saturation) (Fernandez & Goldberg, 1976b; Sadeghi *et al.*, 2007b). Similarly, it was recently demonstrated that naturalistic motion (i.e. motion whose time course matching that of naturally occurring motion) falls outside the linear region of vestibular afferents such that linear models fail to predict the saturated and cutoff responses (Schneider *et al.*, 2015). In order to correctly model the nonlinearities in vestibular afferent responses to motion of high intensity, a linear-nonlinear cascade was used, where the linear

prediction estimated from previously established transfer function of the afferents was subsequently transformed by a static nonlinearity in the form of a sigmoid. This particular nonlinear transformation, which took into account the cutoff and saturation of vestibular afferents' firing rates, was able to accurately predict afferents response to higher intensity motion stimuli (Schneider *et al.*, 2015). In addition to high motion amplitude, motion at higher frequencies was also found to drive both semicircular canal (Ramachandran & Lisberger, 2006) and otolith afferents (Jamali, 2015), especially irregular afferents, into a different nonlinear regime known as phase-locking. In other words, during high intensity motion, vestibular afferents adopt a different coding strategy where instead of using their firing rate to encode the motion, they fire temporally precise action potentials at specific phases of the motion. Altogether, while in most situations vestibular afferents can be considered as a linear system, it is important to acknowledge that nonlinear responses can be generated under more challenging conditions.

## III. Galvanic vestibular stimulation

### A. Overview of galvanic vestibular stimulation

Galvanic vestibular stimulation (GVS) is one of a few techniques that is used to artificially activate the vestibular system, which evokes stereotype behavioural responses (reviewed in Fitzpatrick & Day, 2004). In the case of GVS, electrical current is applied between surface electrodes, placed on the mastoid processes behind the ears of human subjects, where it is relatively near to the vestibular labyrinth located in the inner ear. Compared to other techniques to artificially activate the vestibular system such as caloric and magnetic vestibular stimulation, GVS is more practical in the sense that it is non-invasive (in contrast with the ear irrigation for caloric vestibular stimulation), as well as portable (as opposed to the use of a magnetic resonance imaging scanner

for magnetic vestibular stimulation). Over the past 50 years, GVS studies in humans have used several possible setups of the stimulating electrodes, each activating the vestibular system in a different way. The most typical approach is to deliver currents of opposing polarity, cathodal versus anodal, between the two ears. The applied current then generates a vestibular signal, activating central vestibular processing of a virtual head movement, which in turn evokes vestibular-related behavioural responses. Considering that the vestibular system has three core functions: gaze stabilization, postural and balance control, and self-motion, GVS-evoked behavioural responses can be categorized into three groups of similar nature. First, it has been observed that GVS evokes distinct types of eye movements in the horizontal and torsional plane (Zink *et al.*, 1997; Watson *et al.*, 1998; Kleine *et al.*, 1999; Schneider *et al.*, 2000; MacDougall *et al.*, 2003). Second, there are well-defined postural responses during GVS such as temporally defined postural electromyographic responses in the leg muscles (Nashner & Wolfson, 1974; Britton *et al.*, 1993; Fitzpatrick *et al.*, 1994) and body sway (Lund & Broberg, 1983; Inglis *et al.*, 1995b; Day *et al.*, 1997a; Wardman *et al.*, 2003a). Third, in the presence of GVS, subjects have reported different perception of self-motion, including rotation (reviewed in Reynolds & Osler, 2012) and rocking, as well as the sensation of being tilted (reviewed in Cohen *et al*., 2011) despite the fact that the subjects were physically static.

As described above, early vestibular processing of physiological stimuli has been well established. In contrast, less is known about how the vestibular system responds to artificial electrical stimulation. Despite the growing popularity of GVS to manipulate the vestibular system of human subjects, how this technique activates the peripheral vestibular system remains a topic of debate. Previous human studies have attempted to infer the underlying mechanisms mediating GVS-evoked behavioural responses. However, it is difficult to interpret the effects of this type of

stimulation at the neuronal level because of the wide variety in GVS-evoked responses to consider. While there have also been neurophysiological studies in animals directly investigating the vestibular afferent activity to electrical stimulation, as discussed in the following section, there are certain limitations in deducing the effects of GVS on the human vestibular system based on prior animal studies. Hence, the central focus of this thesis is to investigate the neuronal mechanisms underlying the GVS activation of the peripheral vestibular system. To do so, I recorded from primary vestibular afferents in nonhuman primates during GVS. It has been previously shown that nonhuman primates are an optimal model for humans, in particular, having similar oculomotor and visual systems. As such, to validate that the effects of GVS in nonhuman primate are similar to those experienced in humans, I also recorded eye movements in the animals under similar stimulation paradigm as previously done in humans. Taken together, the findings presented in this thesis would provide a neural correlate for GVS-evoked ocular responses in humans.

### B. Electrical stimulation of vestibular afferents in animal models

The current understanding of how GVS activates the peripheral vestibular system is based on neurophysiological recordings performed in a number of species including cats (Ezure *et al.*, 1983), pigeons (Lifschitz, 1973), rodents (Courjon *et al.*, 1987; Baird *et al.*, 1988; Kim & Curthoys, 2004; Kim *et al.*, 2011) and squirrel monkeys (Goldberg *et al.*, 1982; Goldberg *et al.*, 1984). Although there exists the caveat that most of the aforementioned studies delivered electrical current to electrodes implanted inside the ear (only one study had used surface electrodes (Kim & Curthoys, 2004); see Fig. 1.5), which is a situation much different than transmastoid stimulation conducted in human GVS studies, their results to date provide the only source of insight in how GVS activates the human vestibular system.

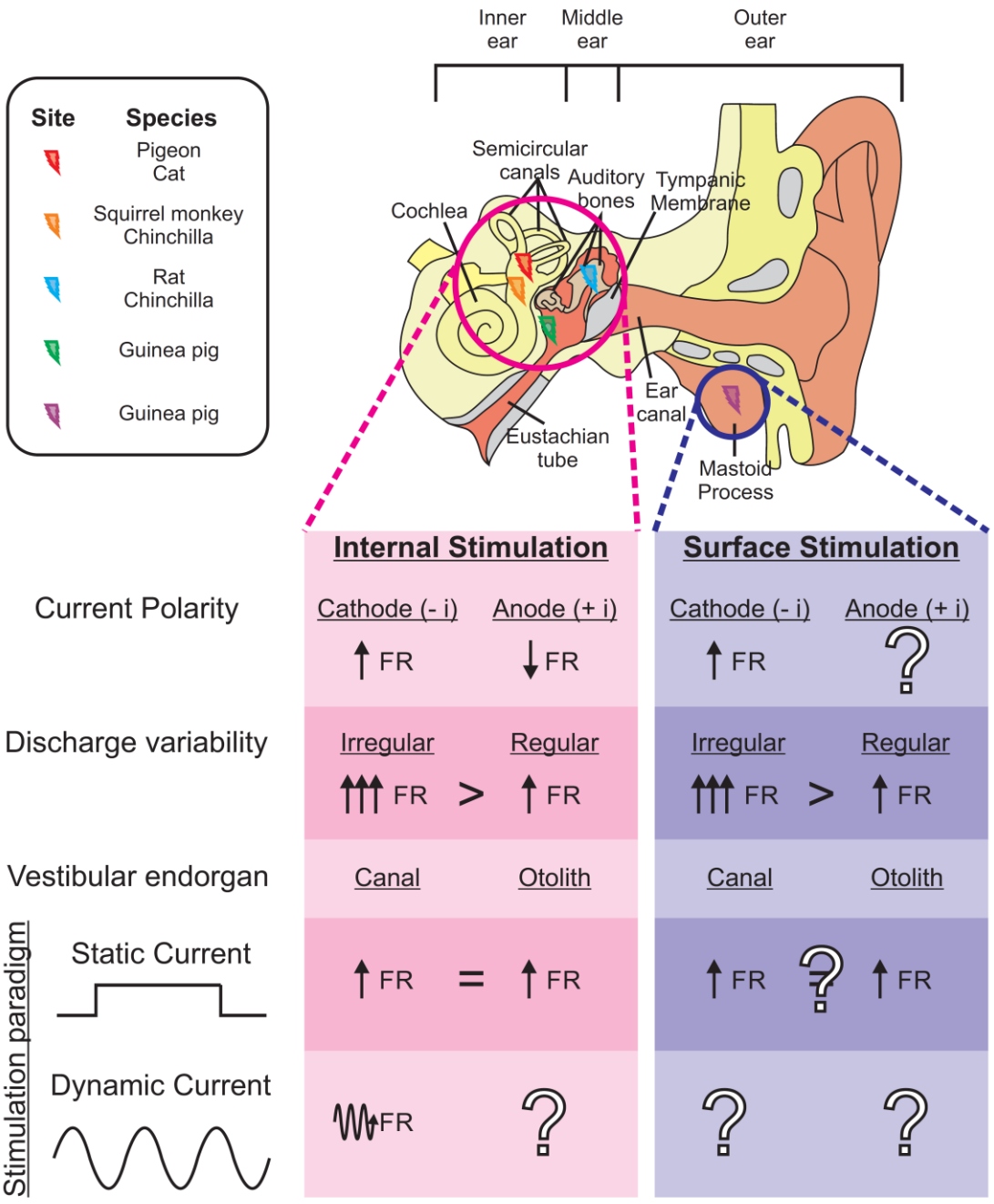


**Figure 1.5: Literature overview of the effects of electrical stimulation of vestibular afferents**
The top diagram shows the stimulating electrode sites and species from previous animal studies that have recorded vestibular afferents in response to electrical current stimulation. The bottom schematic what is currently known in terms of current polarity (cathode versus anode), discharge variability of afferents (irregular versus regular), and responses to static and dynamic current stimulation of afferents innervating different vestibular endorgans (canal versus otolith). Straight arrows indicate an increase or decrease in firing rate. Wavy arrow (bottom) indicates modulation of firing rate following the dynamic current waveform.

First, based on the results of prior animal studies using internally implanted electrodes, there are three widely accepted conclusions concerning vestibular afferent responses to electrical current stimulation (Fig. 1.5, pink box). (1) it has been consistently shown that cathodal current causes an increase in the firing rate of vestibular afferents while an anodal current elicits a decrease in firing rate (Goldberg *et al.*, 1984; Kim & Curthoys, 2004). (2) There are many reports that irregular afferents are more sensitive to electrical stimulation compared to regular afferents, which as reviewed above is one functional difference between the two types of afferents. Furthermore, several groups have demonstrated that the normalized galvanic sensitivity of afferent responses to constant current stimulation had a strong positive correlation with CV*, following a power law (Goldberg *et al.*, 1984; Baird *et al.*, 1988; Kim & Curthoys, 2004). (3) Constant current stimulation evokes responses from both canal and otolith afferents as they share similar relationships between normalized galvanic sensitivity and CV* (Goldberg *et al.*, 1984; Kim & Curthoys, 2004). Although it is often assumed that human vestibular afferents demonstrate these three characteristic responses during GVS (Fitzpatrick & Day, 2004), there remains the limitation in associating internal electrical stimulation in animal to surface transmastoid stimulation in humans. Hence, the first goal of this thesis is to investigate whether these response characteristics of vestibular afferents hold true during electrical stimulation delivered on the surface. To test this, I recorded the activity of canal and otolith afferents during constant current transmastoid stimulation, a paradigm typically conducted in humans.

Second, to date, the dynamic responses of vestibular afferents to electrical stimulation have not been well described. Our understanding of the dynamic responses of vestibular afferents to electrical stimulation is limited to a few animal studies, which have delivered sinusoidal modulated electrical stimulation at the level of the inner ear, focused only on semicircular canal afferents

(Goldberg & Smith, 1982; Ezure *et al.*, 1983; Kim *et al.*, 2011). While these studies demonstrated that canal afferents modulate their firing rate to the sinusoidal electrical current, from which the frequency responses were found to be markedly less than the frequency response to natural vestibular stimulation (Goldberg *et al.*, 1982; Kim *et al.*, 2006), it remains unknown whether otolith afferents share the same response dynamic as canal afferents. Hence, the second goal of this thesis is to characterize the frequency response to electrical stimulation of both otolith and canal afferent over the physiological relevant frequency range (0-25 Hz) and to determine whether they display similar gain and phase lead as a function of frequency. Accordingly, since our stimulation setup is analogous to those used to apply GVS in humans, the findings presented in this thesis provide a better representation of the dynamic effects of GVS in humans.

In addition, as reviewed above, vestibular afferents encode physiological stimulation (i.e. motion of low intensity) in a linear regime, which has been modelled with established transfer functions. This raises the question whether we can build linear models to predict afferent responses to GVS. In this context, prior animal studies present conflicting results regarding the linearity of vestibular afferent responses to electrical stimulation. On the one hand, Goldberg et al. (1984) found a largely linear relationship between changes in afferents' firing rate and constant current amplitude (-70 to +70 μA). On the other hand, Kim and Curthoys (2004) observed that although normalized galvanic sensitivities also linearly correlated with cathodal current amplitudes, irregular afferents in particular had an asymmetrical response to currents of opposing polarity: The magnitude of increase in firing rate to cathodal current was greater than the magnitude of the decrease in responses to anodal current. While the former study suggests that linearity in afferent responses is continuous between the cathodal and anodal current, the latter study proposes that afferents have different linear regimes to currents of opposing polarity. Thus, in my thesis, I will

also explore whether vestibular afferents respond linearly to GVS by means of linear system identification previously used to assess linearity of vestibular afferents to motion (Sadeghi *et al.*, 2007a; Jamali *et al.*, 2013). Furthermore, I address whether there is polarity-induced asymmetry in vestibular afferent responses.

Notably, the mechanism mediating the artificial activation of early vestibular processing by electrical stimulation, including GVS, remains a controversial topic. From one point of view, it is thought that electrical stimulation bypasses both the vestibular endorgans and the hair cells to stimulate directly on the trigger site of vestibular afferents. Goldberg *et al*. (1984) found that cathodal current delivered either in the perilymphatic space or the endolymphatic space (which has a positive electrical potential, opposite to the perilymph) of the vestibule evoked an increase in vestibular afferent responses. Since an increase in afferent firing rate is independent of the site of stimulation, they argued that hair cells were not involved in mediating vestibular afferent responses to electrical stimulation. Alternatively, results from a recent GVS human study suggests that electrical current modulates directly the transmembrane potential in vestibular hair cells on the basis that GVS-evoked ocular reflex was reduced in patients with damaged and loss of hair cells due to gentamicin vestibulotoxicity, compared to normal subjects (Aw *et al.*, 2008). While this thesis does not address the issue in the site of activation in the peripheral vestibular system, recognizing that there are different potential sites is necessary to fully understand the vestibular afferent responses to electrical stimulation of any form, particularly GVS.

## C. Modelling the GVS-evoked behavioural responses in humans

It is widely accepted that GVS activates the human vestibular system. As discussed previously, GVS evokes three main categories of vestibular-related behavioural responses: Eye movements, postural responses, and virtual motion perception. To better understand the mechanism mediating GVS-evoked behavioural responses, Fitzpatrick and Day (2004) first developed a model of GVS activation of the peripheral vestibular system under the assumptions largely based on electrical stimulation studies in animals reviewed above: (1) Cathodal and anodal current GVS elicit equal increase and decrease, respectively, in the firing rate of vestibular afferents. (2) GVS activates non-selectively all vestibular afferents (canal and otoliths). (3) With previously described anatomical organizations of the organizations of the semicircular canals (Blanks *et al.*, 1975) and otolith organs (Tribukait & Rosenhall, 2001; Tribukait *et al.*, 2005), the motion encoded by each canal and otolith afferents are equally summed together, resulting in a net vector of virtual head rotation and translation. (4) The resulting virtual rotational and translational vectors evoked by GVS are interpreted as head perturbations by the brain, which in turn would generate the compensatory vestibular-related reflexes. According to these assumptions, different net virtual motion vectors – and consequently, different behavioral responses – are expected under different GVS setups (see Fig. 1.6; semicircular canal model: (Fitzpatrick & Day, 2004); otolith model: Supplementary materials in (Mian *et al.*, 2010)). Thus, the observed patterns in GVS-evoked behavioural responses in humans – in particular, the direction of the evoked responses – have been compared with the model prediction as a means of validating the neurophysiological assumptions in the model.

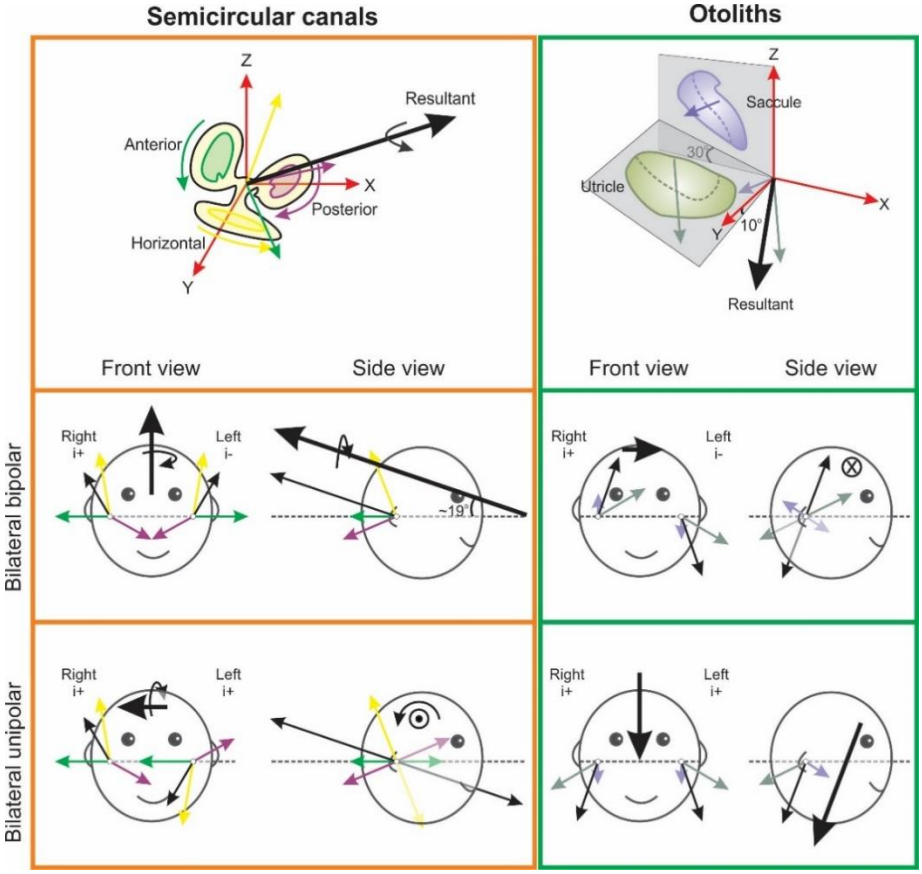


**Figure 1.6: Model of GVS activation of the peripheral vestibular system**
Orange boxes: Vector summation of semicircular canals responses to GVS. (Top) The resultant rotation vector for the sum of the rotation vectors for the horizontal (yellow), anterior (green) and posterior (purple) canals in the left labyrinth in response to cathodal current. (Middle) Bilateral bipolar stimulation (cathode on the left and anode on the right) would result in a net rotation vector that is tilted ~19 degrees above the Reid's line (dashed line in side view), where rotation is towards the cathode stimulation side. (Bottom) Bilateral unipolar stimulation (anode on both sides) would result in a net rotation vector aimed at the right ear, which equals to a pitch rotation toward the back of the head (bottom two panels adapted from Fitzpatrick & Day, 2004). Cathode stimulation on both side would result in a pitch rotation toward the front of the head. Green boxes: Vector summation of otoliths responses to GVS. (Top) The resultant translation vector for the sum of the translation vectors for the utricle (light green) and saccule (light purple) in the left labyrinth in response to cathodal current (adapted from supplementary materials in Mian *et al*., 2010). (Middle) Bilateral bipolar stimulation (cathode on the left and anode on the right) would result in a net translation vector toward the left ear (or a tilt vector toward the right ear). (Bottom) Bilateral unipolar stimulation (anode on both sides) would result in a net translation vector toward the back and the ground. Cathodal stimulation on both sides would result in a net translation vector of the opposite direction. Note here that the amplitude and direction of translation vectors in bottom two panels are not accurate. They are rough sketches based on supplementary materials in (Mian *et al.*, 2010).

There is evidence in favour of this model and its assumptions (Fitzpatrick & Day, 2004). Under the commonly used bilateral bipolar GVS, it is predicted the equal activation (cathodal side) and inhibition (anodal side) of all semicircular canal afferents would result in a virtual rotation toward the cathodal stimulation side whose axis would be tilted upward by about 19 degrees above the Reid's line (Fitzpatrick & Day, 2004). When subjects pitched their head down by about 71 degrees such that the virtual axis of rotation is aligned with the earth vertical axis, a perception of whole-body yaw rotation toward the cathode stimulation side is expected and has been confirmed experimentally in multiple studies (Fitzpatrick *et al.*, 2002; Day & Fitzpatrick, 2005; St George *et al.*, 2011; Peters *et al.*, 2015). This model also predicts that during head upright position, the virtual rotation towards the cathode stimulation side is compensated by evoked-reflexes that are directed toward the anode. This agrees with the observed behavioural responses: Induced postural sway (Inglis *et al.*, 1995b; Day *et al.*, 1997a; Day & Cole, 2002; Wardman *et al.*, 2003a) and compensatory eye movements ((Zink *et al.*, 1997; Watson *et al.*, 1998; MacDougall *et al.*, 2003) were consistently found to be directed toward the anode stimulation side.

Although the evidence presented above suggests that the model correctly assumes the physiological mechanisms mediating GVS-evoked responses, there remain shortcomings in the model and its assumptions based on other behavioural and neurophysiological studies. First, the semicircular canal model under unipolar bilateral GVS fails to predict the correct direction of the anteroposterior sway (Cauquil *et al.*, 2000; Day *et al.*, 2010). It was suggested that this discrepancy could be resolved if the model assumes instead that afferents of the three canals are activated with different sensitivity (Day *et al.*, 2011). Second, while it is presumed that both canal and otolith afferents are activated equally, the expected translational vector from the otolith afferents under different GVS setups repeatedly fails to predict the direction of the observed evoked reflexes

(Fitzpatrick & Day, 2004; Mian *et al.*, 2010). This raises the issue whether GVS equally activates the semicircular canal and otolith pathways (Mian *et al.*, 2010; Day *et al.*, 2011). Notably, it remains an ongoing debate whether GVS-evoked vestibular reflexes are the outputs of the semicircular canals, or otolith pathways, or a combination of both? (Cohen *et al.*, 2011; 2012; Curthoys & MacDougall, 2012; Reynolds & Osler, 2012). Third, the assumption that cathodal and anodal current have equal but opposite effects on vestibular afferents does not agree with the prior animal study that have shown there is an asymmetrical change in the firing rate of vestibular afferent to cathodal and anodal current (Kim & Curthoys, 2004). Finally, as discussed previously, there are limitations in predicting the effects of GVS on human vestibular afferents using neurophysiological results in animals receiving internal electrical stimulation.

Taken together, there are uncertainties in the three assumptions of the GVS model proposed by Fitzpatrick and Day (2004). Since the experimental setup presented in this thesis is analogous to that used in human studies, our findings provide a more accurate depiction of how GVS would activate the vestibular afferents. Accordingly, by characterizing the responses of all vestibular afferents (canal versus otolith and irregular versus regular) to different stimulation protocols (e.g. GVS steps of opposing polarity), I address the validity of two current assumptions used to model the GVS activation of the peripheral system: (1) Is there equal activation among all vestibular afferents, and (2) are there equal magnitude changes in firing rate to currents of opposing polarity?

### D. Current and potential applications of GVS

There is a growing number in research on GVS in various fields, from the basic science of understanding the function of the vestibular system to GVS as a potential entertainment device. In

this section I provide an overview of a few current and potential applications of GVS, as well as the importance of neurophysiological recordings in advancing GVS technology.

First, GVS is presently a common tool to study the function of the vestibular system because it has the advantage of activating solely the vestibular system, unlike natural vestibular stimulation requiring head motion in space and most likely activating other sensory channels such as somatosensory and proprioception. Another advantage of GVS over natural vestibular stimulation is that sinusoidal and stochastic GVS can cover a wider range of frequencies, exceeding the capability of any motor normally used to generate motion. Accordingly, recent studies have applied dynamic GVS in order to understand the frequency responses of vestibular reflexes responsible for postural control (Forbes *et al.,* 2015). For instance, the typical GVS-evoked electromyogram responses consisting of short and medium latency responses were shown to cover different frequency ranges (Dakin *et al.,* 2007). Furthermore, GVS-evoked reflexes in appendicular and axial muscles are found to be responsive to stimulation of low (up to 25 Hz) and high (up to 70 Hz) frequency ranges, respectively (reviewed in Forbes *et al*., 2015). However, the frequency response of vestibular afferents to transmastoid stimulation remains unknown, leading to inaccurate computational models of the dynamics of GVS activation of the vestibular system (Forbes *et al.,* 2013; Héroux *et al.,* 2015). Hence, as mentioned above, one focus of this thesis is to characterize the response dynamics of vestibular afferents to GVS with the goal in developing a correct model of GVS-to-afferent system.

Second, there is increasing interest in using stochastic GVS for other clinical and biomedical applications. Recently, it was found that the magnitude of destabilization in postural sway (but not eye movements) evoked by stochastic GVS can be reduced after multiple presentations of the artificial stimulation, suggesting that GVS can induce central vestibular

adaptation (Dilda *et al.*, 2014b). Therefore, it is thought that central vestibular adaption to repeated stimulation of stochastic GVS on astronauts prior to flight (Moore *et al.*, 2011; Dilda *et al.*, 2014b; Moore *et al.*, 2015) or pre-habilitating patients prior to vestibular lesion (Magnusson *et al.*, 2011) would reduce the destabilizing effects of a new disorienting environment or perturbations in the vestibular system, respectively. While GVS is often known to disturb our balance, as in the case above, it may be possible to improve postural and locomotor stability using stochastic GVS of sub-threshold level (i.e. low current amplitude), which was demonstrated both in balance-deficient patients and normal subjects (Mulavara *et al.*, 2011; Iwasaki *et al.*, 2014; Goel *et al.*, 2015; Kataoka *et al.*, 2015; Mulavara *et al.*, 2015; Samoudi *et al.*, 2015; Wuehr *et al.*, 2016). It is believed that improvement to balance is due to stochastic resonance, a phenomenon where the presence of the low non-zero noise (GVS) in a nonlinear system enhances the detection of a normally undetectable signal (vestibular input). Despite the growing number in human studies investigating these two different applications of stochastic GVS, there is an absence of physiological evidence. Do central vestibular neurons, but not vestibular afferents, adapt to repeated presentation of stochastic GVS? And is there stochastic resonance at the level of vestibular afferents if presented with low levels of stochastic GVS and weak physiological vestibular stimulation (i.e. motion)? While I do not address these questions directly, they motivate future works (discussed in Chapter 4) using the experimental setup described in this thesis.

Finally, in addition to the clinical applications, GVS may potentially be used as a navigation tool (Maeda *et al.*, 2005a; Fitzpatrick *et al.*, 2006). Based on the GVS model for semicircular canals described above, when the head is pitched downward such that the net virtual rotation would occur in the yaw plane, it was shown that GVS can cause deviation to the walking path (Fitzpatrick *et al.*, 2006). This demonstrates the possibility of applying GVS in navigation,

where a walking individual is steered to the correct direction with the appropriate current stimulus. Besides navigation, illusory perception of motion evoked by GVS may help to improve virtual reality simulations, either for training or entertainment purposes (Maeda *et al.*, 2005b; Reed-Jones *et al.*, 2007; Cevette *et al.*, 2012). In particular, to reduce the sickness during simulation, such as dizziness and disorientation due to mismatch between visual and vestibular signals during simulations, it was suggested that GVS can evoke the matching vestibular responses (Cevette *et al.*, 2012). However, as discussed in the section above, there are uncertainties in current models of predicting GVS-evoked virtual motion. Furthermore, the latter application requires an understanding of how GVS activates the vestibular system relative to physiological vestibular stimulation (i.e. motion). Accordingly, in addition to characterizing the vestibular afferent responses to GVS, I also compare these effects to those induced by motion. While the findings presented in this thesis will provide new insights necessary in establishing a more physiological model of GVS-activation of the vestibular periphery, it is important to note that more neurophysiological work in central vestibular processing areas is needed to fully understand how GVS activates of the vestibular system.

## IV. Thesis goals summary

The overarching objective of my thesis is to characterize the vestibular afferent responses under transmastoid GVS, a stimulation setup used in humans. My results have important implications not only in furthering our basic understanding of the human vestibular system during transmastoid GVS but also in advancing GVS as a tool for numerous applications. The first aim of this thesis is to validate the nonhuman primate model for the effects of GVS in humans by comparing GVS-evoked eye movements in nonhuman primates to those previously reported in

humans. I provide evidence that the effects of GVS on nonhuman primates' behaviour are similar to humans. This important finding allows us to justify our assumption that vestibular afferent responses recorded under transmastoid stimulation in nonhuman primates would be similar to those of the human vestibular system (Chapter 2 and 3). The second aim of this thesis is to characterize both semicircular canal and otolith afferents, consisting of both regularly and irregularly discharging afferents under the application of dynamic (Chapter 2) and static (Chapter 3) currents to determine whether the effects of transmastoid GVS differ between the innervating endorgans and/or discharge variability of the vestibular afferents. I present findings that the response dynamics of canal and otolith afferents are comparable but these responses depend on the type of afferents (i.e. regular versus irregular). In meeting the second aim, this thesis also provides the dynamics of vestibular afferents to GVS necessary in future models of GVS-evoked vestibular reflexes, as well as the neurophysiological evidence to resolve the controversy of the vestibular origins mediated GVS-evoked behavioural responses. The third aim of this thesis is to compare vestibular afferent responses to physiological (i.e. rotational and translational motion) versus artificial (i.e. GVS) stimuli (Chapter 2). This information is important in developing GVS techniques as an alternative to natural vestibular stimulation. The final aim of this thesis is then to determine whether there are nonlinearities in vestibular afferent responses to GVS (Chapter 3). Altogether, the findings of this thesis provides new insights in how the transmastoid GVS is encoded by vestibular afferents, which yields necessary information in developing accurate models of the vestibular pathways and improving the clinical and biomedical application of GVS.

# Chapter 2: Dynamics of vestibular afferents to transmastoid galvanic vestibular stimulation

## I. Introduction

As we move around in the world, the vestibular system in the inner ear detects head motion in space providing the brain with vital information needed for our sense of balance. Investigating the vestibular system in isolation is complicated however because natural vestibular stimuli (i.e. motion) often activate other sensory inputs (i.e. tactile and proprioception). In this context, galvanic vestibular stimulation (GVS), which is current applied on surface electrodes on the mastoid processes behind the ears (Fitzpatrick & Day, 2004), has become an increasingly popular strategy to selectively activate the vestibular system. This non-invasive tool evokes vestibular reflex pathways evoking both ocular (Watson *et al.*, 1998; Zink *et al.*, 1998; MacDougall *et al.*, 2005) and postural (Nashner & Wolfson, 1974; Lund & Broberg, 1983; Day *et al.*, 1997a) responses, and can produce a sensation of self-motion (Wardman *et al.*, 2003b; St George *et al.*, 2011; Hammam *et al.*, 2012).

Numerous human GVS studies have attempted to deduce the physiology underlying the induced behavioural responses and addressed whether GVS-evoked vestibular reflexes are predominately driven by the activation of the semicircular canals or otoliths, or a combination of both. One view is that GVS predominantly activates the otolith system (Cohen *et al.*, 2011; 2012) because it evokes behaviours including tonic ocular torsion (Watson *et al.*, 1998; Zink *et al.*, 1998; MacDougall *et al.*, 2005) and static postural sway (Lund & Broberg, 1983; Inglis *et al.*, 1995b; Day *et al.*, 1997a), which are attributed to the activation of otolith afferents. On the other hand, reports of subjects sensing rotation during GVS (reviewed in Reynolds & Osler, 2012) and results

suggesting that canal afferents play a role in GVS-evoked ocular torsion (Schneider *et al.*, 2000; 2002) support the view that GVS stimulates preferentially canal system. Finally, there is accumulating evidence that GVS activates both the semicircular canal and otolith afferents. For example, constant current GVS produces horizontal and torsional nystagmus, as well as tonic ocular torsion (MacDougall *et al.*, 2002a; MacDougall *et al.*, 2003; MacDougall *et al.*, 2005), and also generates postural sway comprising of static and dynamic components (Wardman *et al.*, 2003a). Despite many efforts in interpreting these evoked behavioural responses, how vestibular afferents respond to GVS remains unknown.

In this study we sought a more direct approach to examine the effects of GVS on vestibular afferent activity. In human studies, the vestibular afferents are activated via transmastoid stimulation. Yet so far, studies aimed at understanding the influence of electrical stimulation on vestibular afferents in animal models delivered stimulation inside the ear such that current is applied in much closer proximity to the vestibular endorgans (Goldberg & Smith, 1982; Ezure *et al.*, 1983; Courjon *et al.*, 1987; Kim & Curthoys, 2004; Kim *et al.*, 2011). This has become a limitation for models that have made assumptions based on these prior animal studies to understand the physiological basis of GVS-evoked behaviours (Fitzpatrick & Day, 2004; Day *et al.*, 2011). Accordingly, we recorded directly from canal and otolith afferents while we delivered GVS to surface electrodes placed behind the ears of macaque monkeys in a bilateral bipolar configuration, a setup typically used in humans, and delivered single sinusoidal GVS. To validate this primate-based model, we recorded eye movements and established that responses were comparable to those evoked in humans. Then, we recorded from individual vestibular afferents and found similar changes in firing rates of both canal and otolith afferents. Importantly, both canal and otolith afferents displayed a noticeable increase in both gain and phase lead that were less

marked than for natural stimuli. These findings demonstrate that semicircular canal and otolith systems are equally activated by transmastoid GVS, with similarly high-pass tuning, and thereby providing for the first time knowledge of these dynamics required for understanding the representation and use of such information in the brain.

## II. Materials and Methods

Three male macaque monkeys (2 *Macaca fascicularis*, Monkey B and H, *and 1 M. mulatta*, Monkey D) were prepared for chronic extracellular recording using aseptic surgical techniques. All experimental protocols were approved by the McGill University Animal Care Committee and were in compliance with the guidelines of the Canadian Council on Animal Care.

### *Surgical procedures*

The surgical preparation for Monkey B and D followed the procedures described previously (Dale & Cullen, 2013). Under new protocol, Monkey H was administered loading doses of carprofen (4 mg/kg sq) and cefazolin (22 mg/kg iv), the latter of which was administered slowly and repeated every two hours for the duration of the surgery, to reduce swelling and prevent infection, respectively. In all three animals, aseptic surgical techniques were used. Under isofluorane anesthesia (0.8 – 1.5%), we secured a stainless steel post to the animal's skull with stainless steel screws and dental acrylic, permitting complete immobilization of the animal's head during the experiment, and implanted a chamber for chronic extracellular recording. Finally, an eye coil, consisting of three loops of Teflon-coated stainless steel wire, was implanted in the right eye behind the conjunctiva (Fuchs & Robinson, 1966). Post-surgery protocol for Monkeys B and D was described previously (Dale & Cullen, 2013). For Monkey H, carprofen (2 mg/kg)

administration was continued daily for 5 days. Buprenorphine (0.01-0.02 mg/kg im) was adminstered postoperative analgesia every 12 hours for 2-5 days, depending on the animal's pain level. In addition, cefazolin (22 mg/kg im) was injected twice within 24 hours after surgery. Animals were given at least 2 weeks to recuperate from the surgery before any experiments began.

*Data acquisition*

During the experiments, monkeys were head-restrained and seated comfortably in a primate chair mounted on top of a vestibular turntable. The left vestibular nerve was found as described (Jamali *et al.*, 2013). Extracellular single-unit activity of primary vestibular afferents (semicircular canal and otolith) was recorded using tungsten microelectrodes (7-10 MΩ and 20-25 MΩ, Frederick-Haer Co., Bowdoinham, ME) (Fig. 2.2A). Neural signals were band-pass filtered from 300 Hz to 3 kHz and sampled at 30 kHz. Head linear acceleration and angular velocity was measured by a three-dimensional linear accelerometer and a one-dimensional angular gyroscope (Watson Inc., Eau Claire, WI), respectively, both firmly secured to the animal's head post. Horizontal and vertical eye positions were measured using the magnetic search-coil technique (Fuchs & Robinson, 1966; Judge *et al.*, 1980). Head linear acceleration, head angular velocity and galvanic vestibular stimulation signals were low-pass filtered at 250 Hz (eight-pole Bessel filter) and sampled at 1 kHz. Neural, behavioural and stimulation data were collected through the Cerebus Neural Signal Processor (Blackrock Microsystems, Salt Lack City, UT). Neural data was imported into either Offline Sorter (Plexon, Dallas, TX) as previously described (Dale & Cullen, 2015) or into a custom-written algorithm in MATLAB (The MathWorks, Natick, MA) to extract action potentials.

Horizontal and vertical eye positions were also measured separately using a modified eye tracker (Chronos Vision, Berlin, Germany) fixed onto the monkey's head post. Offline analysis software Iris (Chronos Vision) was later used to calculate torsional eye position from markers applied near the limbus. Markers consisted of an infrared absorbing cosmetic pigment, Eisenoxid 316/Schwarz (Carl Jäger Tonindustriebedarf GmbH, Erlen, Germany), dissolved in distilled water and were applied near the limbus using a sterile surgical marking pen.

*Experimental design*

*Physiological vestibular stimulation*: Once a unit was isolated, the vestibular endorgan innervated by that fiber was determined based on the responses of the afferent to rotations or translation. To assess that semicircular canal afferents recorded in this study have similar sensitivity to previous studies, these afferents were stimulation with yaw sinusoidal rotation at frequencies 0.5, 1, 2, 4, 8, 10, 12, and 16 Hz with peak velocity of ~40 deg/s. Similarly, otolith afferents were stimulated with translation in the fore-aft ($90^o$) and lateral ($0^o$) axes at ~2 Hz. Because of limitations in our experimental setup, afferents that were predominantly sensitive to stimulation along the vertical axis were not included in our dataset.

*Galvanic vestibular stimulation*: Electrical vestibular stimulation was applied to animals using carbon rubber electrodes (~6 $cm^2$) in a binaural bipolar configuration. The electrodes were coated with Spectra 360 electrode gel (Parker Laboratories, Fairfield, NJ) and secured over the animal's mastoid processes with surgical tape. The stimuli were generated using MATLAB and were delivered as analog signals to a constant current isolation unit (STMISOLA; Biopac Systems Inc., USA) via a QNX-based real-time data acquisition system (Hays Jr *et al.*, 1982) or an arbitrary

waveform generator (Keysight Technologies, Santa Rosa, CA). The current polarity of the stimulation is referred to the polarity of the left stimulating electrode, which was on the same side of the vestibular afferents recorded. In the figures, cathodal and anodal currents are depicted as positive and negative values, respectively. For neural recordings, animals were exposed to a series of sinusoidal current (sinusoid GVS) of frequencies 0.1, 0.2, 0.5, 1, 2, 4, 8, 16, and 25 Hz with peak amplitude of 1 mA. For eye movement recordings, animals were placed in the dark with a target, to which the animal was trained to fixate. Stimulation included sinusoidal current of frequencies from 0.5 to 8 Hz with peak amplitude of 1 mA, and 2 Hz sinusoidal current of peak-to-peak amplitude of 0.5, 0.75, 1, 1.25, and 1.5 mA. Rightward horizontal, upward vertical, and clockwise torsional (i.e. toward the right ear) eye movements are expressed as positive values.

*Data analysis*

Data were imported into MATLAB for analysis using custom-written algorithms. Behavioural signals were digitally filtered at 125 Hz.

*Background discharge*: Afferents were classified based on the regularity of resting discharge, which is evaluated by the normalized coefficient of variation (CV*) as done previously (Goldberg *et al.*, 1984; Massot *et al.*, 2011). Afferents with CV* $\leq$ 0.1 were considered as regular, while those with CV* > 0.1 were considered as irregular (Sadeghi *et al.*, 2009). The afferents' resting discharge was calculated as well.

*Firing rate estimation*: The time-dependent firing rate FR(t) was estimated as follows. First, the spike train R(t) was set as the binary sequence of action potentials with bin width of 1 ms. Then,

R(t) was convolved with a Kaiser window whereby the cut-off frequency was set to 0.1 Hz above twice the sinusoidal stimulus frequency to obtain the estimated FR(t) (Cherif *et al.*, 2008).

*Response dynamic – Sinusoid GVS*: For each afferent, a least-squares regression analysis was used to determine its resting discharge (bias, spk/s), its sensitivity to sinusoidal GVS waveform, and its phase shift relative to sinusoidal GVS waveform, using ≥ 10 cycles of the stimulus. For each frequency of stimulation, the bias, sensitivity ($S_G$) and phase shift (θ) of each afferent in response to sinusoidal GVS were calculated by estimating the coefficients of the following model:

$$FR(t) = bias + S_G \times GVS(t + \theta) \qquad \text{[eq. 2.1]}$$

Linear time invariant model were estimated for the four categories of vestibular afferents from the population frequency responses to sinusoid GVS using the function tfest in Matlab. The best transfer function were chosen using the Akaike information criterion, which optimized goodness of fit and minimal number of parameters.

*Canal response dynamic – Rotation*: For each canal afferent, a least-squares regression analysis was used to determine its resting discharge (bias, spk/s), its sensitivity to head velocity, and its phase shift relative to head angular velocity. For each frequency of rotation, the bias, sensitivity (S) and phase shift (θ) of each afferent in response to sinusoidal head angular velocity Ḣ were calculated by estimating the coefficients of the following model:

$$FR(t) = bias + S \times \dot{H}(t + \theta) \qquad \text{[eq. 2.2]}$$

To correct the gain for the preferred rotation plane for horizontal, anterior and posterior canals, the angular yaw velocity was projected onto the semicircular canal planes as done previously (Carriot

*et al.*, 2014). For each semicircular canal afferent, the decomposed angular velocity of the appropriate plane was then used to estimate the corrected gain.

*Spatial tuning of otolith afferents*: For each otolith afferent, a least-squares regression analysis was used to determine its resting discharge (bias, spk/s), its sensitivity to head acceleration, and its phase shift relative to head linear acceleration. For direction of translational motion (foreaft and lateral) the bias, sensitivity (S) and phase shift (θ) of each afferent in response to sinusoidal head linear acceleration Ḧ were calculated by estimating the coefficients of the following model

$$\mathrm{FR}(t) = \mathrm{bias} + S \times \ddot{H}(t + \theta) \qquad \text{[eq. 2.3]}$$

The maximum sensitivity and preferred direction was estimated using a cosine fit (Angelaki & Dickman, 2000; Purcell *et al.*, 2003; Jamali *et al.*, 2009).

*Comparison of sensitivity to GVS and motion*: In order to compare the sensitivity of vestibular afferents to two different stimuli, the gain was normalized by dividing the values with the gain at 0.5 Hz. Additionally, this allows us to pool all semicircular canal afferents together, as normalization compensates for the difference in preferred axis of rotation.

*Eye movement*: Segments of eye velocity trace (horizontal, vertical and torsional) without saccades were first chosen over at least three cycles of the sinusoidal stimulation. Similar to afferent responses, a least-squares regression analysis was then used to determine the sensitivity and phase shift of the eye velocity relative to sinusoidal GVS waveform using the chosen segments. Torsional eye velocity gain to sinusoidal stimulation of different frequencies and amplitude of torsional eye

velocity to sinusoidal stimulation of different current amplitudes were normalized at the values of 0.5 Hz and 0.5 mA, respectively. The values reported were averaged across five trials.

*Statistical analysis*: Statistical analysis was performed in SPSS (IBM, Armonk, NY) and Excel (Microsoft, Redmond, WA). Statistical significance was set at $p < 0.05$. To analyze the eye movements in response to sinusoidal GVS, a two-way mixed ANOVA with the Greenhouse-Geisser correction was conducted. Animal was the between factor whereas frequency stimulation or current amplitude was the within factor. To analyze the relationship of the gain and phase of vestibular afferent responses to sinusoidal GVS as a function of CV*, linear regressions were conducted. To account for multiple comparisons, a Bonferroni's correction was applied.

*Reporting data*: In terms of the data of vestibular afferent responses to sinusoidal stimulation across frequency, the number of samples are expressed as (min, max), where min and max represents the lowest and higher number of afferents across the frequencies tested. All values are expressed as mean ± SEM.

## III. Results

GVS in humans evokes vestibular-related behavioural responses such as reflexive eye movements. To characterize the effects of GVS on primary vestibular afferents and to determine neural correlates mediating GVS-evoked behaviours, we recorded eye movements and neuronal activity of vestibular afferents during GVS in awake behaving monkeys. The neuronal data set consists of a total of 203 afferents, whose resting discharge and innervated endorgans were characterized prior to GVS. N = 119 were classified as semicircular canal afferents among which

N = 63 were considered regular (mean CV* = 0.06±0.00) and N = 56 were considered irregular (mean CV* = 0.35±0.02). The mean resting discharge rates were 111.24±3.07 spk/s for the regular canal afferents and 96.26±4.40 spk/s for the irregular canal afferents. The remaining N = 84 afferents were classified as otolith afferents, among which N = 30 were considered regular (mean CV* = 0.05±0.00) and N = 54 were considered irregular (mean CV* = 0.38±0.02). The mean resting discharge rates were 79.30±5.22 spk/s for the regular otolith afferents and 62.14±4.20 spk/s for the irregular otolith afferents. The dataset was categorized into the four groups described above for subsequent characterization of afferent responses.

**Sinusoidal eye movements to sinusoidal GVS**

To determine whether transmastoid GVS on nonhuman primate is a useful model for the GVS activation of the human vestibular system, we first assessed whether transmastoid GVS in nonhuman primates evokes comparable eye movements with those reported in humans. Prior human GVS studies have shown that while human subjects fixated at a target, sinusoidal GVS evoked sinusoidal modulated torsional eye movements. Hence, under similar experimental setup, we recorded eye movements in the dark with a fixation target during sinusoidal modulated GVS (Fig. 2.1A). In the presence of 2 Hz single sinusoidal stimulation, we observed eye velocity predominantly in the torsional plane (Fig. 2.1B). First, we characterized the torsional eye velocity as a function of stimulation frequency while keeping the current amplitude at 1 mA. We found that the normalized gain of the torsional eye velocity remained relatively constant across frequencies (two-way mixed ANOVA, $F(2.89, 34.6) = 1.16$, $p > 0.05$) while phase decreased as a function of frequency (two-way mixed ANOVA, $F(1.92, 23.04) = 91.74$, $p < 0.001$), consistently lagging behind the stimulation (Fig. 2.1C).

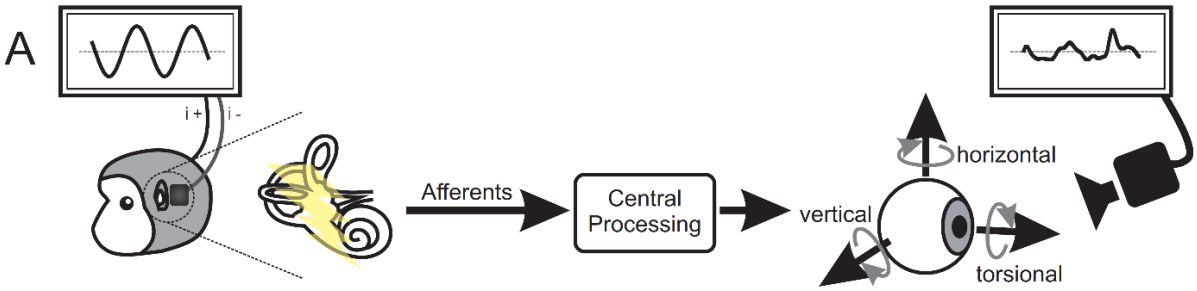
A
i +
i -
Afferents
Central Processing
horizontal
vertical
torsional

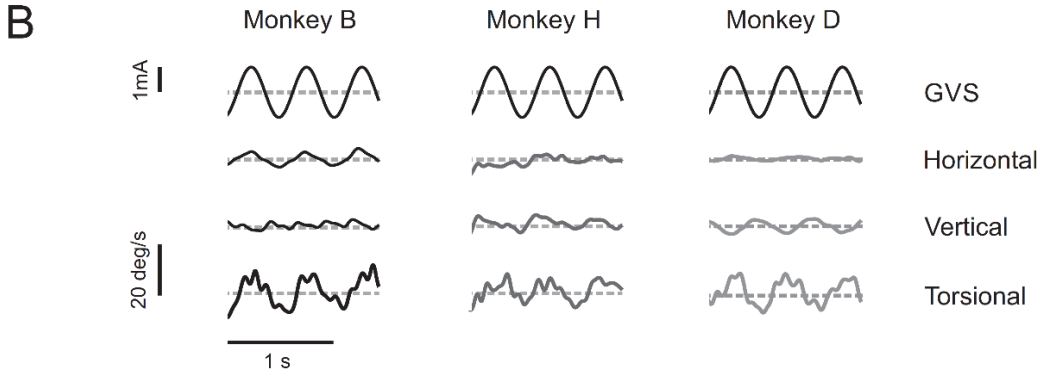
B
Monkey B
Monkey H
Monkey D
1mA
GVS
Horizontal
Vertical
20 deg/s
Torsional
1 s

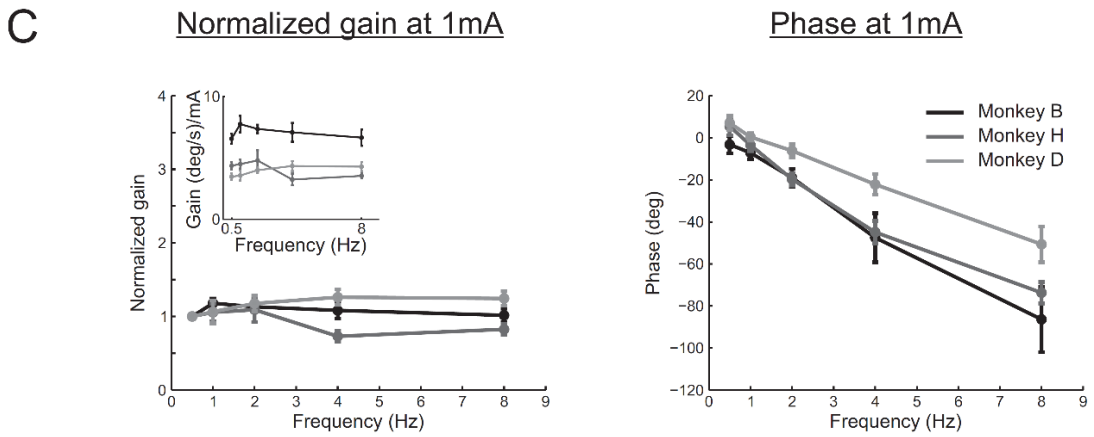
C
Normalized gain at 1mA
Phase at 1mA
Normalized gain
Gain (deg/s)/mA
Frequency (Hz)
Phase (deg)
Monkey B
Monkey H
Monkey D

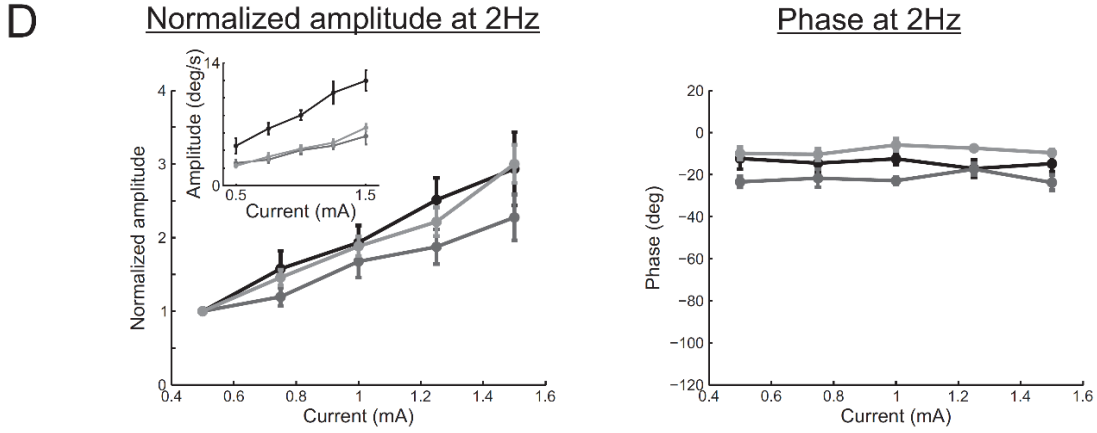
D
Normalized amplitude at 2Hz
Phase at 2Hz
Normalized amplitude
Amplitude (deg/s)
Current (mA)
Phase (deg)

**Figure 2.1.** Torsional eye movements in response to sinusoidal GVS. (A) While we applied sinusoidal GVS between surface electrodes placed on the mastoid processes behind the ears, we recorded the animal's eye movements while it is fixating. (B) Example traces of horizontal, vertical and torsional velocity for three animals to a 2 Hz sinusoidal stimulation of 1 mA in current amplitude. Note that the primary eye component is in the torsional plane because the animals were fixating on a target. (C) Population averaged of the normalized gain and phase of the torsional eye velocity for each of the animal across five trials to sinusoidal stimulation that varied in frequency. The gain was normalized based on the responses at 0.5 Hz. The inset shows the population gain prior to normalization. (D) Population averaged of the normalized magnitude and phase of the torsional eye velocity for each of the animal across five trials to sinusoidal stimulation that varied in current amplitude. The magnitude was normalized based on the responses at 0.5 mA. The inset shows the population gain prior to normalization.

Second, we measured torsional eye velocity during 2 Hz sinusoidal GVS at varying current amplitude. Across the current amplitude (Fig. 2.1D), the normalized magnitude of torsional velocity increased (two-way mixed ANOVA, $F(2.09, 25.07) = 44.308$, $p < 0.001$), while the phase remained constant (two-way mixed ANOVA, $F(3.26, 39.08) = 0.59$, $p > 0.05$) which agrees with human behavioural data (Kleine *et al.*, 1999). Note here that Monkey B had greater evoked eye movements compared to Monkey H (and Monkey D), shown in the insets in Fig. 2.1C and D. Interestingly, as will be discussed below, the difference in magnitude of torsional eye movements between the two animals agreed with the difference in sensitivities of their vestibular afferent responses, where vestibular afferents in Monkey B had a greater sensitivity than those recorded in Monkey H (Fig. S2.1).

**Vestibular afferents respond to sinusoidal GVS**

We next characterized the effects of sinusoidal GVS on the vestibular afferent activity (Fig. 2.2A) to establish any difference in vestibular afferent responses that may dependent on their discharge regularity and/or the innervated endorgans. First, we stimulated semicircular canal afferents with sinusoidal GVS of a broad range of physiologically relevant frequencies (0.1-25 Hz)

of the vestibular system. The responses of the example regular and irregular canal afferents both innervating the posterior semicircular canal during single sinusoidal current of 1 Hz and 4 Hz are shown in Fig. 2.2B. The example canal afferents had firing rates that modulate with the sinusoidal stimulation, with the irregular canal afferent showing a greater modulation compared to regular canal afferent (1 Hz: 25.9 vs 6.2 spk/s/mA; 4 Hz: 28.4 vs 6.7 spk/s/mA). This difference in modulation amplitude between the two types of canal afferents was consistent across our dataset. On average, irregular canal afferents (N = 27-56) displayed a higher gain as a function of frequency than regular canal afferents (N = 28-63, Fig. 2.2D). Furthermore, both regular and irregular canal afferents showed on average similar phase lead increase as a function of frequency. Canal afferents were nearly in-phase with the GVS waveform at low frequencies, and they gradually increased its phase lead to over 40 degrees at 25 Hz. This finding implies that sinusoidal current delivered on the mastoid processes evokes frequency-dependent responses in canal afferents. Furthermore, the frequency response of canal afferents to transmastoid stimulation presented here contrasts previously characterized dynamics of canal afferents to sinusoidal current delivered directly inside the ear (Goldberg *et al.*, 1982; Baird *et al.*, 1988; Kim *et al.*, 2011), which suggests that there are different effects of electrical stimulation delivered inside the ear versus on the surface of the ear.

We next addressed the question whether otolith afferents are also stimulated by sinusoidal GVS and how their responses compared to that of canal afferents. The responses of the example regular and irregular otolith afferents during single sinusoidal current of 1 Hz and 4 Hz are shown in Fig. 2.2C. Both these otolith afferents modulated their firing rates with electrical stimulation, with the irregular otolith afferent firing more spikes per second compared to regular otolith afferent (1 Hz: 16.1 vs 4.5 spk/s/mA; 4 Hz: 17.2 vs 5.2 spk/s/mA). This difference in modulation amplitude was also observed across our dataset. Irregular otolith afferent population (N = 18-54) responded

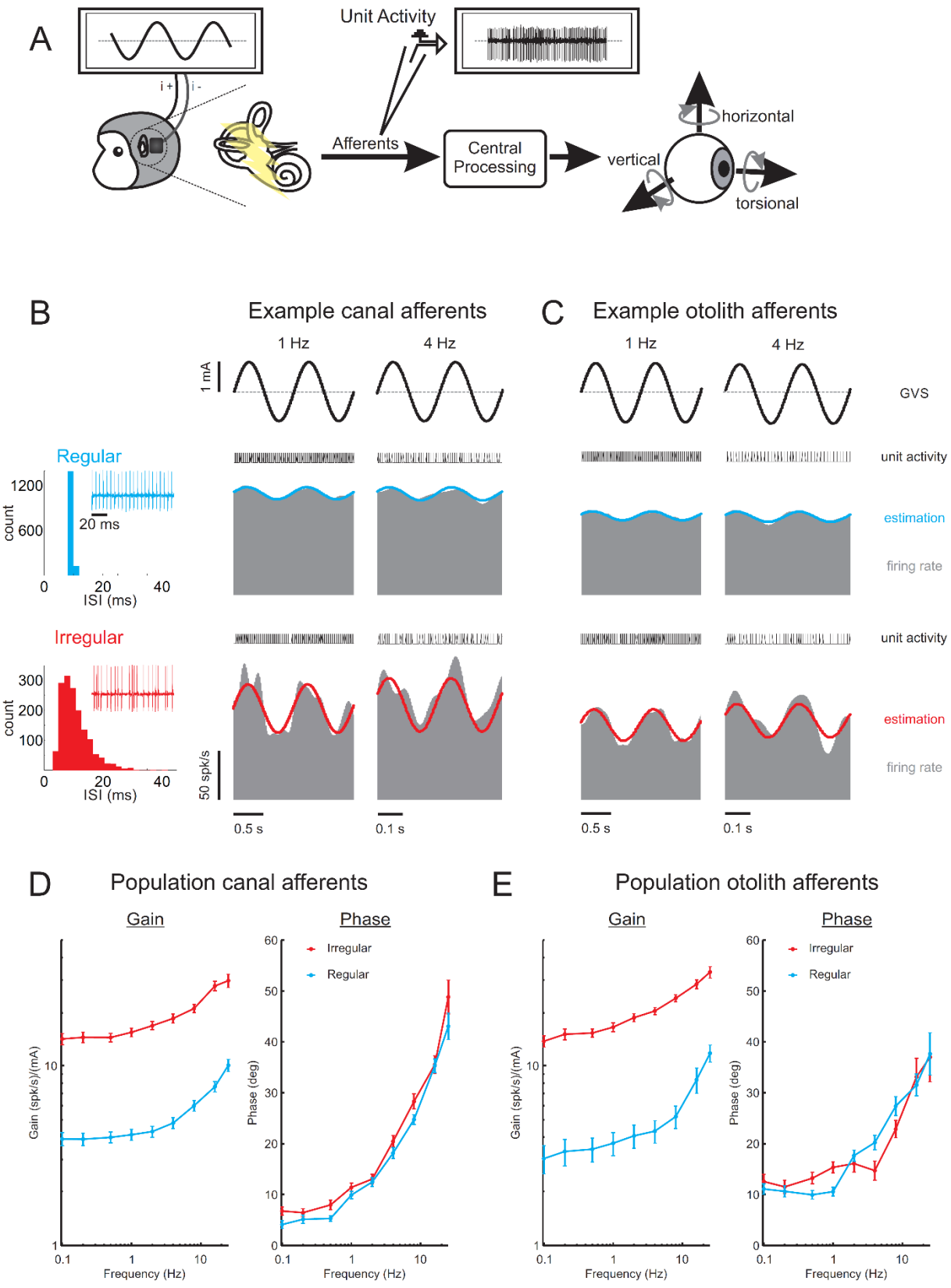
A
Unit Activity
i +
i -
Afferents
Central Processing
horizontal
vertical
torsional
B
Example canal afferents
C
Example otolith afferents
1 Hz
4 Hz
1 mA
GVS
Regular
1200
600
count
20 ms
0
20
40
ISI (ms)
unit activity
estimation
firing rate
Irregular
300
200
100
50 spk/s
0.5 s
0.1 s
D
Population canal afferents
E
Population otolith afferents
Gain
Phase
Irregular
Regular
Gain (spk/s)/(mA)
Phase (deg)
Frequency (Hz)
0.1
1
10
60
50
40
30
20

**Figure 2.2.** Response dynamics of vestibular afferents to sinusoidal GVS. (A) We recorded extracellular single-unit activity from vestibular afferents using tungsten electrodes during sinusoidal GVS. (B) Firing rate (gray) of example regular (blue) and irregular (red) canal afferents to 1 Hz (left) and 4 Hz (right) sinusoidal GVS. Firing rate estimates (solid blue and red line) are found using eq. 2.1. The right insets show the interspike interval (ISI) histogram for the resting discharge of the example canal afferents. Regular afferents have a narrow ISI distribution whereas irregular afferents have a broader ISI distribution. (C) Firing rate (gray) of example regular (blue) and irregular (red) otolith afferents to 1 Hz (left) and 4 Hz (right) sinusoidal GVS. (D) Population averaged gain (left) and phase (right) of regular (blue, N = 28-63) and irregular (red, N = 27-56) canal afferents. (E) Population averaged gain (left) and phase (right) of regular (blue, N = 11-30) and irregular (red, N = 18-54) otolith afferents.

with a higher gain as a function of frequency then regular otolith afferent population (N = 11-30, Fig. 2.2E). Furthermore, both groups had generally a similar phase lead to the GVS as a function of frequency. On average, regular and irregular otolith afferent populations, comparable to their canal counterparts, display a gradual increase in phase lead starting from being nearly in-phase with the GVS waveform at low frequencies to 40 degrees at 25 Hz.

A comparison of canal and otolith afferents' frequency responses to GVS suggests that both canal and otolith afferents are activated in a similar manner (compare Fig. 2.2C and D). To quantify this observation between canal and otolith afferents, we conducted linear regressions for gain and phase as a function of CV* separately at each individual frequency for both canal and otolith afferents, and compared their slopes. For example, Fig. 2.3. shows the plots of gain and phase versus CV* at 2 Hz for canal (open black circles) and otolith (filled gray circles) afferents. First, both canal and otolith afferents were separately found to exhibit an increase in gain as a function of CV*. The gains of canal and otolith afferents can be grouped together (i.e. linear regressions for canal and otoliths were not significantly different, $F(2,195) = 1.03$, $p > 0.0056$, Bonferroni's correction for comparisons at each frequency) and were found to be linearly correlated with CV* ($y = 37.55 x + 3.04$, $r = 0.84$). Second, both canal and otolith afferents had phase lead showing no linear relationship with CV*. Again, the phase leads of canal and otolith

afferents are not significantly different from one another ($F(2,195) = 1.27$, $p > 0.0056$, Bonferroni's correction for comparison at each frequency) and the phase leads of both afferent populations formed the following relationship with CV*: $y = 4.19 x + 13.41$, $r = 0.09$, whose slope was not significantly different from zero. The comparison between canal and otolith afferents for all frequencies are summarized in Table 2.1. Note that "Common ?" column in the table refers to whether the linear regressions of canal and otolith afferents separately were different. We found that at each frequency, that gains of all afferents were linearly correlated with the regularity of the vestibular afferents' resting discharge, whereas their phase leads were generally found to be constant over CV*. This suggests that the main difference among vestibular afferent responses to GVS is that irregular afferents (innervating both canals and otoliths) have a much higher sensitivity to the stimulation compared to regular afferents.

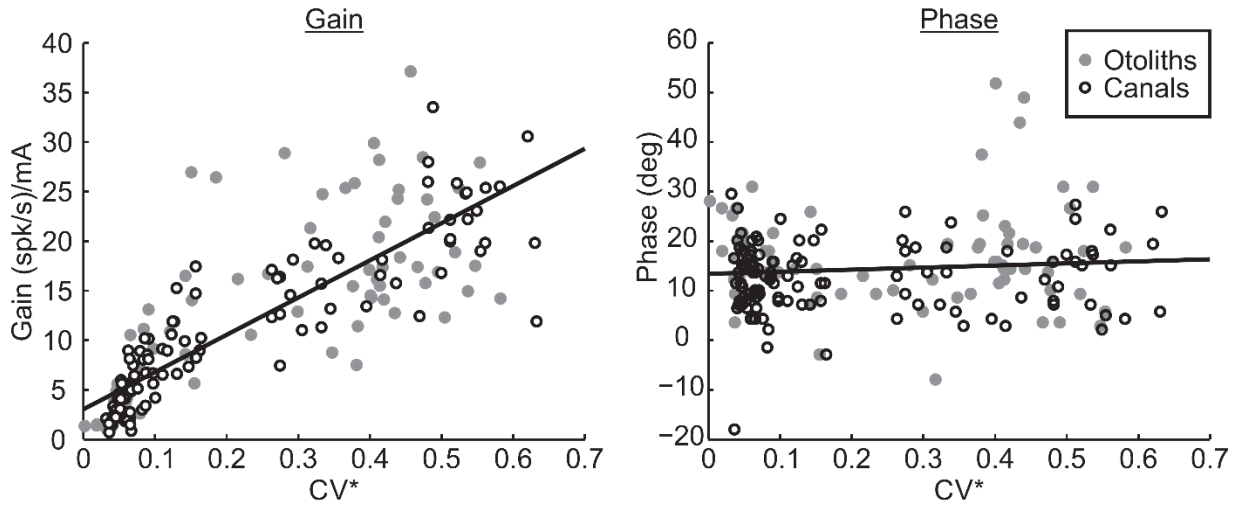


**Figure 2.3.** Comparison of canal and otoliths afferent responses to sinusoidal GVS (A) Gain (left) and phase (right) of canal (open black circles, N = 118) and otolith (filled grey circle, N = 81) to 1 Hz sinusoidal as a function of the resting discharged variability, quantified as CV*.

**Table 2.1.** Comparison between gain and phase of otolith and canals as a function of discharge variability across frequencies.

| Gain | | | | | | | | | | | |
|---|---|---|---|---|---|---|---|---|---|---|---|
| Frequency (Hz) | Common? | P - value | Common | Common R | P - value | Canal | Canal R | P - value | Otolith | Otolith R | P - value |
| 0.1 | F(2,124) = 1.41 | p > 0.00278 | y = 28.50x+2.34 | r = 0.81 | p < 0.00278 | - | - | - | - | - | - |
| 0.2 | F(2,131) = 0.15 | p > 0.00278 | y = 29.99x+2.41 | r = 0.83 | p < 0.00278 | - | - | - | - | - | - |
| 0.5 | F(2,194) = 0.15 | p > 0.00278 | y = 31.07x+2.78 | r = 0.82 | p < 0.00278 | - | - | - | - | - | - |
| 1 | F(2,198) = 0.19 | p > 0.00278 | y = 33.63x+2.90 | r = 0.80 | p < 0.00278 | - | - | - | - | - | - |
| 2 | F(2,195) = 1.03 | p > 0.00278 | y = 37.55x+3.04 | r = 0.84 | p < 0.00278 | - | - | - | - | - | - |
| 4 | F(2,193) = 0.81 | p > 0.00278 | y = 41.89x+3.17 | r = 0.85 | p < 0.00278 | - | - | - | - | - | - |
| 8 | F(2,178) = 1.27 | p > 0.00278 | y = 45.80x+4.43 | r = 0.84 | p < 0.00278 | - | - | - | - | - | - |
| 16 | F(2,140) = 1.86 | p > 0.00278 | y = 60.06x+5.58 | r = 0.87 | p < 0.00278 | - | - | - | - | - | - |
| 25 | F(2,80) = 1.59 | p > 0.00278 | y = 72.17x+7.27 | r = 0.87 | p < 0.00278 | - | - | - | - | - | - |

| Phase | | | | | | | | | | | |
|---|---|---|---|---|---|---|---|---|---|---|---|
| Frequency (Hz) | Common? | P - value | Common | Common R | P - value | Canal | Canal R | P - value | Otolith | Otolith R | P - value |
| 0.1 | F(2,124) = 19.08 | p < 0.00278 | - | - | - | y = 6.79x+3.94 | r = 0.27 | p > 0.00278 | y = 4.41x+10.77 | r = 0.13 | p > 0.00278 |
| 0.2 | F(2,131) = 12.91 | p < 0.00278 | - | - | - | y = 2.78x+5.17 | r = 0.10 | p > 0.00278 | y = 2.35x+7.75 | r = 0.07 | p > 0.00278 |
| 0.5 | F(2,194) = 15.05 | p < 0.00278 | - | - | - | y = 6.24x+5.30 | r = 0.20 | p > 0.00278 | y = 7.75x+10.01 | r = 0.20 | p > 0.00278 |
| 1 | F(2,198) = 4.54 | p > 0.00278 | y = 9.73x+9.69 | r = 0.24 | p < 0.00278 | - | - | - | - | - | - |
| 2 | F(2,195) = 4.73 | p > 0.00278 | y = 4.19x+13.41 | r = 0.27 | p > 0.00278 | - | - | - | - | - | - |
| 4 | F(2,193) = 5.68 | p < 0.00278 | - | - | - | y = 8.32x+17.57 | r = 0.18 | p > 0.00278 | y = -13.87x+20.24 | r = -0.22 | p > 0.00278 |
| 8 | F(2,178) = 1.40 | p > 0.00278 | y = 0.70x+25.50 | r = 0.01 | p > 0.00278 | - | - | | - | - | |
| 16 | F(2,140) = 0.59 | p > 0.00278 | y = -4.56x+35.32 | r = -0.06 | p > 0.00278 | - | - | - | - | - | - |
| 25 | F(2,80) = 3.52 | p > 0.00278 | y = 16.09x+39.72 | r = 0.16 | p > 0.00278 | - | - | - | - | - | - |

**Comparison of vestibular afferent response to GVS and motion**

One open question about the GVS activation of the vestibular system is whether afferent responses evoked by GVS are equivalent to those evoked by motion stimuli. Therefore, to compare vestibular afferent responses to GVS versus motion, we also stimulated the afferents with sinusoidal modulated motion stimuli of similar frequencies. We first recorded individual canal afferent during yaw rotation of frequencies within the physiological relevant range (0.5-16 Hz), as done previously (Sadeghi *et al.*, 2007b; Massot *et al.*, 2011). The responses of the example regular and irregular canal afferents during sinusoidal yaw rotation of 1 Hz and 4 Hz are shown in Fig. 2.4A, where we found, as expected, that the irregular canal afferent was more sensitive compared to regular canal afferent (1 Hz: 0.3 vs 0.1 spk/s/deg/s; 4 Hz: 0.6 vs 0.2 spk/s/deg/s). These results were consistent across our dataset (regular, N = 21-26; irregular, N = 17-21) and were in agreement with previous studies (Sadeghi *et al.*, 2007b; Massot *et al.*, 2011). Fig. 2.4B shows the comparison between the population response dynamics of canal afferents to GVS (data from Fig. 2D) and to yaw rotation. We first noticed that both the normalized sensitivity and phase lead relative to rotation were markedly higher when compared to GVS. Interestingly, we found that while the normalized sensitivity and phase lead relative to rotation were greater in irregular canal afferents than in regular canal afferents, there was no such difference between irregular and regular canal afferent responses to GVS. The evident discrepancies between the canal afferent response dynamics to physiological and artificial vestibular stimuli were most likely caused by the difference in activation of the vestibular system; GVS activates the canal afferents by bypassing the biomechanics of the semicircular canals, which normally mechanically transduces motion into neural activity in the canal afferents.

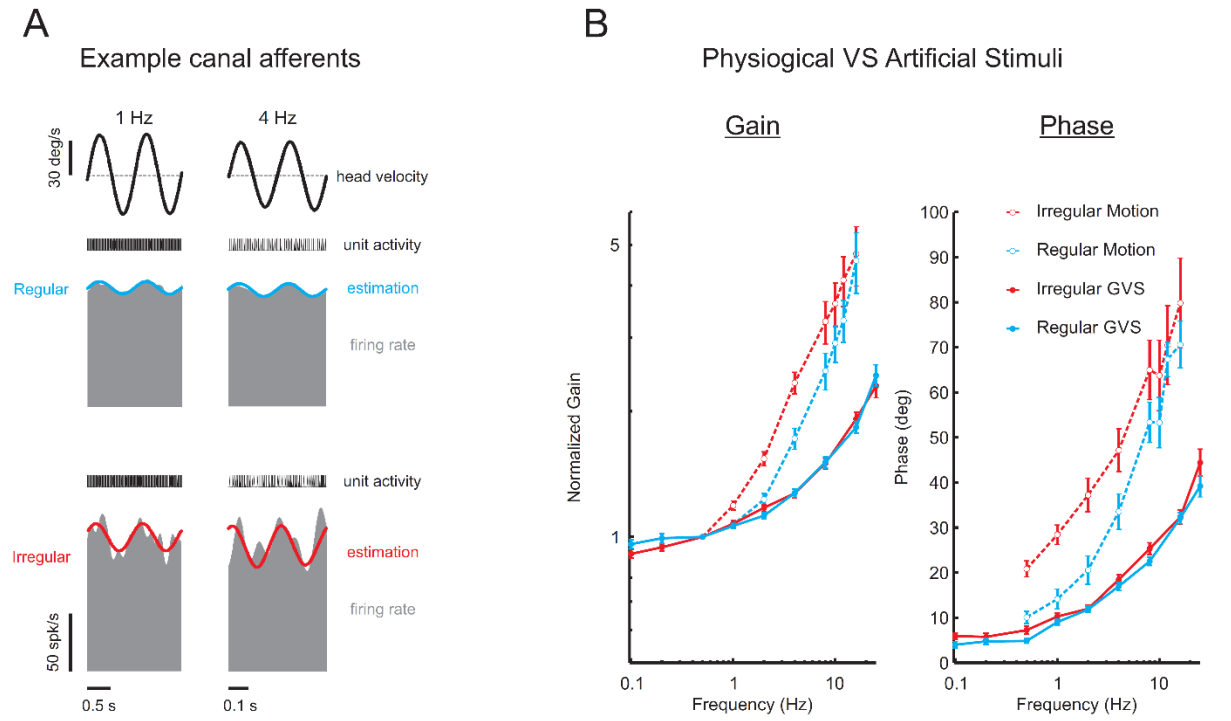


**Figure 2.4.** Comparison of motion and GVS for canal afferents. (A) Firing rate (gray) of example regular (blue) and irregular (red) canal afferents to 1 Hz (left) and 4 Hz (right) head velocity. Firing rate estimates (solid blue and red line) are found using eq. 2.2. (B) Comparison of canal afferent responses to physiological (yaw rotation) and artificial (GVS) stimuli. Population normalized gain (left) and phase (right) to motion for regular (blue dashed line and open circles, N = 21-26) and irregular (red dashed line open circles, N = 17-21) canal afferents. Population normalized gain (left) and phase (right) to sinusoidal GVS for regular (solid blue line) and irregular (solid red line) canal afferents.

We next compared the response dynamics of otolith afferents to GVS and linear head acceleration. Here, we used previously published otolith afferent responses to translational motion (Jamali *et al.*, 2013) to compare with sinusoidal GVS-evoked otolith afferent responses presented here. To ensure that our otolith afferent population was consistent with the previous study, we compared the gain to linear acceleration in the preferred direction at 2 Hz of the otolith afferents in the current and previous datasets. Specifically, we first recorded individual otolith afferent during translation motion (~2 Hz) in both the foreaft and lateral direction, and estimated the gain

at 2 Hz corresponding to the preferred direction of the otolith afferents (see Methods). Fig. 2.5A shows the responses of the example regular and irregular otolith. As expected, these otolith afferents respond differently to translational motion in the foreaft and lateral direction because of its spatial tuning (regular: 33.1 vs 133.5 spk/s/G; irregular: 209.8 vs 253.0 spk/s/ G). We found that in our dataset, irregular otolith afferents have a higher sensitivity to their preferred direction compared to regular afferents (2 Hz: 223.4±31.2 spk/s/G vs 68.6±17.3 spk/s/G), which is consistent with those previously reported (2 Hz: 212.8±25.4 spk/s/G vs 50.6±10.2 spk/s/G; Jamali *et al*., 2013)). Since our otolith afferent population was not significantly different from those in the previous study (t-test, $p = 0.44$ and $p = 0.77$ for regular and irregular otolith afferents, respectively), we used the normalized sensitivity and phase of otolith afferents to linear acceleration from (Jamali *et al.*, 2013) in order to compare with the otolith afferent responses to sinusoid GVS obtained here, shown in Fig. 2.5B. Once again, we found an evident difference between the otolith response dynamics to physiological and artificial stimuli. As is the case in canal afferents, irregular and regular otolith afferents demonstrated similar normalized sensitivity and phase lead to GVS, but not to linear acceleration. However, unlike canal afferents, the difference in relative frequency-dependent increase in the normalized gain was much smaller. Overall, the observed difference in dynamics between artificial and physiological stimuli implies that GVS also bypasses the mechanics of the otolith endorgans, and thereby producing the differences in otolith afferent response dynamics to physiological and artificial motion.

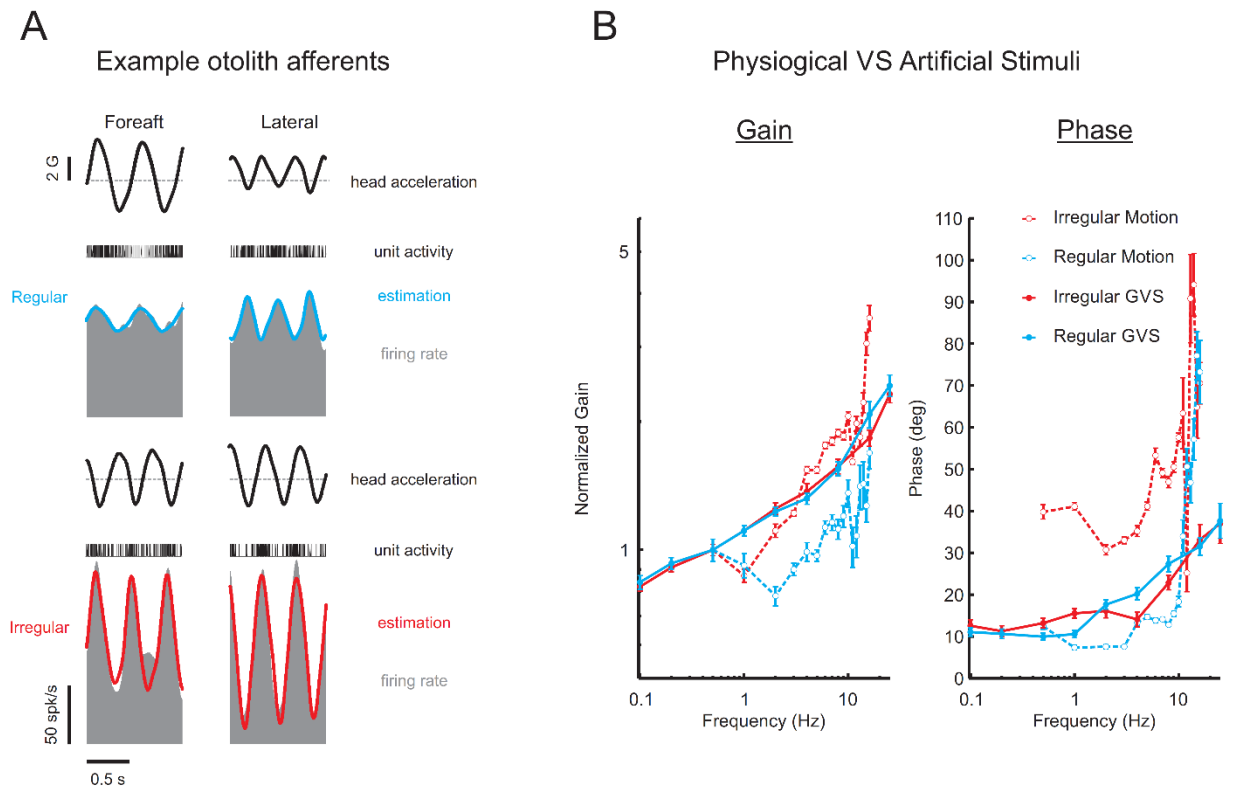


**Figure 2.5.** Comparison of motion and GVS for otolith afferents. (A) Firing rate (gray) of example regular (blue) and irregular (red) otolith afferents to ~ 2 Hz foreaft (left) and lateral (right) head acceleration. Firing rate estimates (solid blue and red line) are found using eq. 2.3. (B) Comparison of otolith afferent responses to physiological (translation motion) and artificial (GVS) stimuli. Population normalized gain (left) and phase (right) to motion (Jamali *et al.*, 2013) for regular (blue dashed line and open circles, N = 6-30) and irregular (red dashed line open circles, N = 4-26) otolith afferents. Population normalized gain (left) and phase (right) to sinusoidal GVS for regular (solid blue line) and irregular (solid red line) otolith afferents.

To better understand the relative activation of vestibular afferents by artificial versus physiological stimuli, we computed the ratio between the gains of vestibular afferents to motion (either rotation or translation) and to GVS as a function frequency. This motion-GVS ratio gives a sense of the equivalent motion corresponding to the current amplitude. Fig. 2.6 shows the population averaged motion-GVS ratio for canal and otolith afferents across the matching frequencies for both stimuli. In general, we found that vestibular afferents, with the exception of regular otolith afferents, show a frequency-dependent increase in the motion-GVS ratio, indicating

that for the same current, the amplitude of equivalent motion increased as a function of frequency. Instead, the equivalent translation in regular otolith afferents for a given current amplitude was independent of frequency (Table 2.2). This result demonstrates that, at the level of individual afferents, it is necessary to take into account the difference in dynamics of vestibular afferent responses to GVS versus motion in order to make predictions of how GVS activates the vestibular system.

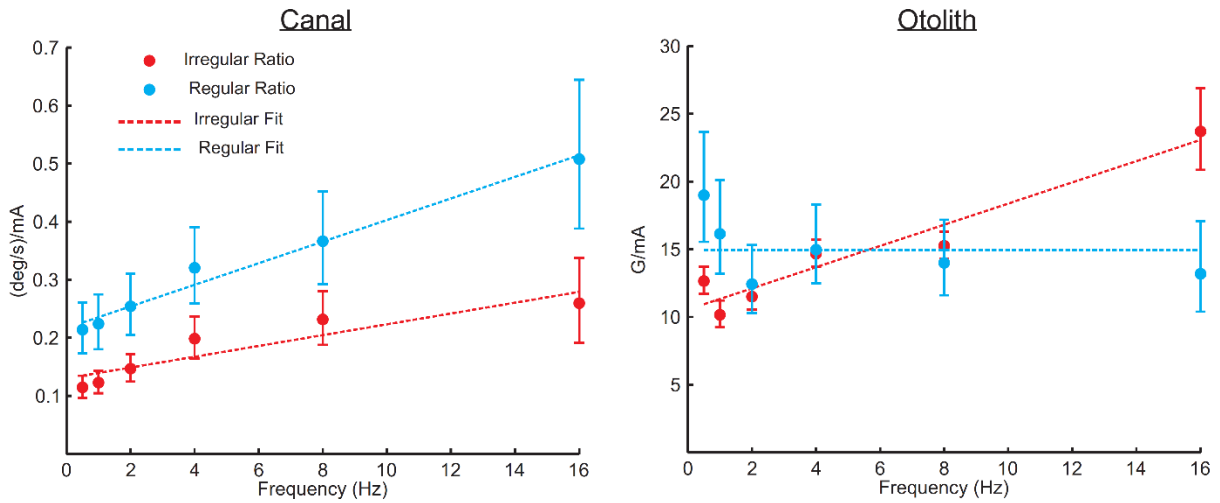


**Figure 2.6.** Motion-GVS ratio for canal (right) and otolith (left) afferent responses. The motion-GVS ratio of both regular and irregular canal afferents, as well as of irregular otolith afferents, increases as a function of frequency. In contrast, the motion-GVS ratio of regular otolith afferents is independent of frequency.

**Table 2.2.** The relation between the motion-GVS ratio and frequency for vestibular afferents.

| | Canal | Otolith |
|---|---|---|
| Regular | $ratio = 0.02f + 0.22$ | $ratio = 14.95$ |
| Irregular | $ratio = 0.01f + 0.13$ | $ratio = 0.78f + 10.55$ |

The comparison of vestibular afferent responses to physiological and artificial stimulation demonstrates that established linear models of canal and otolith afferents with angular head velocity and linear head acceleration, respectively, cannot be used to model vestibular afferent

responses to GVS. Therefore, we estimated transfer functions to the population frequency responses to sinusoidal GVS from Fig. 2.2D and E. Here, since we cannot make any assumption on the number of parameters to include in the model, we fitted the frequency responses to multiple models, each of different form (i.e. varying the number of poles and zeros of the transfer function). We found that the responses of irregular canal afferents were best fitted with a one pole and one zero transfer while the other three afferent groups were modelled after a two poles and two zeros transfer function (Table 2.3). These estimated models provide an approximate representation of how vestibular afferents dynamically respond to GVS as well as the necessary information in developing computational models of vestibular processing of artificial stimulation.

**Table 2.3.** Transfer function of GVS-evoked responses.

| | Canal | Otolith |
|---|---|---|
| Regular | $\frac{25.1(s+92.7)(s+13.6)}{(s+438.0)(s+18.4)}$ | $\frac{16.4(s+47.9)(s+1.5)}{(s+194.5)(s+2.1)}$ |
| Irregular | $\frac{85.4(s+73.3)}{(s+404.5)}$ | $\frac{88.0(s+107.0)(s+4.7)}{(s+456.3)(s+7.3)}$ |

## IV. Discussion

In the present study, we recorded eye movements and the activity of primary vestibular afferents in nonhuman primates during electrical stimulation applied between surface electrodes, a setup comparable to human GVS studies. Similar to human behaviour, we observed sinusoidal modulated torsional eye movements in response to sinusoid GVS. We characterized the frequency responses of primary vestibular afferents to GVS of frequencies within the physiological range (0.1-25 Hz) and found that both semicircular canal and otolith afferents showed similar frequency responses in which their gains and phase leads increased monotonically as a function of frequency. Although both canal and otolith afferents are known exhibit high-pass tuning to physiological

stimulation (i.e. motion) (Sadeghi *et al.*, 2007a; Jamali *et al.*, 2013), here, we demonstrated the difference in activating the vestibular system between physiological and artificial stimulation. Altogether, our results provide insights to the first component in modelling the GVS activation of the vestibular system.

**Comparison with previous animal studies**

Here, we have shown that transmastoid GVS can evoke vestibular afferent responses, both in canal and otolith afferents. Consistent with previous animal studies, which have stimulated vestibular afferents with current mostly delivered inside the ear (Lifschitz, 1973; Goldberg *et al.*, 1984; Baird *et al.*, 1988; Cullen & Minor, 2002; Kim & Curthoys, 2004), we found that irregular afferents were more readily responsive compared to regular afferents. Specifically, we found that the sensitivity of canal and otolith afferents is linearly related to their discharge variability. This finding suggests that regardless of the location of the stimulating electrodes (i.e. on the surface or inside the ear), the effects of electrical stimulation are highly dependent on the discharge variability of the vestibular afferents.

In contrast, we found that the dynamics of vestibular afferent responses differ from those previously reported for internal electrical stimulation (Goldberg *et al.*, 1982; Baird *et al.*, 1988; Kim *et al.*, 2011). Specifically, we found that both canal and otolith afferents shared comparable response dynamics to sinusoidal GVS, where the gain increased by over two folds and the phase lead increased by ~30 degrees across the physiological frequency range (0.1 – 25 Hz). Furthermore, the difference in responses between regular and irregular afferents was only found in the sensitivity but not in the phase lead. This result contrasts with a recent animal study, which showed that canal afferents had smaller and more variable increases in gain and phase lead as a function of frequency

to internally delivered sinusoidal modulated current (Kim *et al.*, 2011). The robust high-pass tuning of vestibular afferents to transmastoid stimulation is unexpected, if we were to consider that current delivered internally is in much closer proximity to activate the vestibular afferents compared to current delivered on the mastoid processes. Specifically, the underlying skin, bone and cerebrospinal fluid together are known to act as a low-pass filter to the electrical activity generated in the brain when recording using external techniques, such as electroencephalography (Srinivasan *et al.*, 1998). Following the same principle, when current is instead delivered on the surface, it should also be low-pass filtered by the skin-bone-CSF ensemble. If that were the case, currents delivered at higher frequencies would be attenuated and the predicted frequency response of vestibular afferents to transmastoid stimulation should be reduced when compared to the dynamics of afferents in response to internal stimulation. This, however, is the opposite of what we observed, with vestibular afferents frequency responses to transmastoid stimulation generally displaying larger gain and phase lead increases. This result indicates that vestibular afferent dynamic responses to GVS cannot be predicted from previously reported responses to internal stimulation.

**Vestibular afferent dynamics: Motion versus GVS**

Our finding that vestibular afferents display different dynamic responses to GVS and motion highlights how these two types of stimuli have different mechanisms of activating the vestibular system. This is consistent with previous animal studies which showed that the dynamics of canal afferent responses to direct electrical stimulation and rotation were dissimilar (Goldberg *et al.*, 1982; Kim *et al.*, 2011). Here, we also found that although canal and otolith afferents have distinct dynamics to their preferred motion, the two types of vestibular afferents have comparable

frequency responses to GVS. This result provides a stronger evidence that GVS activates vestibular afferents by bypassing the biomechanics of both the semicircular canals and otolith organs, which are responsible for the different dynamics to rotation and translation, respectively (Sadeghi *et al.*, 2007a; Jamali *et al.*, 2013). However, it remains to be resolved whether GVS-evoked afferent responses involve the hair cells as well (Goldberg *et al.*, 1984; Aw *et al.*, 2008; Mitchell *et al.*, 2013).

It is also noteworthy to address the question of whether there is an equivalent motion corresponding to GVS-evoked vestibular afferent responses. Previous predictions comparing human behavioural and vestibular afferent responses evoked by motion or electrical stimulation (GVS in humans and direct electrical stimulation in animals) fail to consider that the dynamics of vestibular afferent activity are different during GVS versus motion (Schneider *et al.*, 2000; Fitzpatrick & Day, 2004). Notably, one study has simply assumed that the frequency response of canal afferents to GVS was equivalent to a well-established canal afferent transfer function to rotation, scaled by a constant factor (Héroux *et al.*, 2015). As these estimations are physiologically incorrect, we developed more accurate relationships between motion-evoked and GVS-evoked vestibular responses as a function of frequency. Therefore, the results presented in this study have important implications in estimating the equivalent motion corresponding to GVS-evoked neural activity (Stephan *et al.*, 2005; Schneider *et al.*, 2009) as well as modelling the neural dynamic responses within vestibular pathways activated by GVS (Forbes *et al.*, 2013).

**Behavioural correlates of GVS-evoked vestibular afferent responses**

Here, we demonstrated that the nonhuman primate is a valid model for investigating the effects of GVS on vestibular afferents because the evoked torsional eye movements in animals

during sinusoidal simulation were similar to those reported in humans (Kleine *et al.*, 1999; Schneider *et al.*, 2000; MacDougall *et al.*, 2002b). More importantly, as in human studies (MacDougall *et al.*, 2002b), we observed variability in the gain of torsional eye movements among animals, for example Monkey B produced greater torsional eye velocity compared to Monkey H. The difference in the sensitivity between these animals was also found in afferents. This result suggests that the magnitude in GVS-evoked eye movements (and most likely other behavioural responses) is dependent on the sensitivity of vestibular afferents to GVS. Thus, between-subject variability of GVS-evoked behaviours in humans may in part be explained by afferent responses to GVS differed between subjects.

However, there are certain limitations in linking GVS-evoked vestibular afferent responses to the downstream behaviour, in particular higher-order functions like perception. For instance, Peters *et al.* (2015) recently recorded the frequency-dependent discrimination threshold and phase of virtual rotation perception and attempted to predict the frequency responses of vestibular afferents, where the gain of the vestibular afferents is related to the inverse of discrimination threshold. Since the direction discrimination threshold of virtual motion was found to worsen as a function of frequency (i.e. more current is need for higher frequencies), the authors hypothesized that the gain of the vestibular afferents to GVS would decrease as a function of frequency. However, this contradicts our findings in which we observed a robust increase in gain and phase lead as a function of frequency to transmastoid stimulation. Thus, to model the dynamics of GVS-evoked perception of motion, it is insufficient to solely use the dynamics of vestibular afferent responses to GVS. Motion perception is the result of higher-order brain areas integrating vestibular inputs (Sadeghi *et al.*, 2007a; Massot *et al.*, 2011; Jamali *et al.*, 2013). Here, we have shown that GVS activates all vestibular afferents – both canals and otoliths – in a similar fashion. However,

this type of activation is non-physiological. For example, under physiological vestibular stimuli, half of the otolith afferents would be excited, whereas the other half would be inhibited. Therefore, the integration of vestibular afferents that are unnaturally all activated would likely explain the decline in GVS-evoked motion perception as a function of frequency, even though individually, vestibular afferents show a frequency-dependent increase in gain.

**Implications for future work**

One novelty of the experimental approach used in the present study is that we were able to characterize the dynamics of vestibular afferent responses to transmastoid GVS in a primate-based model and thereby provide more physiologically-relevant mechanisms mediating GVS-evoked responses in humans. Here we have demonstrated that afferent responses to transmastoid stimulation cannot be predicted from responses to internal electrical stimulation nor to natural vestibular stimulation. Notably, both canal and otolith afferents have similar dynamic responses to transmastoid stimulation. In contrast, models of how GVS activates the human peripheral vestibular system to evoke behavioural responses have focused primarily on the semicircular canal afferents, without considering their dynamics to the stimulation (Day *et al.*, 2010; Day *et al.*, 2011; Héroux *et al.*, 2015). Yet, there are other views suggesting that otolith afferents primarily mediate GVS-evoked behaviours (Cohen *et al.*, 2011; 2012). Since our results imply that GVS activate both canal and otolith afferents, we first suggest that both canal and otolith afferent responses do indeed contribute to the evoked responses. However, we also propose that the more important question to now address is how higher-order vestibular areas integrate the combined activity of vestibular afferents to drive GVS-evoked behaviours. In this context, future work will be required

to determine the effects of transmastoid stimulation on central vestibular areas, including the vestibular nuclei, the next stage of vestibular processing.

## V. Conclusion

We conclude that dynamic GVS evokes similar responses in both semicircular canal and otolith afferents. In addition, comparison with the dynamics to kinetic stimuli provides new insight into how vestibular afferents are activated artificially. Therefore, our findings are necessary in the development of physiological and accurate model of GVS activation of the vestibular system.

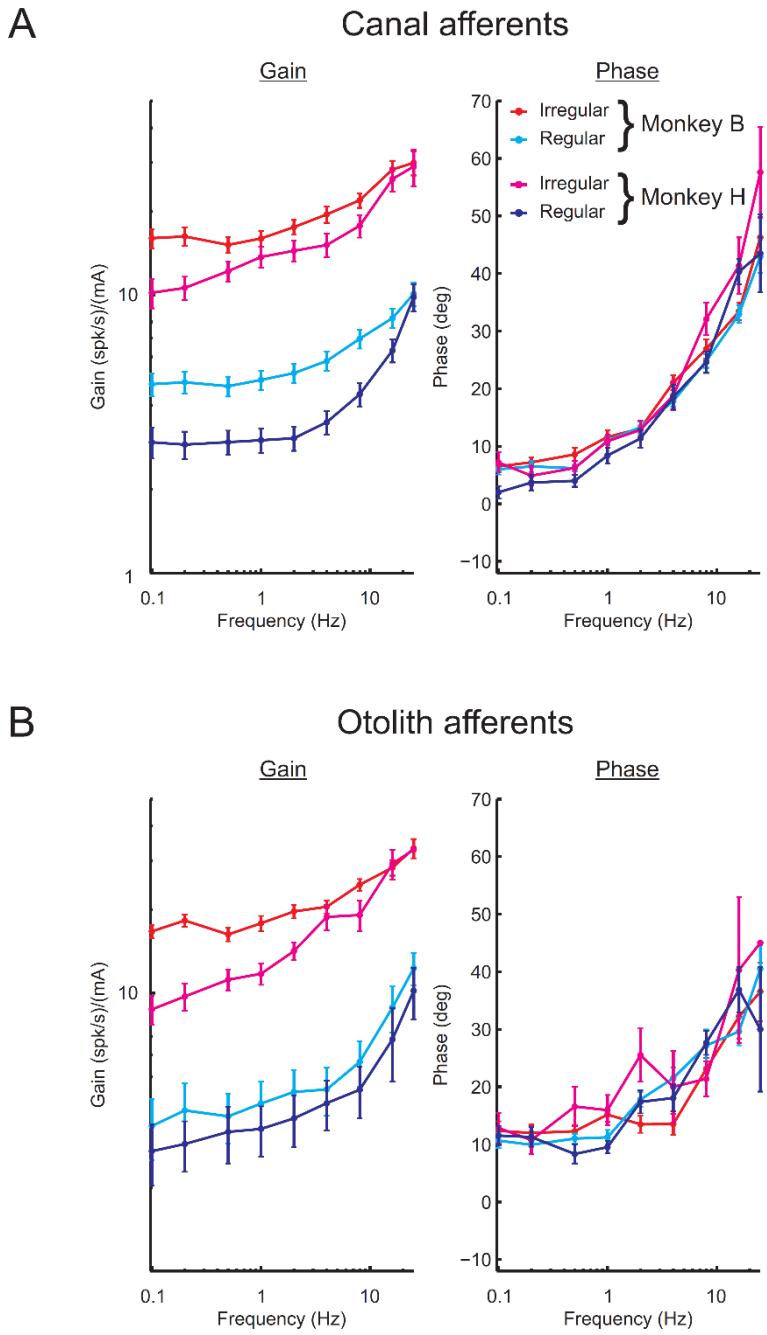


**Figure S2.1.** Comparison of vestibular afferents recorded from two animals. (A) Population averaged gain and phase of regular (Monkey B: light blue, N = 21-36; Monkey H: dark blue, N = 6-27) and irregular (Monkey B: red, N = 21-40; Monkey H: pink, N = 6-16) canal afferents to sinusoidal GVS. (A) Population averaged gain and phase of regular (Monkey B: light blue, N = 8-18; Monkey H: dark blue, N = 3-12) and irregular (Monkey B: red, N = 17-41; Monkey H: pink, N = 1-13) otolith afferents to sinusoidal GVS.

# Chapter 3: Asymmetry in vestibular afferent responses to transmastoid galvanic vestibular stimulation

## I. Introduction

Galvanic vestibular stimulation (GVS) is a technique where current applied to surface electrodes placed on the mastoid processes behind the ears stimulates the vestibular system and consequently evokes behavioural responses in humans such as: eye movements (Watson *et al.*, 1998; Zink *et al.*, 1998; MacDougall *et al.*, 2002b; MacDougall *et al.*, 2003; MacDougall *et al.*, 2005; Dilda *et al.*, 2014a), postural changes (Nashner & Wolfson, 1974; Lund & Broberg, 1983; Day *et al.*, 1997b), and the sensation of self-motion (Wardman *et al.*, 2003b; St George *et al.*, 2011; Hammam *et al.*, 2012). Because GVS is a non-invasive tool that can be used to selectively activate the vestibular system, there is a growing interest in its utility as a clinical tool for the diagnosis of vestibular disorders (Kim *et al.*, 2006; Aw *et al.*, 2013). In addition, the ability of GVS to drive the vestibular system has potential biomedical applications, such as controlling navigation by biasing the trajectory of locomotion via the electrical perturbation of the vestibular system (Maeda *et al.*, 2005a; Fitzpatrick *et al.*, 2006).

To date, however, the physiological mechanisms mediating GVS-evoked responses remain to be fully elucidated. An assumption inherent to most previous studies is that the effects of GVS on the vestibular system can be estimated from neuronal activity recorded during natural vestibular stimulation (i.e. self-motion) or in response to direct electrical stimulation of the inner ear (Fitzpatrick & Day, 2004; Forbes *et al.*, 2013; Héroux *et al.*, 2015). As a result, the prevailing view is that the GVS activation of the peripheral vestibular system is linear because (1) vestibular afferent responses to physiological stimuli (i.e. motion) can be well modelled using linear systems

approaches (Fernandez & Goldberg, 1971; Angelaki & Dickman, 2000; Hullar *et al.*, 2005), and similarly (2) vestibular afferent responses to electrical stimulation of the inner ear are linearly related to current amplitude (Goldberg *et al.*, 1984). Importantly, however, there are many reasons to believe that afferent responses can show significant nonlinearities in response to GVS. First, it has been reported that direct electrical stimulation with currents of opposite polarity produces asymmetrical changes in vestibular afferents' firing rates (Kim & Curthoys, 2004). In addition, high frequency and amplitude self-motion stimuli will drive vestibular afferents into a nonlinear regime (Ramachandran & Lisberger, 2006; Schneider *et al.*, 2011; Schneider *et al.*, 2015). Such nonlinearities may also play a vital role in explaining why low levels of stochastic transmastoid GVS may improve postural and locomotor stability in patients (Mulavara *et al.*, 2011; Iwasaki *et al.*, 2014; Goel *et al.*, 2015; Kataoka *et al.*, 2015; Mulavara *et al.*, 2015; Samoudi *et al.*, 2015; Wuehr *et al.*, 2016). While it has been proposed that stochastic resonance, a phenomenon where adding a low level of noise to a nonlinear system improves the detection of a weak input underlies improvements in patients, there is no direct evidence for this proposal. Thus, an important and open question is whether the peripheral vestibular system shows non-linear responses to transmastoid GVS.

Thus, here we directly investigated whether vestibular afferent responses show significant nonlinearities in response to GVS. To do so, we applied current stimulation onto surface electrodes placed behind the ears of macaque monkeys in a bilateral bipolar configuration and delivered two different but common stimulation paradigms: constant current and stochastic GVS for frequencies (0-25 Hz) that spanned the physiologically relevant range of the vestibular system. We first demonstrated that constant current transmastoid GVS stimulation evoked eye movements in monkeys comparable to those observed in humans. Then to establish the neural correlates

mediating GVS-evoked behaviour, we recorded responses from individual vestibular afferents during the constant current stimulation and found comparable asymmetries in the responses at the onset versus the offset of the stimulation. Similarly, vestibular afferents displayed asymmetric responses to currents of opposite polarity. Notably, response asymmetries were more significant for irregular than regular afferents, for both the semicircular canal and otolith systems. Using a second approach to evaluate linearity, we recorded vestibular afferent responses to stochastic stimulation and determined whether the response dynamics are comparable to those observed when single sinusoidal stimulation are applied individually (Chapter 2). Interestingly, we found deviations in the vestibular afferent responses to these two separate stimuli. These findings reveal nonlinearities in the vestibular afferent activity in response to GVS, which provide new insights in developing of physiologically relevant models and advancing the applications GVS.

## II. Materials and Methods

Three male macaque monkeys (2 *Macaca fascicularis*, Monkey B and H, *and 1 M. mulatta*, Monkey D) were prepared for chronic extracellular recording using aseptic surgical techniques. All experimental protocols were approved by the McGill University Animal Care Committee and were in compliance with the guidelines of the Canadian Council on Animal Care.

### *Surgical procedures*

The surgical preparation for Monkey B and D followed the procedures described previously (Dale & Cullen, 2013). The surgical preparation for Monkey H followed new protocol procedures described in Chapter 2. Briefly, in all animals, aseptic surgical techniques were used, and under isofluorane anesthesia (0.8 – 1.5%), we secured a stainless steel post to the animal's

skull with stainless steel screws and dental acrylic, permitting complete immobilization of the animal's head during the experiments, and implanted a chamber for chronic extracellular recording. Finally, an eye coil consisting of three loops of Teflon-coated stainless steel wire was implanted in the right eye behind the conjunctiva (Fuchs & Robinson, 1966). Post-surgery protocol for Monkeys B and D followed that described previously (Dale & Cullen, 2013); for Monkey H, the procedures are detailed in Chapter 2. Animals were given at least 2 weeks to recuperate from the surgery before any experiments began.

*Data acquisition*

During the experiments, monkeys were head-restrained and seated comfortably in a primate chair mounted on top of a vestibular turntable. The left vestibular nerve was found as described (Jamali *et al.*, 2013). Extracellular single-unit activity of primary vestibular afferents (semicircular canal and otolith) was recorded using tungsten microelectrodes (7-10 MΩ and 20-25 MΩ, Frederick-Haer Co., Bowdoinham, ME) (Fig. 3.2A). Neural signals were band-pass filtered from 300 Hz to 3 kHz and sampled at 30 kHz. Head linear acceleration and angular velocity was measured by a three-dimensional linear accelerometer and a one-dimensional angular gyroscope (Watson Inc., Eau Claire, WI), respectively, both firmly secured to the animal's head post. Horizontal and vertical eye positions were measured using the magnetic search-coil technique (Fuchs & Robinson, 1966; Judge *et al.*, 1980). Head linear acceleration, head angular velocity and galvanic vestibular stimulation signals were low-pass filtered at 250 Hz (eight-pole Bessel filter) and sampled at 1 kHz. Neural behavioural and stimulation data were collected through the Cerebus Neural Signal Processor (Blackrock Microsystems, Salt Lack City, UT). Neural data was imported into either Offline Sorter (Plexon, Dallas, TX) as previously described (Dale & Cullen, 2015) or

into a custom-written algorithm in MATLAB (The MathWorks, Natick, MA) to extract action potentials.

Horizontal and vertical eye positions were also measured separately using a modified eye tracker (Chronos Vision, Berlin, Germany) fixed onto the monkey's head post. Offline analysis software Iris (Chronos Vision) was later used to calculate torsional eye position from markers applied near the limbus. Markers consisted of an infrared absorbing cosmetic pigment, Eisenoxid 316/Schwarz (Carl Jäger Tonindustriebedarf GmbH, Erlen, Germany), dissolved in distilled water and were applied near the limbus using a sterile surgical marking pen.

*Experimental design*

*Galvanic vestibular stimulation*: Electrical vestibular stimulation was applied to animals using carbon rubber electrodes (~6 $cm^2$) in a binaural bipolar configuration. The electrodes were coated with Spectra 360 electrode gel (Parker Laboratories, Fairfield, NJ) and secured over the animal's mastoid processes with surgical tape. The stimuli were generated using MATLAB and were delivered as analog signals to a constant current isolation unit (STMISOLA; Biopac Systems Inc., USA) via a QNX-based real-time data acquisition system (Hays Jr *et al.*, 1982) or an arbitrary waveform generator (Keysight Technologies, Santa Rosa, CA). The current polarity of the stimulation is referred to the polarity of the left stimulating electrode, which was on the same side of the vestibular afferents recorded.

For neural recordings, once a unit was isolated, the vestibular endorgans innervated by that fiber was determined based on the responses of the afferent to rotations or translation. Animals were then exposed to two different electrical stimuli. The first stimulation consists of a repeated sequence of three consecutive constant cathodal or anodal current pulses of 1 mA lasting 40 s and

20 s off period. The second stimulation consisted of a broadband Gaussian stochastic (0-25 Hz) current of maximum peak amplitude of 1 mA.

For eye movement recordings, animals were placed in the dark while exposed to constant cathodal current pulse stimulation of 1 mA. A fixation laser was present in conditions where torsional eye movements were recorded. Rightward horizontal, upward vertical, and clockwise torsional (i.e. toward the right ear) eye movements are expressed as positive values.

*Data analysis*

Data were imported into MATLAB for analysis using custom-written algorithms. Behavioural signals were digitally filtered at 125 Hz.

*Background discharge*: Afferents were classified based on the regularity of resting discharge, which is evaluated by the normalized coefficient of variation (CV*), as done previously (Goldberg *et al.*, 1984; Massot *et al.*, 2011). Afferents with CV* $\leq$ 0.1 were considered regular, while those with CV* > 0.1 where considered irregular (Sadeghi *et al.*, 2009). The afferents' resting discharge was calculated as well.

*Response dynamic – constant current GVS*: The time-dependent firing rate FR(t) was first estimated by convolving the spike train r(t) with a Gaussian (SD = 50 ms). Responses to the constant current pulse were normalized by removing the baseline firing rate calculated two seconds prior to the onset of the stimulation. For each afferent, the average response across the three pulses were taken. We characterized the afferent responses to the pulses into three phases: onset (the maximum or minimum response within the first second after at the start of cathodal or anodal

current stimulation, respectively), steady-state (the mean responses within the last five seconds of the stimulation), and offset (the minimum or maximum responses within the first second after the cathodal or anodal current stimulation was turned off, respectively). We next computed the percent difference between the peak responses at onset and offset. Specifically, we calculated the percent difference for responses to cathodal current stimulation as follows:

$$\text{Percent difference cathodal} = \frac{\text{Onset} - \text{Offset}}{\text{Onset}} \times 100 \qquad \text{[eq. 3.1]}$$

The percent difference for responses to anodal current stimulation is calculated using

$$\text{Percent difference anodal} = \frac{\text{Offset} - \text{Onset}}{\text{Offset}} \times 100 \qquad \text{[eq. 3.2]}$$

since we observed that the offset of anodal current stimulation evoked a greater change in vestibular afferent activity compared to the onset of the stimulation. We then further described the responses with a model with a two exponential decay with time delay:

$$\text{FR}(t) = c_1 + c_2 e^{-c_3(t-t_d)} + c_4 e^{-c_5(t-t_d)} \qquad \text{[eq. 3.3]}$$

The model coefficients and 95% confidence intervals were computed using a bootstrap technique (Carpenter & Bithell, 2000). Briefly, 1999 "new data sets" were generated by random sampling with replacement from the original set of afferents' average responses to the constant current stimulation, for instance irregular canal afferents. For each of iteration, the coefficients were estimated at each time delay, incrementing from 0 ms relative to the onset of the stimulus to 50 ms after the peak response. The estimated coefficients were constrained to be positive. In particular, the bias ($c_1$) is set to be above 0.001. The time delay and corresponding coefficients with the best variance accounted for (VAF) which is calculated by

$$\text{VAF} = 1 - \frac{\text{var}(\text{FR} - \text{est FR})}{\text{var}(\text{FR})} \qquad \text{[eq. 3.4]}$$

were taken as the estimates for that particular iteration. The distribution were obtained for each model coefficient.

*Response dynamic – Broadband stochastic GVS*: For each afferent, response to the stochastic GVS of at least 30 seconds was used to estimate the transfer function using:

$$\mathrm{H(f)} = \mathrm{P_{sr}(f)/P_{ss}(f)} \qquad \text{[eq. 3.5]}$$

where $\mathrm{P_{sr}(f)}$ is the cross-spectrum between the stochastic stimulation and the spike train, and $\mathrm{P_{ss}(f)}$ is the power spectrum of the stochastic stimulation. The gain and phase were then estimated from the transfer function. All spectral quantities were estimated using multitaper techniques with 32 Slepian functions.

*Response dynamic – Sinusoid GVS*: We reanalyzed the data from Chapter 2 to take into account the vestibular afferent responses to constant current stimulation. For each afferent, a least-squares regression analysis was performed to determine the sensitivity ($S_G$) of the cathodal and anodal cycle of the sinusoidal GVS.

$$FR(t) = \mathrm{bias} + S_G \times GVS(t + \theta) \qquad \text{[eq. 3.6]}$$

Here, the resting discharge (bias, spk/s) was kept constant across frequency while the phase shift (θ), determined previously, was kept constant between the fits to cathodal and anodal half-cycles.

*Eye movement:* Segments of eye movement trace (horizontal, vertical and torsional) without saccades were first chosen over at least 20 trials. Slow phase velocity was computed from these segments. Tonic ocular torsion was computed relative to a time point within a one second range before the onset of the stimulation.

*Statistical Analysis*: Statistical analysis was performed in SPSS (IBM, Armonk, NY) and Excel (Microsoft, Redmond, WA). Statistical significance was set at $p < 0.05$.

To assess the dynamics of afferent responses to cathodal current GVS, we conducted a three-way mixed ANOVA with a Greenhouse-Geisser correction, where endorgan (canal versus otolith) and type (regular versus irregular) were the between factors, and phase (onset, steady-state, and offset) was the within factor. Since a two-way significant interaction was revealed for type and phase ($F(1,109)=1.2$, $p > 0.05$), we conducted simple main effects tests. Post-hoc Tukey's tests were conducted and are reported below. To evaluate whether the percent difference at the onset and offset of the stimulation differed among different classes of vestibular afferents, a two-way between factor ANOVA (endorgan and type) was conducted.

To assess the difference in the afferent responses to cathodal versus anodal current GVS, we conducted a three-way mixed ANOVA with a Greenhouse-Geisser correction, where endorgan and type were the between factors, and current polarity was the within factor for each of the three phases. For afferent responses at onset, there was a three-way significant interaction ($F(1, 51) = 6.33$, $p < 0.05$). For afferent responses at steady-state, there was a two-way significant interaction between type and current polarity ($F(1, 51) = 4.20$, $p < 0.05$). For afferent responses at offset, there was a two-way significant interaction between type and current polarity ($F(1, 51) = 12.49$, $p < 0.005$). Simple main effects were conducted for these interactions and are reported below. To evaluate the percent difference at the onset and offset of the stimulation, a two-way between factor ANOVA, endorgan and type, was conducted. To evaluate whether the cathodal and anodal percent difference were similar, we conducted a three-way mixed ANOVA with a Greenhouse-Geisser

correction, where endorgan and type were the between factors, and current polarity was the within factor.

*Reporting data*: All values are expressed as mean ± SEM unless otherwise stated.

## III. Results

The goals of this study were to (1) determine whether the patterns in GVS-evoked eye movements to constant current GVS can be predicted by vestibular afferent activity, and (2) establish whether vestibular afferents exhibit nonlinear responses. To address these questions, we first characterized eye movements and vestibular afferent responses to steps of constant current applied between surface electrodes behind the ears. We then stimulated vestibular afferents with stochastic current and compared to afferent responses to sinusoidal stimulation (Chapter 2) in order to determine nonlinearity in their responses.

### Eye movements to constant cathodal current GVS

To evaluate the effects of constant current GVS, we first characterized the evoked eye movements, in a similar setting compared to human studies. We found that large eye movements were robustly evoked at the onset of the stimulation. In the presence of a target to which the animal was trained to fixate, evoked eye movements were predominantly in the torsional plane. The onset of GVS induced torsional eye movements in the clockwise direction (opposite side of the cathodal side of stimulation) while the stimulation offset caused weaker torsional eye movements in the opposite direction (Fig. 3.1B). During the stimulation, there was an attenuation of eye movements across time (Fig. 3.1C). When the fixation target was absent, GVS elicited horizontal nystagmus,

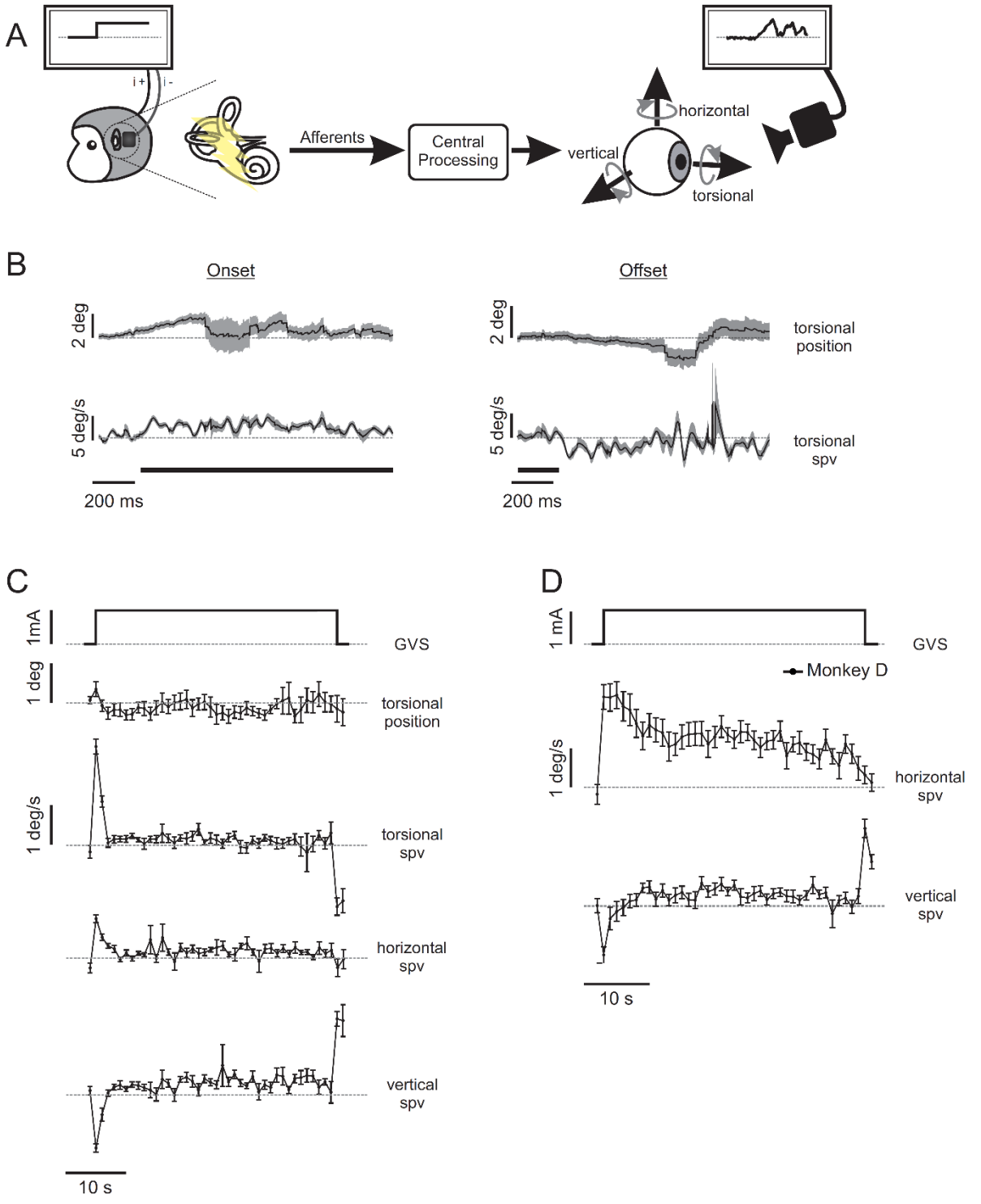


**Figure 3.1.** Eye movements in response to constant current GVS. (A) While we applied constant current GVS between surface electrodes placed on the mastoid processes behind the ears, we recorded the animal's eye movements in the presence or absence of a fixation target. (B) GVS-evoked torsional eye movements with a fixation target. Average torsional eye position and slow

phase velocity (spv) trace at the onset (right) and the offset (left) of the stimulation (thick black bar at the bottom). (C) GVS-evoked eye movement with a fixation target. The average eye movements binned at every one second. Note that there are large eye movements right after the onset of the stimulation and at the offset of the stimulation, primary in the torsional direction, as zoomed in panel above. (D) GVS-evoked eye movements without a fixation target. The average eye movements binned at every one second. Note that in the absence of a fixation target, torsional eye movements were not recorded. Horizontal nystagmus was the dominant evoked-pattern.

with a contralateral slow phase component relative to the cathodal stimulation side (Fig. 3.1D), which were suppressed during trials with fixation (compare with Fig. 3.1C). Except for the onset and offset of the stimulation, vertical nystagmus was less prominent during the stimulation, even without fixation.

**Vestibular afferent dynamics mediate behaviour evoked by constant cathodal current GVS**

Under the same stimulation, we next recorded vestibular afferent activity (Fig. 3.2A) responsible in mediating GVS-evoked eye movements shown in Fig. 3.1. In response to GVS, the example regular (CV*= 0.05) and irregular (CV* = 0.12) canal afferents (Fig. 3.2B, middle row), as well as the regular (CV*= 0.05) and irregular (CV* = 0.26) otolith afferents (Fig. 3.2C, middle row) all increased their firing rate relative to the resting discharge within the two seconds prior to the stimulation. Furthermore, irregular afferents had a more robust response compared to their regular counterparts. These response characteristics were consistent across the population of canal afferents (regular N = 37; irregular N = 33; Fig. 3.2B, bottom row) and otolith afferents (regular N = 20; irregular N = 23; Fig. 3.2C, bottom row). Across the vestibular afferent population, afferent responses to constant current can be qualitatively decomposed into three phases relative to the stimulation: (1) A large transient response at the stimulation onset, (2) a steady-state response during the stimulation, and (3) a large transient response, but of the opposite direction, at the stimulation offset. We next quantified whether the responses within these three phases (Fig. 3.2D-

F) differed across the classes of vestibular afferents. Canal and otolith afferents have comparable responses to the stimulation (a three-way mixed ANOVA, $F(1, 109) = 1.2$, $p > 0.05$) consistent with previous findings (Chapter 2). In addition, we found that irregular afferents had a significantly greater change in activity at the onset versus the offset of the stimulation (post-hoc Tukey's test, $p < 0.05$), but this was not observed for regular afferents (post-hoc Tukey's test, $p > 0.05$). This asymmetry is also illustrated in Fig. 3.2G, which shows the percent difference of the peak responses at the onset and offset of the stimulation was greater for irregular afferents compared to regular afferents (two-way ANOVA, $F(1,109) = 18.6$, $p < 0.001$). Notably, this asymmetrical pattern between onset versus offset was also observed in the eye movements (Fig. 3.1), suggesting that irregular afferents are most likely the source of this asymmetry.

Next, we characterized the dynamics of the vestibular afferent responses to the constant current stimulation by estimating the time constants of the decay. The population step responses were well described with two exponential curves with two time constants (eq. 3.3). Bootstrap technique (see Methods) was used to determine whether the estimated parameters were significant. For each model parameter, we obtained 95% confidence intervals using the percentile method. The estimated bias and the both constants are shown in Table 3.1. Note that the estimated biases agree with the steady-state responses shown in Fig. 3.2E. Interestingly, the large peak and subsequent adaptation found in vestibular afferent responses provide a neural correlate for eye movement responses, which were initially large, but attenuated over the duration of the stimulation (Fig. 3.1C and D).

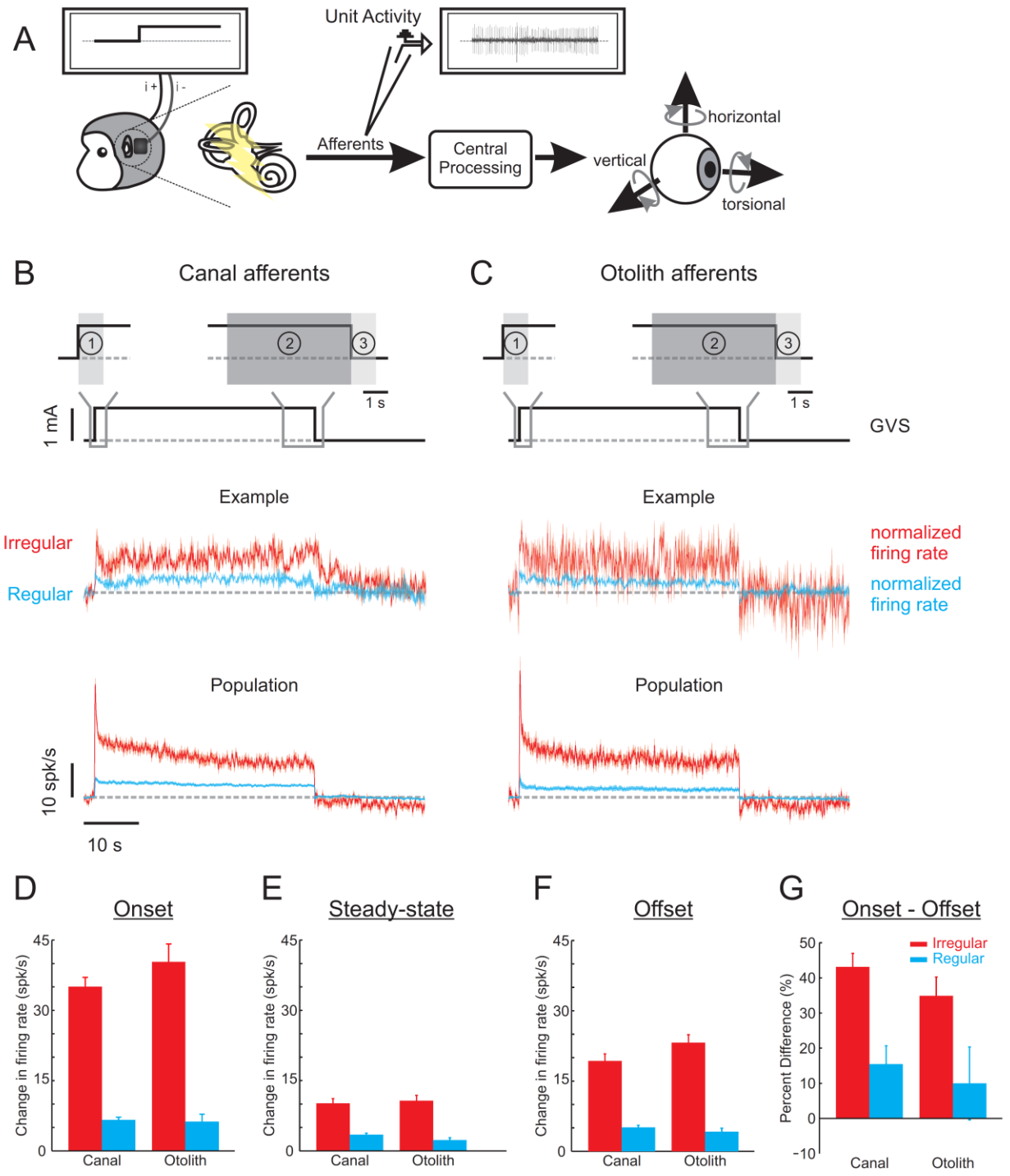


**Figure 3.2.** Response characteristics of vestibular afferents to constant cathodal current GVS. (A) We recorded extracellular single-unit activity from vestibular afferents using tungsten electrodes during constant current GVS. (B) The top row shows the constant cathodal current stimulation and the zoomed-in schematic of the three phases: (1) onset, (2) steady-state, and (3) offset. The middle row shows the average firing rate across three constant current pulses of an example regular (blue) and irregular (red) canal afferents relative to a 2 second baseline prior to the onset of the

stimulation (top row). The bottom row shows the population responses of the regular (N = 37) and irregular (N = 33) canal afferents to the cathodal current, which can be described of having transient and static components. (C) The top row shows the constant cathodal current stimulation and the zoomed-in schematic of the three phases: (1) onset, (2) steady-state, and (3) offset. The middle row shows the average firing rate across three constant current pulses of an example regular (blue) and irregular (red) otolith afferents relative to a 2-second baseline prior to the onset of the stimulation. The bottom row shows the population responses of the regular (N = 20) and irregular (N = 23) otolith afferents to the cathodal current, which can also be described of having transient and static components. (D) The population peak response within the first second after the onset of the stimulation for the different classes of vestibular afferents. (E) The population steady-state response of the last 5 seconds of the stimulation. (F) The population steady-state response of the last 5 seconds of the stimulation. In all three phases, there is a significant difference in response between the discharge regularity of the afferents (regular versus regular; $p < 0.001$), but not the endorgans (canal versus otolith; $p > 0.05$). (G) The population averaged percent difference between the onset and offset responses.

**Table 3.1.** Bias and two time constants estimated from vestibular afferents step responses.

| | Bias | | Short TC | | Long TC | |
|---|---|---|---|---|---|---|
| Afferents | M | 95% CI | M | 95% CI | M | 95% CI |
| Irregular canal | 8.26 | [4.77, 10.47] | 0.25 | [0.17, 0.33] | 17.78 | [7.07, 29.18] |
| Regular canal | 2.88 | [0.73, 3.85] | 0.28 | [0.17, 0.40] | 20.25 | [3.97, 50.18] |
| Irregular otolith | 10.13 | [6.18, 12.74] | 0.25 | [0.12, 0.37] | 7.64 | [1.31, 15.37] |
| Regular otolith | 1.92 | [0.03, 3.08] | 0.32 | [0.12, 0.63] | 10.74 | [0.53, 35.11] |

**Current polarity asymmetry in vestibular afferent responses**

We next investigated whether there were asymmetries in vestibular afferent responses to constant cathodal and anodal current stimulation. Since the change in current flow at the offset of cathodal current stimulation is the same as the change at the onset of anodal current stimulation, the unbalanced responses described above could be linked to asymmetrical responses to currents of opposite polarity. Accordingly, we recorded a separate set of vestibular afferents in responses to cathodal and anodal constant current GVS (regular canal, N = 22; irregular canal, N = 12; regular otolith, N = 9; irregular otolith, N = 12). As expected from previous findings (Chapter 2), constant

anodal current GVS evoked a decrease in firing rate in all vestibular afferents. Again, we can categorized these responses into three phases: Onset, steady-state and offset (Fig. 3.3A).

We then determined whether changes in vestibular afferent activity within the three phases (shown in Fig. 3.3B – D) were different during the cathodal versus anodal stimulation. As expected, changes in the firing rates of irregular afferents were significantly greater than regular afferents (simple main effect tests, $p < 0.05$ for onset, $p < 0.01$ for steady-state, and $p < 0.001$ for offset). In addition, we found that canal and otolith afferents generally exhibit the same responses to constant current stimulation, with the exception of the irregular otolith afferents having greater responses at the onset compared to irregular canal afferents (simple main effect test, $p < 0.05$ for both current polarities). More importantly, in all three phases, irregular afferents, more so than regular afferents, showed unequal responses to currents of opposite polarity (simple main effect test, $p < 0.05$). Notably, changes in firing rates of irregular afferents were greater at the offset of anodal stimulation compared to the offset of cathodal stimulation. At both the onset and the offset of the stimulation, irregular afferents evoked a biased response to a change in current flow toward the cathode. Moreover, the cathodal percent difference in afferent activity was similar to the anodal percent difference (Fig. 3.3E, three-way mixed ANOVA, $p > 0.05$). These results suggest that cathodal and anodal current stimulation have differential effects in vestibular afferent responses, primarily irregular afferents, thereby increasing the complexity of modelling the GVS activation of the peripheral vestibular system.

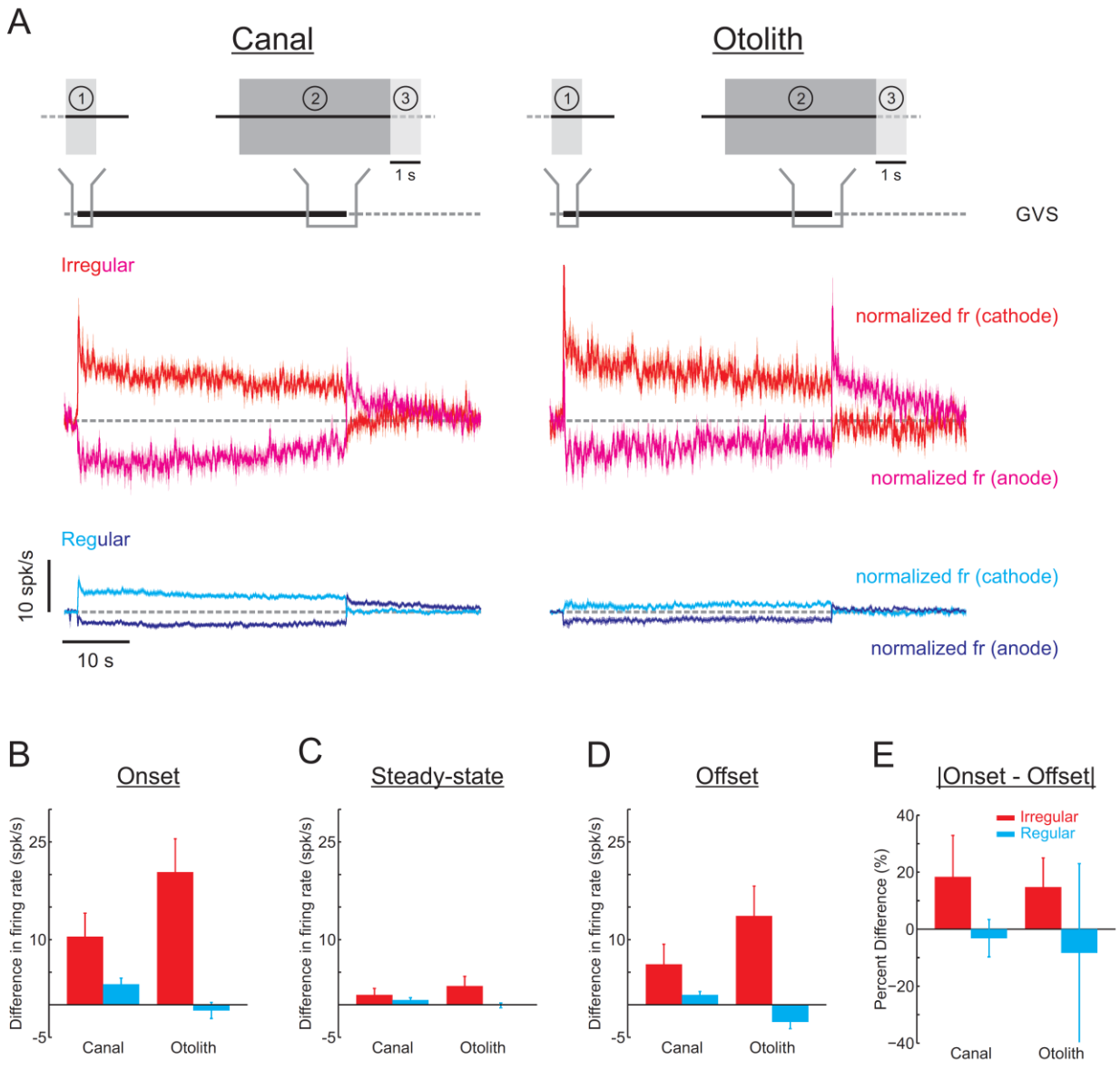


**Figure 3.3.** Comparison of vestibular afferent responses to constant cathodal versus anodal current GVS. (A) Population responses to cathodal (middle trace) and anodal (bottom trace) of the four classes of vestibular afferents (regular canal: N = 22; irregular canal: N = 12; regular otolith: N = 9; irregular otolith: N = 12). The three phases: (1) Onset, (2) steady-state, and (3) offset, are shown on top with the dark line representing the constant current stimulation. (B) The difference in population peak response within the first second after the onset of the stimulation for the different classes of vestibular afferents. (C) The difference in population steady-state response of the last 5 seconds of the stimulation. (D) The difference in population steady-state response of the last 5 seconds of the stimulation. Note here that for B and C, a positive difference indicates that the changes in response to the cathodal condition is greater. In D, a positive difference indicates that the changes in responses to the anodal condition is greater. (E) The difference in the onset/offset asymmetry during cathodal versus anodal current.

**Primary vestibular afferents responds to stochastic stimulation**

A second approach to assess linearity is by using broadband stochastic input and perform standard linear system analysis – a standard method to describe the linearity of the vestibular system to physiological stimuli (Sadeghi *et al.*, 2007a). Moreover, stochastic GVS has been used previously in numerous settings, such as to characterize the frequency responses of muscles associated with the outputs of the vestibular pathways (Forbes *et al.*, 2015). Thus, we examined the activity of vestibular afferents during this type of stimulation. The responses of the example regular and irregular canal afferents to a segment of the stochastic GVS are shown in Fig. 3.4A. We next estimated the frequency response of all vestibular afferents to stochastic stimulation and compared these responses to those observed during sinusoidal GVS (Chapter 2), which are shown in Fig. 3.4B and E for canal (regular, blue, N = 58; irregular, red, N = 48) and otolith (regular, blue, N = 27; irregular, red, N = 37) afferents. We observed that the response dynamics of both regular and irregular canal afferents to the two different GVS paradigms had similar trends: Gain and phase leads increased as a function of frequency. However, the response dynamics to sinusoid and stochastic GVS deviated at low and high frequencies, suggesting that the system is nonlinear.

Based on our finding above that there is an asymmetry in the firing rate change evoked by cathodal and anodal current (i.e. Fig. 3.3), we reanalyzed the vestibular afferent responses to sinusoidal GVS to determine whether these asymmetries were present. First, we computed the difference between the bias estimated in Chapter 2 using eq. 2.1 and the resting discharge of individual afferents. This difference is a measure of asymmetry, where a greater value indicates that the vestibular afferent responds more readily to the cathodal cycle than to anodal cycle. Interestingly, we noticed that this difference increased as a function of frequency, suggesting that

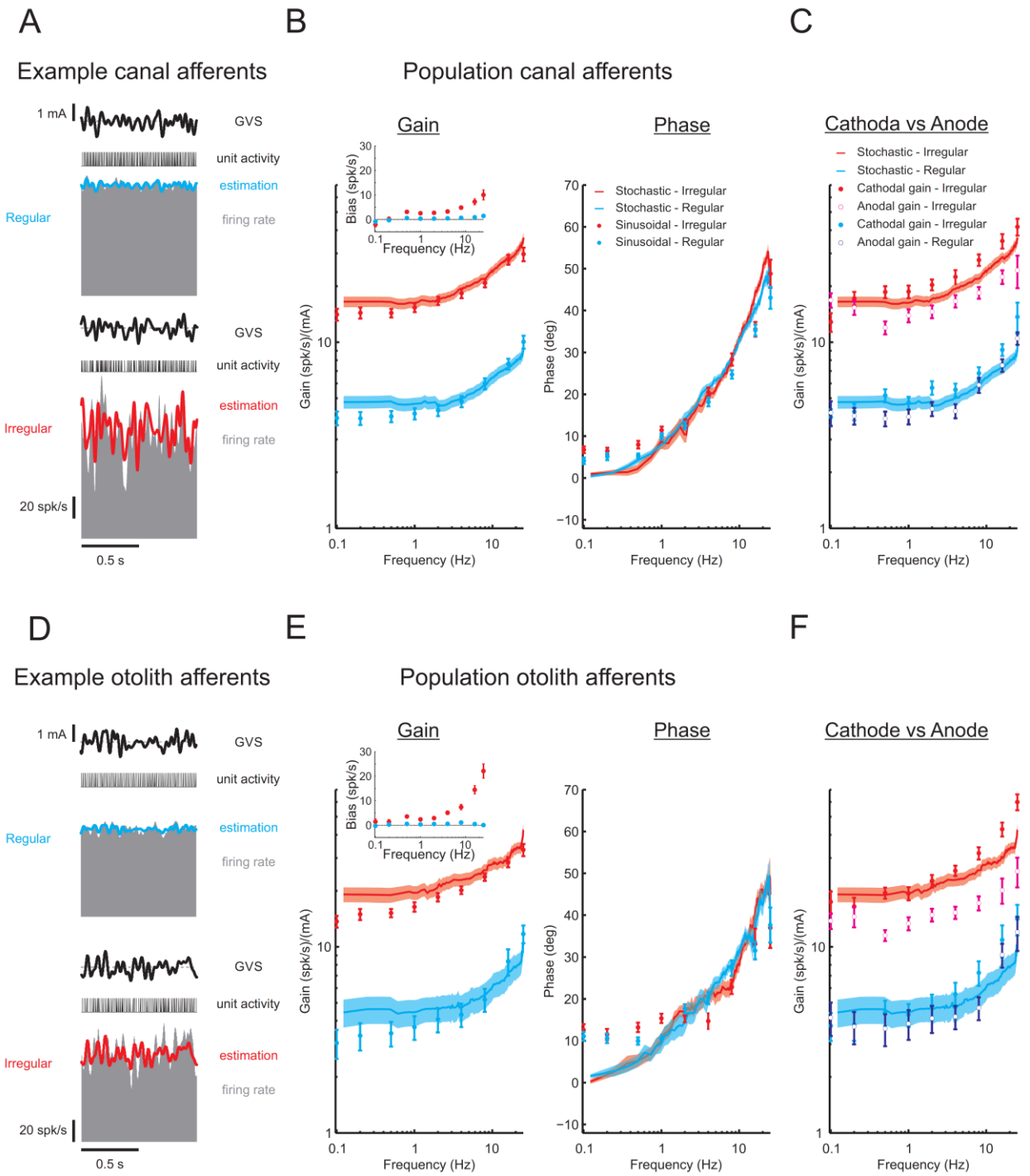


**Figure 3.4.** Response dynamics of vestibular afferents to broadband stochastic GVS. (A) Response of canal afferents. The right panel shows firing rate (gray) of example regular (blue) and irregular (red) canal afferents to segments of broadband stochastic GVS. (B) Population averaged gain (left), and phase (right) for regular (blue, N = 58) and irregular (red, N = 48) canal afferents. Superimposed gain and phase (dots) are the population response dynamics to sinusoidal GVS from Chapter 2. Inset shows estimated bias using eq. 2.1 as a function of frequency for regular (blue) and irregular (red) afferents. (C) The gains using the cathodal (red filled circles) and anodal (pink

open circle) cycles of sinusoidal GVS compared to the gain to the stochastic stimulation. (D) Response of otolith afferents. The right panel shows firing rate (gray) of example regular (blue) and irregular (red) otolith afferents to segments of broadband stochastic GVS. (D) Population averaged gain (left), and phase (right) for regular (blue, N = 27) and irregular (red, N = 37) otolith afferents as a function of frequency. Superimposed gain and phase (dots) are the population response dynamics to sinusoidal GVS from Chapter 2. Inset shows estimated bias using eq. 2.1 as a function of frequency for regular (blue) and irregular (red) afferents. (C) The gains using the cathodal (red filled circles) and anodal (pink open circle) cycles of sinusoidal GVS compared to the gain to the stochastic stimulation.

the level of asymmetry between cathodal and anodal currents were frequency-dependent (top inset in Fig. 3.4B and E). To test this proposal, we next estimated the gain to the cathodal and anodal cycles of GVS separately (Fig. 3.4C and F), and, consistent with our hypothesis, found that vestibular afferents had greater gains for cathodal versus anodal current (Fig. 3.4C and F). Notably, the gain estimated from the stochastic stimulation mostly fell in between the gains to the cathodal and anodal cycles of sinusoidal GVS. Taken together, these results suggest that traditional linear analysis of vestibular afferent responses to stochastic and sinusoidal GVS washes out nonlinearities due to asymmetric responses during cathodal versus anodal current applications.

## IV. Discussion

In the current study, we delivered current to surface electrodes placed behind the ears of macaque monkeys while recording eye movements and primary vestibular afferent activity in order to investigate whether there are nonlinear mechanisms in early vestibular processing of GVS. We first found that constant cathodal current stimulation evoked eye movements, predominantly torsional nystagmus and horizontal nystagmus, with and without a fixation target, respectively. These eye movements were transient with asymmetrical peaks in the response at the onset and offset of the stimulation. Single unit recordings revealed that stimulation evoked similar patterns of asymmetry in vestibular afferent responses. Notably, response asymmetries were more

significant for irregular than regular afferents, for both the semicircular canal and otolith systems. In addition, we found deviations between afferent modulation produced by stochastic GVS versus sinusoidal GVS that is traditionally applied to study behavioural responses using linear system analyses (Chapter 2). This finding provides further support for our conclusion that that vestibular afferents respond nonlinearly to GVS, that had not previously been explored (Chapter 2).

**Polarity dependence of vestibular afferent responses to GVS**

Here, we have shown that constant current cathodal GVS evoked a greater change in vestibular afferent activity than anodal stimulation, primarily for irregular afferents. This is consistent with a previous report showing that irregular afferents had asymmetrical changes in firing rate to currents of opposite polarity delivered directly to the middle ear (Kim & Curthoys, 2004). In contrast, an earlier animal study using electrical stimulation within the inner ear reported a linear relation between vestibular afferent responses and current that was symmetrical across current polarity (Goldberg *et al.*, 1984). One likely explanation for the apparent discrepancy is that the authors excluded irregular afferents that were completely inhibited (i.e. cutoff) to anodal current in their dataset to estimate the linear relationship. Silencing irregular afferents is physiologically easier than to cause saturation of their firing rate (i.e. the magnitude of an inhibitory stimulus is lesser than that of an excitatory stimulus). This property of irregular afferents thus contributes to the asymmetry in their responses to anodal versus cathodal current. However, in most of the vestibular afferent responses reported here, anodal GVS did not drive the vestibular afferents into cutoff, which suggests that additional mechanisms drive the unbalanced responses. Since vestibular afferents show no such asymmetrical response to natural vestibular stimulation (i.e. linear response to motion (Sadeghi *et al.*, 2007a; Jamali *et al.*, 2013)), we speculate that the

amount of depolarization and hyperpolarization at the cellular level caused by cathodal and anodal current, respectively, is unequal. Moreover, the morphological differences between the regular and irregular afferents as well as the hair cell types that the afferents innervate may explain why predominantly irregular afferents have asymmetrical responses. More importantly, the presence of polarity-induced asymmetry would also provide an explanation for why responses at the onset and offset of the constant current stimulation characterized in this study were asymmetric.

**Behavioural correlates of constant current GVS-evoked vestibular afferent responses**

With our finding that constant cathodal and anodal current GVS evoke unbalanced changes in vestibular afferent activity, primarily irregular afferents, it raises the question of whether the asymmetries are reflected in evoked behaviours. Here, we found that the magnitude of transient eye movements evoked at the onset and offset of the cathodal stimulation was asymmetrical, agreeing with the neural responses. Similar patterns of asymmetry in the eye movements between the onset and offset of GVS have also been reported in humans (MacDougall *et al.*, 2003). However, in the same study, MacDougall *et al.* (2003) found that the average magnitude of eye movements during the cathodal current stimulation was comparable to that during the anodal current stimulation. Similarly, postural responses in humans during GVS are reported to be symmetrical when evoked by cathodal and anodal current (Cauquil *et al.*, 1997; Day *et al.*, 2010). One possibility for this inconsistency between neural responses and behaviours evoked by GVS of opposite current polarity is that the behavioural responses are driven by the combined activity of all vestibular afferents. Thus, how central vestibular processing areas integrate both regular afferent input, which shows less asymmetrical responses, and irregular afferent input, which shows asymmetrical responses, would influence whether behavioural responses exhibit symmetrical

and/or asymmetrical patterns. Accordingly, more physiological models in predicting behaviours induced by GVS should allow for the differences between regular and irregular afferents, such as their sensitivity to GVS and the symmetry/asymmetry to current polarity.

It is also noteworthy to elucidate how the dynamics of vestibular afferents to constant current GVS drive the dynamics in evoked responses. Here, we characterized the vestibular afferent responses into the three phases relative to the stimulation: A large transient response at the stimulation onset, a steady-state response during the stimulation, and a large transient response, but of opposite direction, at the stimulation offset. This is consistent with the time course of GVS-evoked postural sway, which begins with a rapid change in tilt position at the GVS onset, then becomes more stable during the stimulation, and finally ends with a fast sway movement in the opposite direction at the GVS offset (Inglis *et al.,* 1995a; Day *et al.*, 1997a; Wardman *et al.*, 2003a).

In addition, we found that canal afferents had a longer time constant to steps of cathodal current stimulation than to rotations of constant angular velocity. Under rotational stimulation, canal afferents have a time constant of 5 s, which is extended centrally, by means of velocity storage, to 20 s. The prolonged time constant corresponds to the decay in vestibulo-ocular reflex and perception of rotation in response to a rotation of constant angular velocity (Raphan *et al.*, 1979; Shaikh *et al.,* 2013). In contrast, we found that afferent responses to constant currents showed a transient decrease and then remained relatively stable. Consistent with these dynamics, the time constants of the decay in eye movements (MacDougall *et al.*, 2002b) and perception of virtual rotation induced by GVS (St George *et al.*, 2011) during constant GVS exceeded 80 s. Notably, the slower dynamics of GVS-evoked responses compared to those induced by motion suggests that there is a limitation in applying GVS as an exact replicate for natural vestibular stimuli.

**Stochastic GVS, vestibular afferent activity, and its implications for future work**

One novelty in this study is that we recorded vestibular afferent responses to stochastic GVS – an increasingly popular stimulation protocol to activate the human vestibular system for a growing number of applications. Here, comparison of vestibular afferent responses to the stochastic and sinusoidal stimulation (Chapter 2) revealed that afferents exhibited nonlinear responses to GVS, in contrast to our previous assumptions that afferent responses to the transmastoid stimulation can be modelled by linear transfer functions (Chapter 2). Furthermore, since this nonlinearity cannot be predicted by their responses to natural stochastic vestibular stimulation (i.e. motion), where there exists a linear regime (Sadeghi *et al.*, 2007a; Massot *et al.*, 2011; Jamali *et al.*, 2013), our results have important implications in understanding the effects of stochastic GVS in humans. For example, many studies have recorded responses in muscle associated with vestibulo-spinal reflex during stochastic GVS to elucidate the frequency response of the vestibular system (reviewed in Forbes *et al.*, 2015). Our findings provide evidence that these responses are indeed driven by the vestibular system, at least within the physiological frequency range (0-25 Hz). However, recent studies have used GVS stimulation of frequency range up to 75 Hz (Forbes *et al.*, 2013; Forbes *et al.*, 2014). Thus, additional work is needed to determine whether vestibular afferents can be electrically driven at much higher frequencies than their relevant frequency range of the vestibular system.

In one potential biomedical application, stochastic GVS of low current amplitude has recently been used to improve postural and locomotor stability (e.g. (Pal *et al.*, 2009; Mulavara *et al.*, 2011; Mulavara *et al.*, 2015)). The hypothesized mechanism mediating these improvements is known as stochastic resonance, where a subthreshold noise helps a nonlinear system detect a weak signal. Our findings address two key elements necessary in stochastic resonance: A nonlinear

system, and subthreshold noise. First, we have shown the vestibular afferent responses to GVS in a nonlinear fashion, which supports that stochastic resonance may be evoked in the vestibular system with artificial stimuli. Second, since we have shown that vestibular afferents respond to the stimulation of 1 mA in peak amplitude, this suprathreshold noise sets an upper limit of the optimal current amplitude. This upper limit is consistent with prior human studies, which on average, have observed postural and locomotor stability with stochastic stimulation under 1 mA (Pal *et al.*, 2009; Mulavara *et al.*, 2011; Mulavara *et al.*, 2015). However, future experiments will be needed to investigate whether low amplitude stochastic GVS undetectable by vestibular afferents can elicit stochastic resonance.

## V. Conclusion

We conclude that the effects of GVS upon vestibular afferent responses are more complex than is commonly assumed. Specifically, our results provide evidence that GVS produces nonlinear responses in the peripheral vestibular system, most notably substantive asymmetries in the responses of irregular vestibular afferent for cathodal versus anodal currents. Thus, taken together, our findings provide new insights into how GVS activates of the vestibular system, which will be vital to advancing our development of new clinical and biomedical applications.

# Chapter 4. General Summary and Discussion

The purpose of this thesis was to elucidate the effects of transmastoid GVS on primary vestibular afferent responses in order to provide a more accurate neural correlate to GVS-evoked behavioural responses in humans. The four main goals of this thesis were to (1) validate the primate-based model, (2) characterize both canal and otolith afferents to static and dynamic GVS, typically used in human GVS studies, (3) determine the similarities and differences in afferents response dynamics to GVS versus motion, and finally (4) assess linearity in vestibular afferent responses to GVS in order to better understand how GVS-evoked behavioural responses arise.

First, by using single-unit recording of all vestibular afferents (i.e. both canal and otolith afferents of a wide range of discharge variability) under different GVS protocols, I showed that both canal and otolith afferents have similar response dynamics that cannot be predicted by their responses to natural vestibular stimuli (i.e. motion). Second, by recording eye movements during similar stimulation paradigms, I validated the nonhuman primate as a useful model for studying the physiological basis of GVS, since the patterns of eye movements evoked by GVS are comparable to those previously reported in humans (Zink *et al.*, 1997; Watson *et al.*, 1998; Kleine *et al.*, 1999; Schneider *et al.*, 2000; MacDougall *et al.*, 2003). My results show similar patterns in the dynamics of eye movements and vestibular afferent activity in response to GVS, and thereby providing the neural correlates mediating evoked eye movements. These findings and their implications in modelling GVS-activation of the vestibular system and in advancing GVS for clinical and biomedical applications are discussed below.

## I. Modelling GVS activation of the vestibular system

One main finding in my research is the remarkable similarity between canal and otolith afferent responses to static (constant current) and dynamic (e.g. sinusoidal) GVS. Yet to date, there remains an ongoing debate of whether GVS-evoked behavioural responses observed in humans are a result of the activation of primarily otolith pathways (Cohen *et al.*, 2011; 2012), canals pathways (Reynolds & Osler, 2012), or the contributions from both (Curthoys & MacDougall, 2012). Given my results, it is evident that GVS-evoked behaviours are driven by the activation of all vestibular afferents. I suggest instead that there exist conflicting views because interpreting the neural mechanisms from a wide range of GVS-evoked behavioural responses is a daunting task. It becomes more challenging as the contexts in which these experiments were conducted have additional effects influencing the evoked responses. For example, as in other studies (MacDougall *et al.*, 2002b; MacDougall *et al.*, 2003), I found that eye movements evoked in the presence of a fixation target suppressed the movements in the horizontal plane, which were observed in the darkness. Therefore, the direct approach used in the present study is more reliable in elucidating the physiological basis of GVS-evoked behaviour. As discussed below, it would be of interest in the future to investigate how higher order vestibular neurons integrate the combined activity of all vestibular afferents during GVS.

In my thesis research, I further found that the dynamics of vestibular afferent responses to GVS differ markedly from their responses to motion. Thus, we estimated a relationship between the equivalent motion corresponding to GVS-evoked vestibular afferent responses as a function of frequency, since GVS has become an increasingly popular alternative to activate the vestibular system. For instance, as GVS evokes perception of self-motion, this technique could potentially be used to create sensations of motion in virtual reality. Often the mismatch between the self-

motion induced by the immersive visual but virtual environment and the self-motion detected by the vestibular system causes symptoms of motion sickness (Johnson, 2005). In this context, emulating motion-evoked vestibular responses using GVS has been suggested necessary to create a "realistic" experience in the virtual environment of flight and driving simulators (Malcik, 1968; Reed-Jones *et al.*, 2007; Cevette *et al.*, 2012) as well as virtual reality headsets (Entrim 4D, Samsung). Thus, my findings of a frequency-dependent equivalency between motion- and GVS-evoked vestibular afferent responses (Fig. 2.4 – 2.6) have provided an initial starting place for developing GVS stimuli that would produce more physiological dynamics in afferent activity. However, it is important to note that this advance will likely not be sufficient to fully equate motion perception evoked by kinetic stimuli versus GVS since the artificial stimulation simultaneously activates all vestibular afferents in a non-physiological manner. Thus, more work is needed to determine whether GVS can be manipulated to induce sensation of motion similar to those induced physiologically. One key element to apply GVS in virtual reality is the ability to generate perception of self-motion in three dimensions. Thus far, it has been demonstrated that perception of rotation in three dimensions is possible with the addition of GVS electrodes placed on the temples (Aoyama *et al.*, 2015). However, it would be of interest to investigate whether further innovations to GVS including approaches to optimize stimulation between multiple electrodes can provide a sense of physiologically realistic motion. Further development of the approach combined with psychophysical studies will be needed to determine the limits of this technology. In addition, neurophysiological studies in higher-order areas such as cortex and cerebellum – which integrate the vestibular afferent inputs to generate motion perception – will provide insight into how the brain actually combines inputs are integrated during GVS versus actual motion.

## II. Nonlinearity in GVS activation of the peripheral vestibular system

It is commonly assumed that vestibular afferent responses to GVS are linear based on the assumptions that (1) well-established linear model can predict the afferent responses to physiological vestibular stimuli (Fernandez & Goldberg, 1971; Angelaki & Dickman, 2000; Hullar *et al.*, 2005) and (2) the relationship between changes of firing to internal electrical stimulation and current amplitude have been shown to be linear (Goldberg *et al.*, 1984). Subsequently, many studies have modelled GVS activation of the vestibular afferents as a linear system (Fitzpatrick & Day, 2004; Forbes *et al.*, 2013; Héroux *et al.*, 2015). For example, in the model proposed by Fitzpatrick and Day (2004), the authors assumed that cathodal and anodal GVS evokes equal but opposite changes in the firing rate of vestibular afferents. Furthermore, behavioural studies have generally reported symmetrical responses to GVS currents of opposite polarity (Cauquil *et al.*, 1997; MacDougall *et al.*, 2003; Day *et al.*, 2010). Thus, our initial assumption in Chapter 2 was that linear models can well predict vestibular afferent responses to GVS. However, the main finding presented in Chapter 3 of this thesis is that vestibular afferents, primarily irregular afferents, showed asymmetrical responses to cathodal versus anodal current, with a bias toward the cathode. In light of this result, we re-examined the vestibular afferent responses to sinusoidal GVS and found that vestibular afferents (and again primarily irregular afferents), had a higher sensitivity to the cathodal compared to the anodal cycle of the stimulation. Interestingly, the level of asymmetry seems to be frequency-dependent.

It is also noteworthy that motion of high frequency and intensity can drive vestibular afferents into nonlinearities including cutoff (i.e. completely silenced the afferent responses), saturation (i.e. vestibular afferents have a maximum firing rate), and phase-locking (Ramachandran & Lisberger, 2006; Schneider *et al.*, 2011; Jamali, 2015; Schneider *et al.*, 2015).

Therefore, it would not be surprising that for a sufficiently large GVS current, the activated vestibular afferents would exhibit similar nonlinear responses. Since I did not observe strong evidence of these nonlinearities in my study, it is most likely that the current amplitude and the stimulation frequency were too low. Other studies using more direct and thus stronger electrical stimulation inside the ear have reported that anodal current silenced irregular afferent activity (Goldberg *et al.*, 1984; Baird *et al.*, 1988) and signs of saturation to cathodal current (Goldberg *et al.*, 1984). Thus, it would be of interest to determine the intensity of GVS required to elicit similar nonlinearities. Finally, it is important to emphasize that since changes in vestibular afferent responses to inhibitory and excitatory motion stimuli were comparable, the asymmetrical responses to cathodal versus anodal current reported in this thesis are inherent to the artificial stimulation that bypasses the receptor cells to directly activate the afferents. Accordingly, further work aimed at understanding GVS responses nonlinearities will need to consider the cellular mechanisms of GVS activation at the level of the peripheral vestibular system.

## III. Future work

The findings presented in my research are necessary in elucidating the physiological basis of GVS-evoked behavioural responses. Interestingly, in recent years, numerous studies have applied increasingly complex GVS protocols to activate the vestibular system. In this context, further research will be needed to uncover the neural basis of the behavioural and perceptual effects of these novel GVS paradigms. For example, stochastic GVS of high frequency content (reaching up to 75 Hz) is currently used to investigate the frequency responses of the vestibular pathways (Forbes *et al.*, 2013; Forbes *et al.*, 2014). In this thesis, I focused my investigation on GVS within the physiological relevant frequency range of the vestibular system (up to 25 Hz). Further work

will be required to determine whether higher frequency stimulation (i.e., up to 75 Hz) would (1) elicit robust vestibular afferent responses, and if so, (2) drive vestibular afferents into phase-locking regime.

In addition, an increasingly popular area of research is improving postural and locomotor stability in balance deficient patients with the application low levels of stochastic GVS (e.g. (Pal *et al.*, 2009; Mulavara *et al.*, 2011; Iwasaki *et al.*, 2014; Goel *et al.*, 2015; Kataoka *et al.*, 2015; Mulavara *et al.*, 2015)). The predominant hypothesis is that adding a low level of noise to a nonlinear system improves the detection of a weak input – a phenomenon known as stochastic resonance. Although my finding that vestibular afferent responses to stochastic GVS are nonlinear, which is one of the key elements of stochastic resonance, it remains a question of whether subthreshold stochastic GVS would in fact enhance the detection of a weak vestibular signal.

One benefit of the experimental approach presented in this study is that it can directly test whether vestibular afferents exhibit stochastic resonance. As such, I propose the following experiment. Since the stochastic GVS used in this thesis is suprathreshold, I would need to first determine current amplitudes that are low enough to not evoke vestibular afferent responses. To do so, I could gradually decrease the amplitude of the stochastic stimulation. By characterizing the coherence between the vestibular afferent responses to the stimulation, I would then find the range of low amplitudes that are subthreshold level. To then investigate whether stochastic resonance occurs in early vestibular processing, I would record vestibular afferents being simultaneously stimulated by low levels of stochastic GVS, in which the amplitude ranges would be determined above, and sinusoidal motion stimuli whose amplitude is right at the neuronal detection threshold (Sadeghi *et al.*, 2007a; Massot *et al.*, 2011; Jamali *et al.*, 2013). If indeed stochastic resonance

does occur, then the low current amplitude stochastic GVS should improve the vestibular afferent responses to detect the weak motion stimuli.

It is important to note that while my findings provide better understanding in vestibular afferent responses to GVS, it is also fundamental to explore how these evoked responses are integrated at the next stage of vestibular processing. There are still many questions that require more than just the dynamics of vestibular afferents to resolve. For instance, how are otolith and canal afferents, which are demonstrated in this thesis to be non-selectively activated by GVS, integrated by the vestibular nuclei and higher order processing to generate the complexity and diversity in GVS-evoked behavioural responses? Although previous animal studies have recorded vestibular nuclei neurons during electrical stimulation inside the ear (Wilson *et al.*, 1979; Courjon *et al.*, 1987), assumptions based on these results face the same limitations that vestibular responses to GVS cannot be predicted by those to internal electrical stimulation. Accordingly, future experiments focused on recording neurons in the vestibular nuclei under similar GVS paradigms presented in this thesis are crucial. Analysis of such recordings, would provide new insight into a fundamental question: Are nonlinearities in neural responses to GVS more evident at the level of vestibular nuclei? And if so, what are the underlying mechanisms?

## IV. Concluding remarks

Despite the growing literature on GVS and its multiple potential applications, how the vestibular system responds to GVS is not fully understood. To date, studies have attempted to infer the effects of GVS on the human vestibular system using predictions based on GVS-evoked behavioural responses or assumptions based on neurophysiological recordings during internal electrical stimulation (reviewed in Fitzpatrick & Day, 2004). However, the former assessment

lacks the direct investigation of vestibular pathways while the latter estimation lacks the GVS electrodes setup as performed in humans. My Master's thesis provides a direct link between transmastoid stimulation and neurophysiological recordings of the vestibular system – specifically the vestibular afferents that normally convey motion information to the brain. Last but not least, the characterization of the effects of GVS on vestibular nerve activity has important implications to further develop model of GVS activation and advance GVS-based technologies.

# References


Angelaki, D.E. & Cullen, K.E. (2008) Vestibular system: the many facets of a multimodal sense. *Annu. Rev. Neurosci.*, **31**, 125-150.

Angelaki, D.E. & Dickman, J.D. (2000) Spatiotemporal processing of linear acceleration: primary afferent and central vestibular neuron responses. *Journal of neurophysiology*, **84**, 2113-2132.

Aoyama, K., Iizuka, H., Ando, H. & Maeda, T. (2015) Four-pole galvanic vestibular stimulation causes body sway about three axes. *Scientific reports*, **5**.

Aw, S., Todd, M., Aw, G., Weber, K. & Halmagyi, G. (2008) Gentamicin vestibulotoxicity impairs human electrically evoked vestibulo-ocular reflex. *Neurology*, **71**, 1776-1782.

Aw, S.T., Aw, G.E., Todd, M.J. & Halmagyi, G.M. (2013) Enhanced vestibulo-ocular reflex to electrical vestibular stimulation in Meniere's disease. *Journal of the Association for Research in Otolaryngology*, **14**, 49-59.

Baird, R., Desmadryl, G., Fernandez, C. & Goldberg, J. (1988) The vestibular nerve of the chinchilla. II. Relation between afferent response properties and peripheral innervation patterns in the semicircular canals. *Journal of neurophysiology*, **60**, 182-203.

Blanks, R., Curthoys, I. & Markham, C. (1975) Planar relationships of the semicircular canals in man. *Acta oto-laryngologica*, **80**, 185-196.

Britton, T., Day, B., Brown, P., Rothwell, J., Thompson, P. & Marsden, C. (1993) Postural electromyographic responses in the arm and leg following galvanic vestibular stimulation in man. *Experimental brain research*, **94**, 143-151.

Carpenter, J. & Bithell, J. (2000) Bootstrap confidence intervals: when, which, what? A practical guide for medical statisticians. *Statistics in medicine*, **19**, 1141-1164.

Carriot, J., Jamali, M., Chacron, M.J. & Cullen, K.E. (2014) Statistics of the vestibular input experienced during natural self-motion: implications for neural processing. *The Journal of Neuroscience*, **34**, 8347-8357.

Cauquil, A.S., Bousquet, P., Salon, M.-C.C., Dupui, P. & Bessou, P. (1997) Monaural and binaural galvanic vestibular stimulation in human dynamic balance function. *Gait & Posture*, **6**, 210-217.

Cauquil, A.S., Martinez, P., Ouaknine, M. & Tardy-Gervet, M.-F. (2000) Orientation of the body response to galvanic stimulation as a function of the inter-vestibular imbalance. *Experimental brain research*, **133**, 501-505.

Cevette, M.J., Stepanek, J., Cocco, D., Galea, A.M., Pradhan, G.N., Wagner, L.S., Oakley, S.R., Smith, B.E., Zapala, D.A. & Brookler, K.H. (2012) Oculo-vestibular recoupling using galvanic vestibular stimulation to mitigate simulator sickness. *Aviation, space, and environmental medicine*, **83**, 549-555.

Cherif, S., Cullen, K.E. & Galiana, H.L. (2008) An improved method for the estimation of firing rate dynamics using an optimal digital filter. *Journal of neuroscience methods*, **173**, 165-181.

Cohen, B., Yakushin, S.B. & Holstein, G.R. (2011) What does galvanic vestibular stimulation actually activate? *Frontiers in neurology*, **2**.

Cohen, B., Yakushin, S.B. & Holstein, G.R. (2012) What does galvanic vestibular stimulation actually activate: response. *Frontiers in neurology*, **3**.

Colclasure, J.C. & Holt, J.R. (2003) Transduction and adaptation in sensory hair cells of the mammalian vestibular system. *Gravitational and Space Biology Bulletin*, **16**.

Courjon, J., Precht, W. & Sirkin, D. (1987) Vestibular nerve and nuclei unit responses and eye movement responses to repetitive galvanic stimulation of the labyrinth in the rat. *Experimental brain research*, **66**, 41-48.

Cullen, K.E. (2012) The vestibular system: multimodal integration and encoding of self-motion for motor control. *Trends in neurosciences*, **35**, 185-196.

Cullen, K.E. & Minor, L.B. (2002) Semicircular canal afferents similarly encode active and passive head-on-body rotations: implications for the role of vestibular efference. *J Neurosci*, **22**, 1-7.

Curthoys, I.S. & MacDougall, H.G. (2012) What galvanic vestibular stimulation actually activates. *Frontiers in neurology*, **3**.

Dakin, C.J., Son, G.M.L., Inglis, J.T. & Blouin, J.S. (2007) Frequency response of human vestibular reflexes characterized by stochastic stimuli. *The Journal of physiology*, **583**, 1117-1127.

Dale, A. & Cullen, K.E. (2013) The nucleus prepositus predominantly outputs eye movement-related information during passive and active self-motion. *Journal of neurophysiology*, **109**, 1900-1911.

Dale, A. & Cullen, K.E. (2015) Local population synchrony and the encoding of eye position in the primate neural integrator. *The Journal of Neuroscience*, **35**, 4287-4295.

Day, B., Cauquil, A., Bartolomei, L., Pastor, M. & Lyon, I. (1997a) Human body-segment tilts induced by galvanic stimulation: a vestibularly driven balance protection mechanism. *The Journal of Physiology*, **500**, 661.

Day, B., Severac Cauquil, A., Bartolomei, L., Pastor, M. & Lyon, I. (1997b) Human body-segment tilts induced by galvanic stimulation: a vestibularly driven balance protection mechanism. *The Journal of Physiology*, **500**, 661-672.

Day, B.L. & Cole, J. (2002) Vestibular-evoked postural responses in the absence of somatosensory information. *Brain*, **125**, 2081-2088.

Day, B.L. & Fitzpatrick, R.C. (2005) Virtual head rotation reveals a process of route reconstruction from human vestibular signals. *The Journal of physiology*, **567**, 591-597.

Day, B.L., Marsden, J.F., Ramsay, E., Mian, O.S. & Fitzpatrick, R.C. (2010) Non-linear vector summation of left and right vestibular signals for human balance. *The Journal of physiology*, **588**, 671-682.

Day, B.L., Ramsay, E., Welgampola, M.S. & Fitzpatrick, R.C. (2011) The human semicircular canal model of galvanic vestibular stimulation. *Experimental brain research*, **210**, 561-568.

Dilda, V., Morris, T.R., Yungher, D.A., MacDougall, H.G. & Moore, S.T. (2014a) Central adaptation to repeated galvanic vestibular stimulation: implications for pre-flight astronaut training.

Dilda, V., Morris, T.R., Yungher, D.A., MacDougall, H.G. & Moore, S.T. (2014b) Central adaptation to repeated galvanic vestibular stimulation: implications for pre-flight astronaut training. *PloS one*, **9**, e112131.

Eatock, R.A. & Hurley, K.M. (2003) Functional development of hair cells. *Current topics in developmental biology*, **57**, 389-448.

Eatock, R.A. & Songer, J.E. (2011) Vestibular hair cells and afferents: two channels for head motion signals. *Annual review of neuroscience*, **34**, 501-534.

Ezure, K., Cohen, M. & Wilson, V. (1983) Response of Cat Semicircular Canal Merents to Sinusoidal Polarizing Currents: Implications for Input-Output Properties of Second-Order Neurons.

Fernandez, C. & Goldberg, J.M. (1971) Physiology of peripheral neurons innervating semicircular canals of the squirrel monkey. II. Response to sinusoidal stimulation and dynamics of peripheral vestibular system. *J Neurophysiol*, **34**, 661-675.

Fernandez, C. & Goldberg, J.M. (1976a) Physiology of peripheral neurons innervating otolith organs of the squirrel monkey. I. Response to static tilts and to long-duration centrifugal force. *Journal of neurophysiology*, **39**, 970-984.

Fernandez, C. & Goldberg, J.M. (1976b) Physiology of peripheral neurons innervating otolith organs of the squirrel monkey. II. Directional selectivity and force-response relations. *Journal of neurophysiology*, **39**, 985-995.

Fernandez, C. & Goldberg, J.M. (1976c) Physiology of peripheral neurons innervating otolith organs of the squirrel monkey. III. Response dynamics. *Journal of neurophysiology*, **39**, 996-1008.

Fitzpatrick, R., Burke, D. & Gandevia, S.C. (1994) Task-dependent reflex responses and movement illusions evoked by galvanic vestibular stimulation in standing humans. *The Journal of Physiology*, **478**, 363.

Fitzpatrick, R.C., Butler, J.E. & Day, B.L. (2006) Resolving head rotation for human bipedalism. *Current Biology*, **16**, 1509-1514.

Fitzpatrick, R.C. & Day, B.L. (2004) Probing the human vestibular system with galvanic stimulation. *Journal of Applied Physiology*, **96**, 2301-2316.

Fitzpatrick, R.C., Marsden, J., Lord, S.R. & Day, B.L. (2002) Galvanic vestibular stimulation evokes sensations of body rotation. *Neuroreport*, **13**, 2379-2383.

Forbes, P.A., Dakin, C.J., Vardy, A.N., Happee, R., Siegmund, G.P., Schouten, A.C. & Blouin, J.-S. (2013) Frequency response of vestibular reflexes in neck, back, and lower limb muscles. *Journal of neurophysiology*, **110**, 1869-1881.

Forbes, P.A., Siegmund, G.P., Happee, R., Schouten, A.C. & Blouin, J.-S. (2014) Vestibulocollic reflexes in the absence of head postural control. *Journal of neurophysiology*, **112**, 1692-1702.

Forbes, P.A., Siegmund, G.P., Schouten, A.C. & Blouin, J.-S. (2015) Task, muscle and frequency dependent vestibular control of posture. *Frontiers in Integrative Neuroscience, 8, 2015*.

Fuchs, A.F. & Robinson, D.A. (1966) A method for measuring horizontal and vertical eye movement chronically in the monkey. *Journal of Applied Physiology*, **21**, 1068-1070.

Goel, R., Kofman, I., Jeevarajan, J., De Dios, Y., Cohen, H.S., Bloomberg, J.J. & Mulavara, A.P. (2015) Using Low Levels of Stochastic Vestibular Stimulation to Improve Balance Function. *PloS one*, **10**, e0136335.

Goldberg, J., Fernandez, C. & Smith, C. (1982) Responses of vestibular-nerve afferents in the squirrel monkey to externally applied galvanic currents. *Brain research*, **252**, 156-160.

Goldberg, J. & Smith, C. (1982) Responses of vestibular-nerve afferents in the squirrel monkey to externally applied galvanic currents. *Brain research*, **252**, 156-160.

Goldberg, J., Smith, C. & Fernandez, C. (1984) Relation Between Discharge Regularity and Responses to Externally Applied Galvanic Currents in Vestibular Nerve Merents of the Squirrel Monkey.

Goldberg, J.M. (2000) Afferent diversity and the organization of central vestibular pathways. *Experimental Brain Research*, **130**, 277-297.

Goldberg, J.M. & Fernandez, C. (1980) Efferent vestibular system in the squirrel monkey: anatomical location and influence on afferent activity. *Journal of neurophysiology*, **43**, 986-1025.

Hammam, E., Dawood, T. & Macefield, V.G. (2012) Low-frequency galvanic vestibular stimulation evokes two peaks of modulation in skin sympathetic nerve activity. *Experimental brain research*, **219**, 441-446.

Hays Jr, A., Richmond, B. & Optican, L. (1982) Unix-based multiple-process system, for real-time data acquisition and control.

Héroux, M.E., Law, T.C., Fitzpatrick, R.C. & Blouin, J.-S. (2015) Cross-modal calibration of vestibular afference for human balance. *PloS one*, **10**, e0124532.

Hullar, T.E., Della Santina, C.C., Hirvonen, T., Lasker, D.M., Carey, J.P. & Minor, L.B. (2005) Responses of irregularly discharging chinchilla semicircular canal vestibular-nerve afferents during high-frequency head rotations. *Journal of neurophysiology*, **93**, 2777-2786.

Inglis, J., Shupert, C., Hlavacka, F. & Horak, F. (1995a) Effect of galvanic vestibular stimulation on human postural responses during support surface translations. *Journal of neurophysiology*, **73**, 896-901.

Inglis, J.T., Shupert, C.L., Hlavacka, F. & Horak, F. (1995b) Effect of galvanic vestibular stimulation on human postural responses during support surface translations. *Journal of neurophysiology*, **73**, 896-901.

Iwasaki, S., Yamamoto, Y., Togo, F., Kinoshita, M., Yoshifuji, Y., Fujimoto, C. & Yamasoba, T. (2014) Noisy vestibular stimulation improves body balance in bilateral vestibulopathy. *Neurology*, **82**, 969-975.

Jamali, M. (2015) Neural strategies for encoding self-motion: role of spike-timing varibility in the vestibular periphery.

Jamali, M., Carriot, J., Chacron, M.J. & Cullen, K.E. (2013) Strong correlations between sensitivity and variability give rise to constant discrimination thresholds across the otolith afferent population. *The Journal of Neuroscience*, **33**, 11302-11313.

Jamali, M., Sadeghi, S.G. & Cullen, K.E. (2009) Response of vestibular nerve afferents innervating utricle and saccule during passive and active translations. *Journal of neurophysiology*, **101**, 141-149.

Johnson, D.M. (2005) Introduction to and review of simulator sickness research. DTIC Document.

Judge, S.J., Richmond, B.J. & Chu, F.C. (1980) Implantation of magnetic search coils for measurement of eye position: an improved method. *Vision research*, **20**, 535-538.

Kataoka, H., Okada, Y., Kiriyama, T., Kita, Y., Nakamura, J., Morioka, S., Shomoto, K. & Ueno, S. (2015) Can Postural Instability Respond to Galvanic Vestibular Stimulation in Patients with Parkinson's Disease? *Journal of movement disorders*.

Kim, H.J., Choi, J.Y., Son, E.J. & Lee, W.S. (2006) Response to galvanic vestibular stimulation in patients with unilateral vestibular loss. *The Laryngoscope*, **116**, 62-66.

Kim, J. & Curthoys, I.S. (2004) Responses of primary vestibular neurons to galvanic vestibular stimulation (GVS) in the anaesthetised guinea pig. *Brain research bulletin*, **64**, 265-271.

Kim, K.-S., Minor, L.B., Della Santina, C.C. & Lasker, D.M. (2011) Variation in response dynamics of regular and irregular vestibular-nerve afferents during sinusoidal head rotations and currents in the chinchilla. *Experimental brain research*, **210**, 643-649.

Kleine, J.F., Guldin, W.O. & Clarke, A.H. (1999) Variable otolith contribution to the galvanically induced vestibulo-ocular reflex. *Neuroreport*, **10**, 1143-1148.

Lifschitz, W.S. (1973) Responses from the first order neurons of the horizontal semicircular canal in the pigeon. *Brain research*, **63**, 43-57.

Lund, S. & Broberg, C. (1983) Effects of different head positions on postural sway in man induced by a reproducible vestibular error signal. *Acta Physiologica Scandinavica*, **117**, 307-309.

MacDougall, H., Brizuela, A., Burgess, A., Curthoys, I. & Halmagyi, G. (2005) Patient and normal three-dimensional eye-movement responses to maintained (DC) surface galvanic vestibular stimulation. *Otology & Neurotology*, **26**, 500-511.

MacDougall, H., Brizuela, A., Curthoys, I. & Halmagyi, G. (2002a) Three-Dimensional Eye-Movement Responses to Surface Galvanic Vestibular Stimulation in Normal Subjects and in Patients. *Annals of the New York Academy of Sciences*, **956**, 546-550.

MacDougall, H.G., Brizuela, A.E., Burgess, A.M. & Curthoys, I.S. (2002b) Between-subject variability and within-subject reliability of the human eye-movement response to bilateral galvanic (DC) vestibular stimulation. *Experimental brain research*, **144**, 69-78.

MacDougall, H.G., Brizuela, A.E. & Curthoys, I.S. (2003) Linearity, symmetry and additivity of the human eye-movement response to maintained unilateral and bilateral surface galvanic (DC) vestibular stimulation. *Experimental brain research*, **148**, 166-175.

Maeda, T., Ando, H., Amemiya, T., Nagaya, N., Sugimoto, M. & Inami, M. (Year) Shaking the world: galvanic vestibular stimulation as a novel sensation interface. ACM SIGGRAPH 2005 Emerging technologies. ACM, City. p. 17.

Maeda, T., Ando, H. & Sugimoto, M. (Year) Virtual acceleration with galvanic vestibular stimulation in a virtual reality environment. Virtual Reality, 2005. Proceedings. VR 2005. IEEE. IEEE, City. p. 289-290.

Magnusson, M., Karlberg, M. & Tjernström, F. (2011) 'PREHAB': Vestibular prehabilitation to ameliorate the effect of a sudden vestibular loss. *NeuroRehabilitation*, **29**, 153-156.

Malcik, V. (1968) Performance decrement in a flight simulator due to galvanic stimulation of the vestibular organ and its validity for success in flight training. *Aerospace medicine*, **39**, 941-943.

Massot, C., Chacron, M.J. & Cullen, K.E. (2011) Information transmission and detection thresholds in the vestibular nuclei: single neurons vs. population encoding. *Journal of neurophysiology*, **105**, 1798-1814.

Mian, O.S., Dakin, C.J., Blouin, J.S., Fitzpatrick, R.C. & Day, B.L. (2010) Lack of otolith involvement in balance responses evoked by mastoid electrical stimulation. *The Journal of physiology*, **588**, 4441-4451.

Mitchell, D.E., Dai, C., Rahman, M.A., Ahn, J.H., Della Santina, C.C. & Cullen, K.E. (2013) Head Movements Evoked in Alert Rhesus Monkey by Vestibular Prosthesis Stimulation: Implications for Postural and Gaze Stabilization. *PloS one*, **8**, e78767.

Moore, S.T., Dilda, V. & MacDougall, H.G. (2011) Galvanic vestibular stimulation as an analogue of spatial disorientation after spaceflight. *Aviation, space, and environmental medicine*, **82**, 535-542.

Moore, S.T., Dilda, V., Morris, T.R., Yungher, D.A. & MacDougall, H.G. (2015) Pre-adaptation to noisy Galvanic vestibular stimulation is associated with enhanced sensorimotor performance in novel vestibular environments. *Frontiers in systems neuroscience*, **9**.

Mulavara, A.P., Fiedler, M.J., Kofman, I.S., Wood, S.J., Serrador, J.M., Peters, B., Cohen, H.S., Reschke, M.F. & Bloomberg, J.J. (2011) Improving balance function using vestibular stochastic resonance: optimizing stimulus characteristics. *Experimental brain research*, **210**, 303-312.

Mulavara, A.P., Kofman, I.S., De Dios, Y.E., Miller, C., Peters, B.T., Goel, R., Galvan-Garza, R. & Bloomberg, J.J. (2015) Using low levels of stochastic vestibular stimulation to improve locomotor stability. *Frontiers in systems neuroscience*, **9**.

Nashner, L.M. & Wolfson, P. (1974) Influence of head position and proprioceptive cues on short latency postural reflexes evoked by galvanic stimulation of the human labyrinth. *Brain research*, **67**, 255-268.

Pal, S., Rosengren, S.M. & Colebatch, J.G. (2009) Stochastic galvanic vestibular stimulation produces a small reduction in sway in Parkinson's disease. *Journal of Vestibular Research*, **19**, 137-142.

Peters, R.M., Rasman, B.G., Inglis, J.T. & Blouin, J.-S. (2015) The gain and phase of virtual rotation evoked by electrical vestibular stimuli. *Journal of Neurophysiology*.

Purcell, I.M., Newlands, S.D. & Perachio, A.A. (2003) Responses of gerbil utricular afferents to translational motion. *Experimental brain research*, **152**, 317-322.

Purkyně, J.E. (1823) *Commentatio de examine physiologico organi visus et systematis cutanei: quam pro loco in gratioso medicorum ordine rite obtinendo die XXII Decembris MDCCCXXIII*. typis Universitatis.

Rabbitt, R.D. (1999) Directional coding of three-dimensional movements by the vestibular semicircular canals. *Biological cybernetics*, **80**, 417-431.

Rabbitt, R.D., Damiano, E.R. & Grant, J.W. (2004) Biomechanics of the semicircular canals and otolith organs *The vestibular system*. Springer, pp. 153-201.

Ramachandran, R. & Lisberger, S.G. (2006) Transformation of vestibular signals into motor commands in the vestibuloocular reflex pathways of monkeys. *Journal of neurophysiology*, **96**, 1061-1074.

Raphan, T., Matsuo, V. & Cohen, B. (1979) Velocity storage in the vestibulo-ocular reflex arc (VOR). *Experimental Brain Research*, **35**, 229-248.

Reed-Jones, R.J., Reed-Jones, J.G., Trick, L.M. & Vallis, L.A. (Year) Can galvanic vestibular stimulation reduce simulator adaptation syndrome. Proceedings of the 4th International Driving Symposium on Human Factors in Driver Assessment, Training and Vehicle Design. City. p. 534-540.

Reisine, H., Simpson, J. & Henn, V. (1988) A geometric analysis of semicircular canals and induced activity in their peripheral afferents in the rhesus monkey. *Annals of the New York Academy of Sciences*, **545**, 10-20.

Reynolds, R.F. & Osler, C.J. (2012) Galvanic vestibular stimulation produces sensations of rotation consistent with activation of semicircular canal afferents. *Frontiers in neurology*, **3**, 104.

Sadeghi, S.G., Chacron, M.J., Taylor, M.C. & Cullen, K.E. (2007a) Neural variability, detection thresholds, and information transmission in the vestibular system. *The Journal of neuroscience*, **27**, 771-781.

Sadeghi, S.G., Goldberg, J.M., Minor, L.B. & Cullen, K.E. (2009) Efferent-mediated responses in vestibular nerve afferents of the alert macaque. *Journal of neurophysiology*, **101**, 988-1001.

Sadeghi, S.G., Minor, L.B. & Cullen, K.E. (2007b) Response of vestibular-nerve afferents to active and passive rotations under normal conditions and after unilateral labyrinthectomy. *Journal of neurophysiology*, **97**, 1503-1514.

Samoudi, G., Jivegård, M., Mulavara, A.P. & Bergquist, F. (2015) Effects of stochastic vestibular galvanic stimulation and LDOPA on balance and motor symptoms in patients with Parkinson's disease. *Brain stimulation*, **8**, 474-480.

Schneider, A.D., Cullen, K.E. & Chacron, M.J. (2011) In vivo conditions induce faithful encoding of stimuli by reducing nonlinear synchronization in vestibular sensory neurons. *PLoS Comput Biol*, **7**, e1002120.

Schneider, A.D., Jamali, M., Carriot, J., Chacron, M.J. & Cullen, K.E. (2015) The increased sensitivity of irregular peripheral canal and otolith vestibular afferents optimizes their encoding of natural stimuli. *Journal of Neuroscience*, **in press**.

Schneider, E., Bartl, K. & Glasauer, S. (2009) Galvanic Vestibular Stimulation Combines with Earth-Horizontal Rotation in Roll to Induce the Illusion of Translation. *Annals of the New York Academy of Sciences*, **1164**, 116-118.

Schneider, E., Glasauer, S. & Dieterich, M. (2000) Central processing of human ocular torsion analyzed by galvanic vestibular stimulation. *Neuroreport*, **11**, 1559-1563.

Schneider, E., Glasauer, S. & Dieterich, M. (2002) Comparison of human ocular torsion patterns during natural and galvanic vestibular stimulation. *Journal of neurophysiology*, **87**, 2064-2073.

Shaikh, A.G., Palla, A., Marti, S., Olasagasti, I., Optican, L.M., Zee, D.S. & Straumann, D. (2013) Role of cerebellum in motion perception and vestibulo-ocular reflex—similarities and disparities. *The Cerebellum*, **12**, 97-107.

Srinivasan, R., Tucker, D.M. & Murias, M. (1998) Estimating the spatial Nyquist of the human EEG. *Behavior Research Methods, Instruments, & Computers*, **30**, 8-19.

St George, R.J., Day, B.L. & Fitzpatrick, R.C. (2011) Adaptation of vestibular signals for self-motion perception. *The Journal of physiology*, **589**, 843-853.

Stephan, T., Deutschländer, A., Nolte, A., Schneider, E., Wiesmann, M., Brandt, T. & Dieterich, M. (2005) Functional MRI of galvanic vestibular stimulation with alternating currents at different frequencies. *Neuroimage*, **26**, 721-732.

Tribukait, A. & Rosenhall, U. (2001) Directional sensitivity of the human macula utriculi based on morphological characteristics. *Audiology and Neurotology*, **6**, 98-107.

Tribukait, A., Rosenhall, U. & Österdahl, B. (2005) Morphological characteristics of the human macula sacculi. *Audiology and Neurotology*, **10**, 90-96.

Wardman, D.L., Day, B.L. & Fitzpatrick, R.C. (2003a) Position and velocity responses to galvanic vestibular stimulation in human subjects during standing. *The Journal of physiology*, **547**, 293-299.

Wardman, D.L., Taylor, J.L. & Fitzpatrick, R.C. (2003b) Effects of galvanic vestibular stimulation on human posture and perception while standing. *The Journal of physiology*, **551**, 1033-1042.

Watson, S.R., Brizuela, A.E., Curthoys, I.S., Colebatch, J.G., MacDougall, H.G. & Halmagyi, G.M. (1998) Maintained ocular torsion produced by bilateral and unilateral galvanic (DC) vestibular stimulation in humans. *Experimental brain research*, **122**, 453-458.

Wilson, V., Peterson, B., Fukushima, K., Hirai, N. & Uchino, Y. (1979) Analysis of vestibulocollic reflexes by sinusoidal polarization of vestibular afferent fibers. *Journal of neurophysiology*, **42**, 331-346.

Wuehr, M., Nusser, E., Krafczyk, S., Straube, A., Brandt, T., Jahn, K. & Schniepp, R. (2016) Noise-enhanced vestibular input improves dynamic walking stability in healthy subjects. *Brain stimulation*, **9**, 109-116.

Zink, R., Bucher, S., Weiss, A., Brandt, T. & Dieterich, M. (1998) Effects of galvanic vestibular stimulation on otolithic and semicircular canal eye movements and perceived vertical. *Electroencephalography and clinical neurophysiology*, **107**, 200-205.

Zink, R., Steddin, S., Weiss, A., Brandt, T. & Dieterich, M. (1997) Galvanic vestibular stimulation in humans: effects on otolith function in roll. *Neuroscience letters*, **232**, 171-174.